This is to certify that the
thesis entitled

A Self Tuning Electromagnetic Shutter

presented by

Raoul Ouatagom Ouedraogo Jr.

has been accepted towards fulfillment
of the requirements for the

M.S. degree in Electrical Engineering

Edward J. Rothwell
Major Professor's Signature

20 August 2008
Date

A Self Tuning Electromagnetic Shutter

By

Raoul Ouatagom Ouedraogo Jr.

A THESIS

Submitted to
Michigan State University
in partial fulfillment of the requirements
for the degree of

MASTER OF SCIENCE

Electrical Engineering

Department of Electrical and Computer Engineering

2008

ABSTRACT

A Self Tuning Electromagnetic Shutter

By

Raoul Ouatagom Ouedraogo Jr.

A self-tuning electromagnetic shutter (STEMS) is a slotted metallic surface with computer-controlled switchable shorting wires placed across the slots. By opening and closing the shorting wires, the transmissitivity of the surface may be adjusted. In particular, the surface may be placed into open and closed states, creating an electronically-controllable iris. Since the states of the switches needed to create a selected transmissitivity depend on frequency, a binary search technique, such as a genetic algorithm, is used to find an acceptable state. A feedback signal, such as from a receiving probe, is used to judge whether a given state produces the desired behavior.

To investigate the feasibility of STEMS, and to study its dependence on frequency, polarization, and angle of incidence, the STEMS is used to seal the opening to a cubical box containing a monopole antenna. The monopole is used as a receiving probe to measure the coupling from an incident electric field into the box. A closed STEMS is sought by minimizing the field entering the box, while an open STEMS is sought by maximizing the received field.

To my parents and my wife: Justin, Charlotte & Clarice Ouedraogo

ACKNOWLEDGMENTS

There are many people who deserve acknowledgment for both the work contained in this thesis, and the countless other things that I was able to be involved in throughout my first two years at Michigan State University. First and foremost, a special thanks to Dr. E. Rothwell for being a very resourceful and exceptional adviser, and also for always making time to help and provide guidance to your students. Thanks to Dr. B. Shanker and Dr. L. Campbell for all your helpful inputs and for agreeing to serve on my masters committee.

A thank you is also in order for Gary Dexter and my classmates Lynn G., Michael A., Nate K. and Rodolph S. for cheering me up and supporting me throughout the two years. A big thank you to Brian G., Chien .H and Andrew T. for helping me with the experimental set up and assisting me with the codes. Thank you to Dr. John E. Ross, for allowing me to use GA-NEC for my simulations and also for providing helpful input. Another thank you to the MSU ECE shop for fabricating the STEMS.

A special acknowledgment to my parents, Justin and Charlotte O., for their tremendous sacrifice to get me where I am, and for their unconditional love and support. Also to my in-laws and Ms. Julie K. who have loved and supported me as their own throughout my studies. My deepest gratitude is reserved for my wife, Clarice O., who has always been understanding and supportive of me throughout my studies. Without your help and support, all this would not have been possible. You are my angel and I love you with all my heart.

TABLE OF CONTENTS

LIST OF TABLES

LIST OF FIGURES

Images in this thesis are presented in color

KEY TO SYMBOLS AND ABBREVIATIONS

- STEMS: Self Tuning Electromagnetic Shutter
- GA: Genetic Algorithm
- NEC: Numerical Electromagnetic Code
- GA-NEC: Genetic Algorithm based Numerical Electromagnetic Code
- NI-DAQ: National Instrument Data Acquisition
- MEMS: Micro Electromechanical systems
- EAR: Equal Area Rule
- LAPACK: Linear Algebra PACKage
- FACTR: Linear Algebra Factor
- MoM: Method of Moment
- EFIE: Electric Field Integral Equation

CHAPTER 1

INTRODUCTION

Genetic algorithms (GAs) are a special class of evolutionary computational schemes that have been utilized for a variety of applications in electromagnetics, such as designing self-structuring antennas (SSA), and frequency selective surfaces (FSS). Combining the ideology of SSA and FSS, a new class of electromagnetics devices called self tuning electromagnetic shutter (STEMS) is introduce in this thesis.

STEMS is a slotted metallic surface capable of adjusting its transmissivity through the use of computer-controlled switches. In particular, the surface may be placed into open and closed states, creating an electronically-controllable iris. Though similar to the idea of reconfigurable filters, the fundamental differences between STEMS and those existing devices will be shown in the literature review contained in chapter 2. The chapter also provides the theory behind the operation of STEMS along with their conceptual design.

A cavity approach has been undertaken to analyze the performance of STEMS and chapter 3 provides detailed coverage of this approach, as well with an insight into the wire grid modeling of closed conducting surfaces using the Numerical Electromagnetic Code 4 (NEC4).

Chapter 4 presents a detailed coverage of the steps followed to design the final STEMS template, along with a detailed analysis of the results obtained from the simulation of the STEMS.

Chapter 5 presents a prototype STEMS built at Michigan State University, including experimental results attesting of the capability of STEMS to attain both open and closed states over a broad frequency range through the use of the genetic algorithm. Chapter 5 also provides an insight into the random distribution of states within a random sample space of 50000 at various frequencies.

A conclusion to this thesis is given in chapter 6, in addition to possible future work.

Finally, appendix A provides a description of the genetic algorithm and random search codes that are used to analyze the STEMS.

CHAPTER 2

CONCEPT AND THEORY

2.1 Introduction

It is important to point out that at the start of this project there was no specific literature on devices capable of electronically creating both transparent and opaque surfaces. Microwave filters such as frequency selective surfaces (FSS), though fundamentally different from STEMS, were the only devices slightly similar. As a results, they will be referenced frequently in this chapter.

Traditionally, electromagnetic filters such as FSS are planar structures made of periodic metallic screens, usually backed by a dielectric slab. When exposed to electromagnetic waves, the metallic screen, made of unit cells, resonates at frequencies depending on both the characteristics of the substrate and the geometry of the unit cells [1]. These devices can be made to behave as lowpass, highpass, bandstop, or bandpass filters. In order to achieve the desired results, several variables have to be taken into consideration in the design process. For instance, the shape, spacing and orientation of the metallic elements, along with the dielectric properties and thickness of the substrate, have to be simultaneously adjusted prior to being used as a filtering device on a reflector antenna.

Even though coupling with the reflector antenna itself and other devices present at the vicinity of the filter can be taken into consideration during the design process, there is still the effect of environmental conditions and unforeseen elements. These

effects can adversely impact the performance of the filter, rendering it useless in the current condition. To solve this problem, techniques such as the use of varactors, micro-electromechanical systems (MEMS) and optimizers have been employed by several authors [21]-[24] to design broadband and multiband filters.

This thesis introduces a different type of planar surface with a new concept that combines the ideology of the filters explained above with the concept of self structuring antennas (SSA). The introduced surface, referred to as self tuning electromagnetic shutter (STEMS), is capable of creating both open and closed surfaces for various angles of incidence over a broad range of frequencies. A STEMS is a non-periodic slotted metallic surface with computer-controlled electro-mechanical switches placed across the slots. By turning the switches on and off, the transmissitivity of the surface can be adjusted to be transparent or opaque to incoming waves.

In section 2.2 of this chapter, the concept of STEMS is explained while the STEMS template is discussed in section 2.3; sections 2.4-2.6 discuss the remaining elements associated with the STEMS operations that are the receiver, microprocessor and the search algorithm. This chapter also provides a review of the literatures that helped provide insight into the current project.

2.2 STEMS design concept

In this section, the concept of STEMS design is presented. A grid of unidentical metallic patches interconnected by electromechanical switches represents the stems template. By changing the states of the switches, the electrical characteristics of the surface can be adjusted into open and closed states at any given frequency. To

determine the performance of each STEMS template configuration, the STEMS is used to seal the opening of a conducting box that contains a probe connected to a receiver. The term *configuration* is used in this thesis to represent the combination of 'on' or 'off' states of the switches.

The probe within the box is used to measure the level of signal that passes through the STEMS. The receiver in turn provides a feedback signal to a computer that analyzes the received signal and uses an evolutionary computational scheme (a genetic algorithm in this case) to generate a new switch configuration. The main goal of the STEMS is very simple: to successfully model a transparent or opaque surface at any desired frequency by changing the switch configurations. A block diagram of the STEMS is shown in Figure 2.1 and a detailed explanation of each component is provided in the following sections.

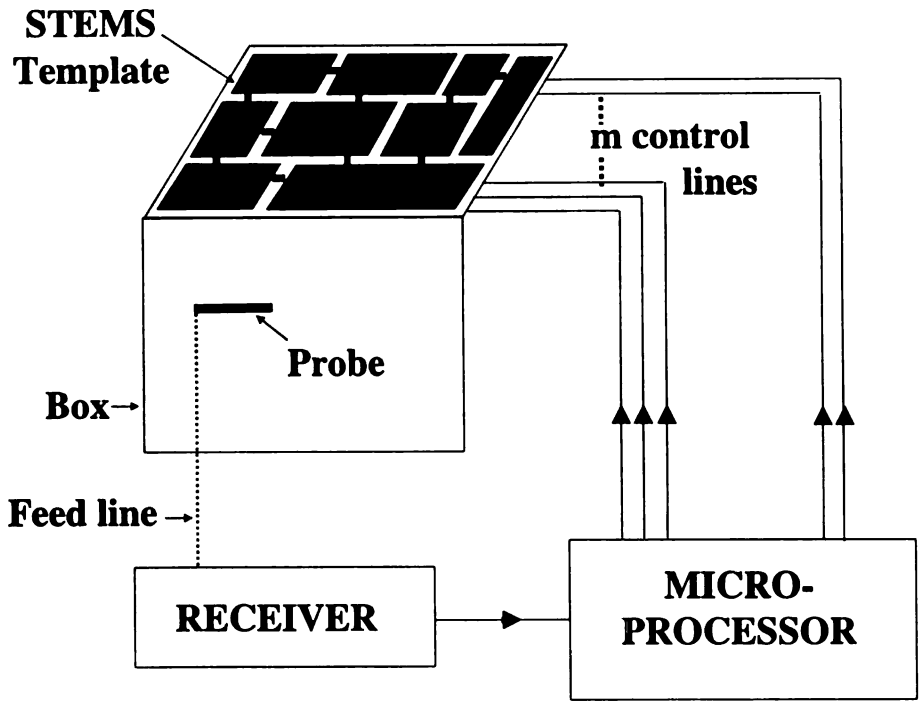

Figure 2.1. Block Diagram of STEMS

2.3 Self Tuning Electromagnetic Shutter Template

The STEMS template as shown in Figure 2.2 is the main building block of the system. It is a slotted metallic surface composed of unidentical patches interconnected by a matrix of controllable switches. A switch can be set to a 'on' or 'off' state, and a template using n switches can be arranged into a total of (2^n) switch configurations. Since the switches are used to connect the patches, by turning the switches on or off, the current flow through neighboring patches changes, altering the electrical characteristics of the surface. Another view is that the switches control the electrical length of the slots, hence determining the field transmitted through the slots The switches on the surface are purposely placed in an asymmetric manner to avoid instances of different switch configurations yielding the same frequency response. This guarantees a unique template configuration for every set of switch states.

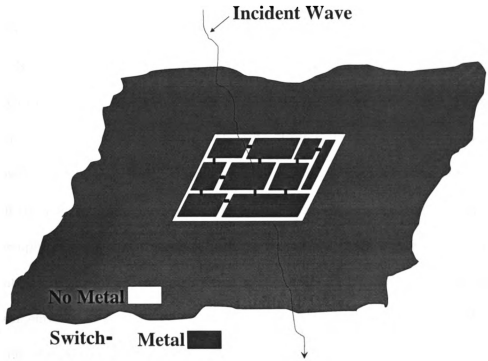

Figure 2.2. Self Tuning Electromagnetic Shutter

2.4 Box and Probe

The Box and the probe are important components used to test the STEMS. The box is made of six continuous metallic walls that provide complete shielding against incoming plane waves. The probe is a monopole antenna located inside the box and used to receive signals from the outside. When all six walls of the box are present, the probe is completely shielded from all incoming electromagnetic waves and unable to receive signals. The box and probe have been designed using the numerical electromagnetic code (NEC4) and chapter 3 provides a detailed explanation of the design process.

To evaluate the performance of the STEMS, one of the sides of the box is removed and the probe is used to measure the strength of the incoming plane wave. The open box is then sealed with the STEMS template as shown in Figure 2.3 and the received signal strength on the probe is measured for various switch configurations. The ratio of the open box signal to the signal from the box sealed with the STEMS determines the ability of the stems to create either an open or closed surface. Simulated and experimental results shown in chapters 4 and 5 demonstrate that the STEMS is capable of performing efficiently in an open, closed or intermediate states for various frequencies and angles of incidence of incoming waves.

It should be noted that this is not the only way to test the STEMS. It could be used in many different applications that do not include boxes. The box technique is selected because it is easy to implement and sufficient to prove the concept of STEMS.

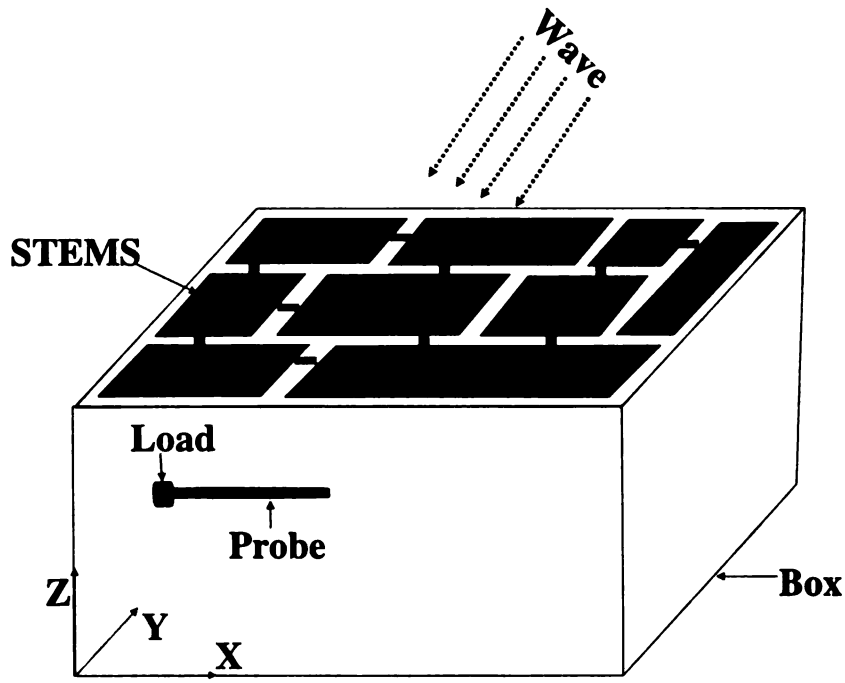

Figure 2.3. Box with probe covered by a STEMS

2.5 Receiver

To configure the STEMS, a feedback signal is required to ascertain its performance. For the test configuration shown in Figure 2.1, the feedback signal is the probe current as measured using a receiver. A receiver such as a vector voltmeter or field intensity meter can be used to measure the induced current on the probe for a given optimized switch configuration at a single frequency. More sophisticated devices such as network analyzers can then be used to obtained a sweep of the induced current over a broad frequency range. Network analyzers can also be used to optimize the STEMS at multiple frequencies, although this is not implemented in this thesis. The quantity measured by the receiver is then sent to the microprocessor for processing. Every subsequent switch configuration depends on the value of the quantity measured by the receiver and extra care should be put toward proper calibration of the receiver.

2.6 Microprocessor

The microprocessor represents the control unit of the STEMS structure and all the computations are made here. The information sent by the receiver is quantified by the microprocessor and used to determine the subsequent switch configuration. In order to optimize the switch setting to meet the requested design criteria, the microprocessor is programmed with an evolutionary search algorithm. In the present work, a laptop is used to perform all the duties of the micro processor and a genetic algorithm is used as the search algorithm. The computer communicates with the receiver and the STEMS template using the National Instruments data acquisition driver software NI-DAQ.

2.7 Search Algorithm

A robust and efficient search algorithm is essential to the operations of STEMS. It determines how fast the STEMS can find a template configuration capable of yielding the desired characteristics at any given frequency and angle of incidence. For a template with n switches, there are 2^n possible configurations. As the number of switches (n) is increased, the number of possible configurations increases quickly to overwhelming values. As an example, a template with 16 switches has a total of $65,536$ possible switch configurations while doubling the switch number to 32 leads to $4,295,000,000$ switch configurations. With such numbers, coupled with the time it takes to measure the frequency response associated with each switch configuration, doing an exhaustive search might take months. A random search could be implemented to find acceptable states among all possible configuration but, as its name implies, the search is random and might take a long time to find a configuration with the required characteristics. As a result, a robust self evolving computational scheme becomes indispensable for quickly finding the needed switch configuration. Since it is fairly simple to represent the two states of each switch with a binary string, a binary genetic algorithm has been investigated as the search algorithm for the STEMS. An in depth description of the genetic algorithm is provided in chapters 4 and 5.

2.8 Literature Review

A Self Tuning Electromagnetic Shutter is a new class of electromagnetic devices capable of exhibiting characteristics of both a closed and open surface. It combines

the ideology of self-structuring antennas [26]-[32], with the concept of microwave filters such as frequency selective surfaces [1]. Frequency selective surfaces are devices that were first introduced in the late 1950s at the Ohio State University [1]. The concept was generated from an Air Force program focused on investigating tuned surfaces capable of limiting the range of frequencies over which an antenna would be a principal source of echo. Dr. B. A. Munk approached the issue by combining the basic physics of interaction between elements with the Moment of Method principles, leading to the idea of FSS. Classical FSS used as electromagnetic filters are planar structures composed of an assembly of periodic metallic elements called unit cells, usually backed by one or several dielectric layers Figure 2.4.

The frequency response of the FSS depends on the geometry of the unit cell and its properties depend on the mutual interactions of the periodic elements. Therefore, to observe a desired frequency response, a large number of unit cells must be present. When the FSS is illuminated by an incoming wave, it behaves as a band pass or band stop filter, depending on the type of elements used and their frequency of resonance. Band pass characteristics are obtained by using slot elements while band stops are obtained via the use of dipole type elements.

This marks a very profound difference from the concept of STEMS, where a single surface, made of non identical elements can be tuned at any desired frequency to exhibit both open and closed surfaces with narrow or broad band characteristics. It is also important to note that the overall size of the STEMS may be small compared to the electromagnetic filters mentioned above. The electrical length of the STEMS

presented in this thesis is approximately $\frac{\lambda}{2}$ at its lowest operational frequency. This dimension represents the electrical length of a single FSS unit cell and a matrix of several unit cells has to be employed to get the desired frequency response

Traditional FSSs suffer from the fact that they are narrow band and exhibit a single stopband or passband characteristic. Intensive work has been put forth toward designing multiband FSS. One technique used by several authors[2]-[8] has been to take advantage of multiple resonant elements such as fractal antennas and multi rings or loops. Using such elements as unit cells of the periodic surface enables for the design of band pass or band stop filters with resonances equivalent to those of the elements.

Another technique used to obtain multi-resonance is to use a multi layered or stacked FSS [1], [9], [10]. In this approach two or more FSS screens backed by dielectric layers are used to obtain multiband characteristics or to improve other design specifications. A combination of both techniques has also been presented as a successful method of achieving multiband characteristics.

Even though desired frequency response can be obtained with these techniques, it comes at a high cost of time consuming trial and error analysis in simultaneously tuning the elements of the periodic surface (shape and spacing between elements) and the characteristics of the dielectric.

To avoid the strenuous process of selecting the proper variables, such as unit cell element shape, spacing between elements, orientation and dielectric properties, genetic algorithms have been used as search algorithms to synthesize the design of FSS [11]- [15]. This process still suffers from the fact that the designs are final and

they lack the ability to adapt to changing conditions such as interactions with other devices or environmental effects.

Lumped elements and MEMS, in combination with search algorithms have been used as a way to design reconfigurable frequency selective surfaces [16]-[25]. Though frequency tunability is obtained through these techniques, the concept and design is the same as that of classical FSS, therefore, they are still fundamentally different from STEMS.

One of the most crucial elements to the understanding of STEMS is the concept of self structuring antennas (SSA). They were were first introduced by Dr. E. Rothwell and his team at Michigan State University [26]. SSAs are antennas made of an arrangement of wires or patches interconnected via switches Figure 2.5 . By changing the states of the switches, the electrical characteristics of the antenna are changed as well [26]-[32]. The switches are controlled via a microprocessor that uses an optimizer to determine the best switch state that will produce the desired antenna properties. This new methodology has been proven to yield excellent results and the same approached is used in this thesis.

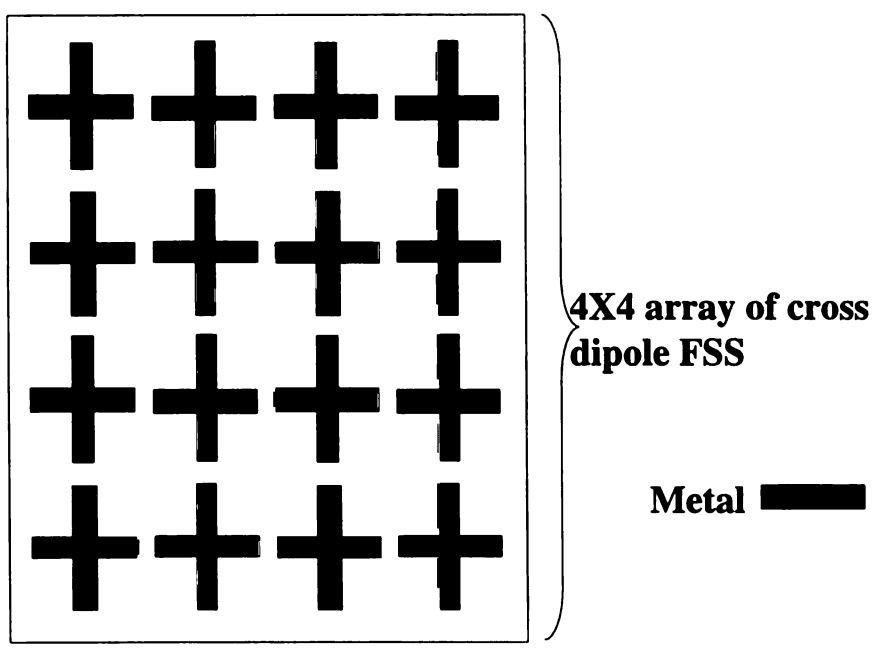

Figure 2.4. Frequency Selective Surface

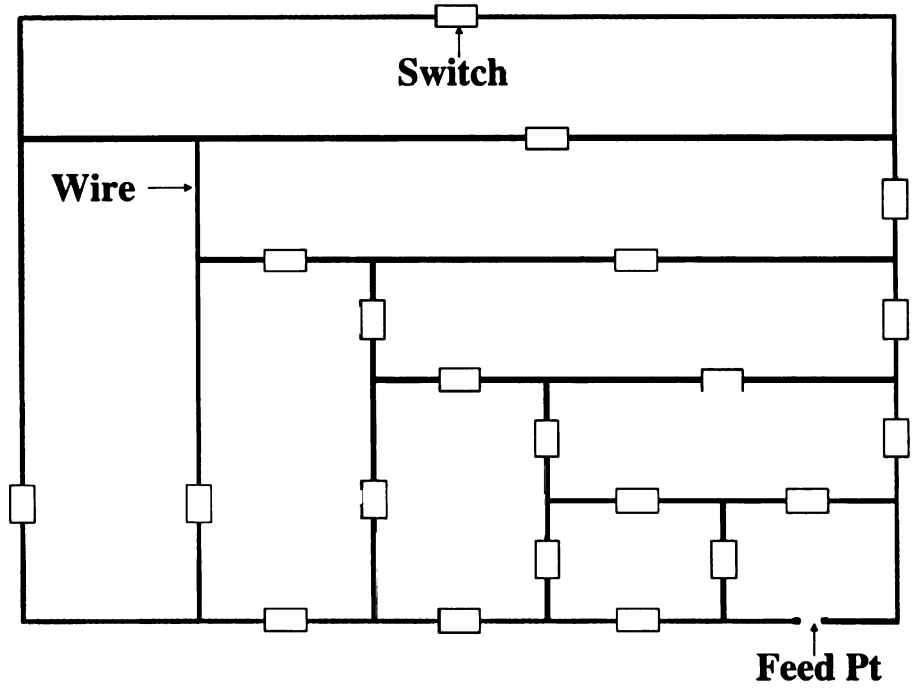

Figure 2.5. Self Structuring Antenna

2.9 Conclusion

In this chapter, the concept and theory of self tuning electromagnetic shutters is presented. A discussion of the concept of STEMS is presented in section 2.2 while the fundamental components along with a block diagram of STEMS are provided in sections 2.3-2.7. A literature review showing the different ideologies used to generate the concept and design methodology of STEMS is also presented in section 2.8.

The next chapter presents in detail the approach used to analyze the performance of STEMS.

CHAPTER 3

NEC4 OVERVIEW AND BOX DESIGN

3.1 Introduction

To analyze the effectiveness of the self tuning electromagnetic shutter, a closed conducting box containing a probe is designed. One of the sides of the box is removed and the probe is used to measure the signal strength of an incoming plane wave as shown in Figure 3.1. The open box is then sealed with the STEMS template as shown in Figure 3.2 and the received signal strength on the probe is measured for various switch configurations. The ratio of the open box signal to the signal from the box sealed with the STEMS determines the shutter effectiveness to either shut itself or to be transparent to incoming waves.

To ensure accuracy in the results, it is crucial that the designed box effectively shields the probe within its interior from external fields. To simulate the STEMS, box, and probe, an electromagnetic simulation package developed at the Lawrence Livermore National Laboratory [33] called NEC4 (Numerical Electromagnetic Code, version 4) is selected. This chapter presents modeling guidelines for NEC4 along with the designed box and simulated results of its effectiveness.

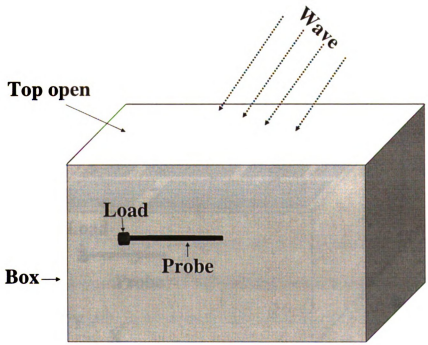

Figure 3.1. Box with top open

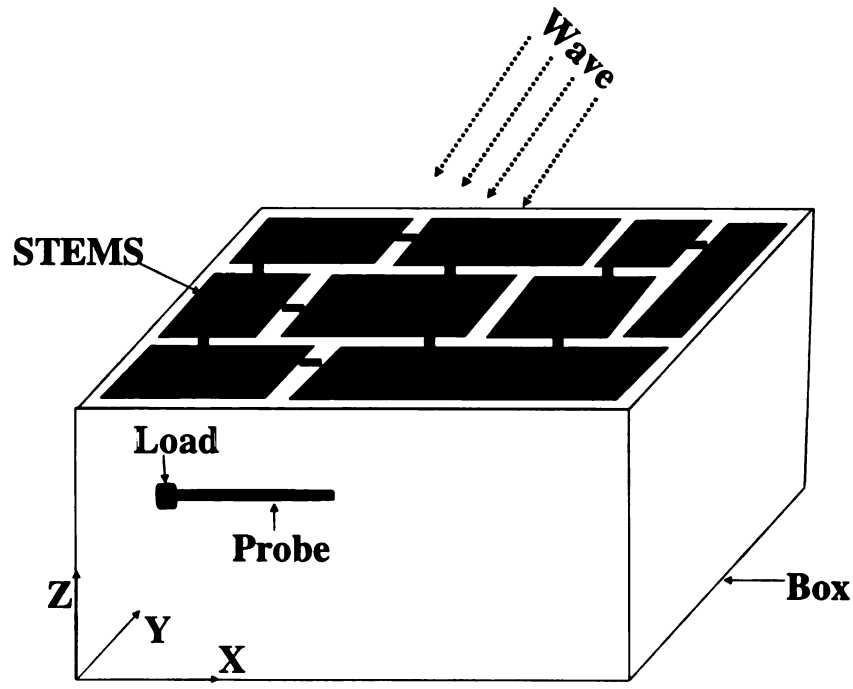

Figure 3.2. Box with top covered by a STEMS

3.2 NEC4 Modeling Guidelines

NEC4 is a method of moments computer program for analyzing the electromagnetic response of antennas and scatterers. It utilizes the electric field integral equation for modeling thin wires and the magnetic field integral equation for modeling closed perfectly conducting surfaces. The code has been used throughout the years with great success in the analysis of various complex geometries including ships, airplanes and automobiles, [36] - [39]. Modeling objects in NEC4 can be done using wires or surface patches depending on the characteristics of the structure being analyzed. Surface patches are only used in NEC4 to model closed perfectly conducting surfaces while a wire grid model is used for all open surface models [33]. STEMS are not perfectly closed conducting surfaces because of their slotted aperture. Therefore, only the wire grid model is used in this section.

Wire modeling in NEC4 involves both electrical and geometrical factors. Every wire in the model is parsed into several segments and each wire segment is defined by its radius, a, and its length, Δ, as shown in Figure 3.3. Electrically, the most crucial aspects are the ratios of each segment length to its radius, and to the wavelength λ. Generally, the value of Δ is selected to be 0.1λ or less at the center frequency, but smaller values of Δ with $\Delta \leq 0.05\lambda$ are required for modeling critical regions such as corners. Selecting the appropriate segment radius is relative to the conditions imposed by the thin wire approximation kernel used by NEC4. This approximation imposes the condition that the wire radius is selected such that $\frac{2\pi a}{\lambda} << 1$. Under these conditions, every wire is reduced to a current filament on the axis of the wire;

this assumes that the current is uniformly distributed around the circumference of the wire and only the axial component of the current is considered.

For a single thin wire of axial path Γ the axial current $I(u)$ due to an incident field $\vec{E}^S$ can be determined by solving the electric field integral equation (EFIE) given in Eq-3.1 of [40] as

$$\int_\Gamma [\frac{\partial I(u')}{\partial u'}\frac{\partial}{\partial u} + k^2(\hat{u}\cdot\hat{u}')I(u')]g(u|u')du' = -\frac{jk}{\eta}\hat{u}\cdot\vec{E}^i(u), \tag{3.1}$$

where the term $g(u|u')$ represents the reduced Green's function kernel of the integral equation

$$g(u|u') = \oint f(s')\frac{e^{-jkR(0,u|s',u')}}{4\pi R(0,u|s',u')}ds' \tag{3.2}$$

When the conditions imposed on the radius a and the segment length Δ are met, Eq-3.2 can be simplified by using the approximated reduce Green's function given by

$$g(u|u') = \frac{e^{-jkR(0,u|s',u')}}{4\pi R(0,u|s',u')}. \tag{3.3}$$

It was found in [40] that the error introduced by using the thin wire approximation in computing the current on the wire is related to the ratio $\frac{\Delta}{a}$ and is given by

$$\frac{d_u - d_{1u}}{d_u} = \frac{(a/\Delta)^2}{4ln(2\Delta/a)}. \tag{3.4}$$

A plot of the error introduced for various values of Δ/a is shown on Figure 3.4. Analyzes of this plot shows that a minimum value of $\frac{\Delta}{a}$=3.55 is needed to maintain the error below 1%.

Several authors have successfully used previous versions of NEC4 to model continuous conducting surfaces by use of a wire grid model and it is found that optimum results can be obtained for a value of $\frac{\Delta}{a}$=2π, [41]-[43]. This observation is known as the equal area rule (EAR), and it states that the surface area of the segments in the grid should be made equal to the surface area of the solid surface being modeled as demonstrated in Figure 3.5. Using the equal area rule as a reference, the next section discusses the design of the Box using NEC4.

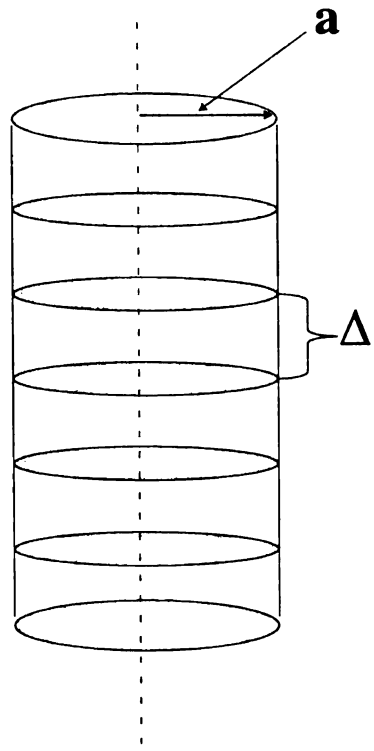

Figure 3.3. Wire segmentation

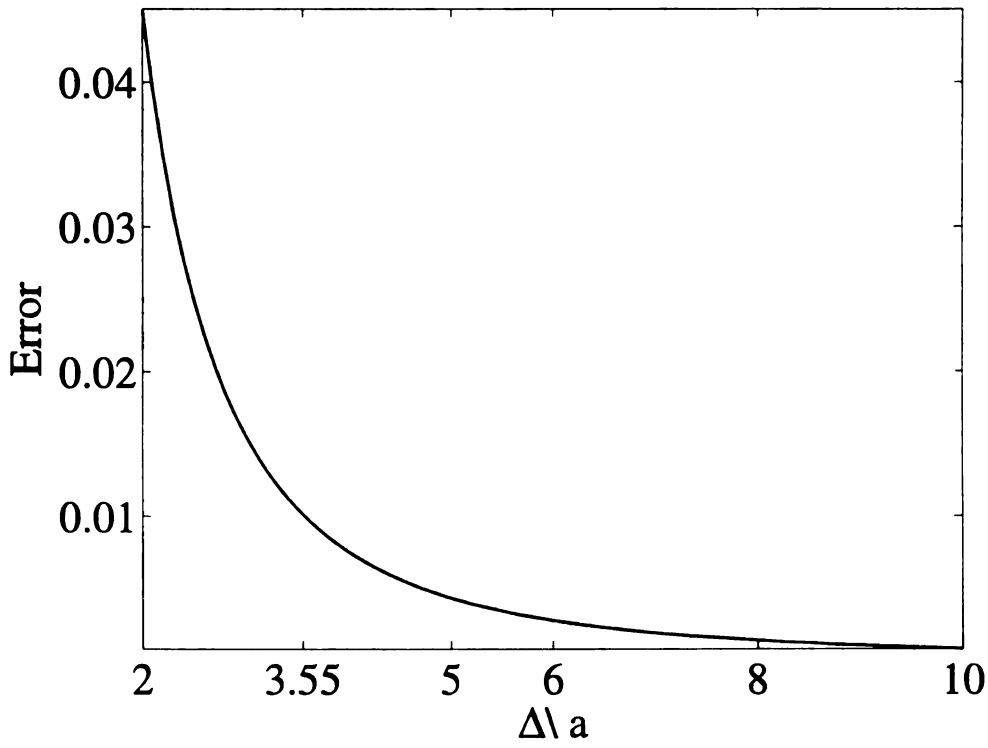

Figure 3.4. Thin Wire Approximation error

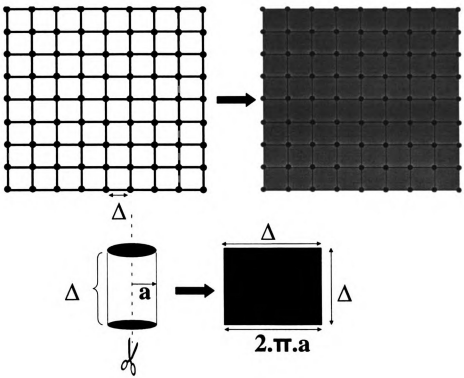

Figure 3.5. Equal Area Rule Representation

3.3 Box Design

As discussed in section 3.1, the shutter effectiveness of the STEMS can be determined through the use of a box. By mounting the STEMS template on the opening of a box, a probe is used to measure the intensity of the field that passes through the STEMS template into the box. The box is defined by its width W, its length L and height H. It is made of 6 continuous conducting surfaces and each surface is represented as an array of identical wire grids as shown in Figure 3.5.

Modeling the continuous conducting surfaces of the box using wire grids introduces a number of variables that could affect both the accuracy and simulation time. With reference to section 3.2, the accuracy of the simulation depends on the values of the segment radius, a, and length, Δ,. Every wire is parsed into multiple segments and the total current is determined by computing the currents at the centers of all the segments. As a result, increasing the number of segments per wire leads to better accuracy but also an increase in the total computation time.

It is important to mention that the total number of segments used to model a box of arbitrary dimensions does not need to change if the dimensions of the box are changed. This can be proven by referring to the discussion on cavities provided in [40] and [44]. By analogy to the cavity, the resonant frequencies of the box are dependent on its dimensions (H, W, L) as given by

$$fr = \frac{c}{2} * \sqrt{(\frac{m}{H})^2 + (\frac{n}{W})^2 + (\frac{p}{L})^2}, \tag{3.5}$$

where the integer values m, n and p determine the modes of the box being excited

and c is the speed of light in vacuum. By utilizing the relationship $\lambda = cf_r$, it is observed that a change in the resonant frequency also leads to a change in the wavelength λ. Therefore, for any given box the ratio $\frac{\Delta}{\lambda}$ can be kept the same as the dimensions of the box are changed just by altering the length of the segments Δ.

In order to determine an optimum $\frac{\Delta}{a}$ ratio suitable for the analysis of the STEMS template, various cubical boxes, $W = L = H$, with different wire radii but identical segment length have been designed. Each cavity has a side length of $L = 29.3cm$ and segment length of $\Delta = 9.75cm$. Those dimensions give a total of 28 segments per wire and 9408 segments for the whole box. The reasons for selecting $L = 29.3cm$ are explained in chapter 5.

Given those dimension and using Eq-3.5, the resonant frequency of the dominant TE_{101} mode is determined to be $777.04MHz$ with $\lambda = 38.6cm$. This yields a $\frac{\Delta}{\lambda}$ ratio of 0.025, well below the value of 0.05 mentioned in [33]. It should be pointed out that analysis at close proximity of the resonant frequency are not considered in this thesis because of the properties of cavities at resonance. In [33] and [44], it is shown that at resonance, the computed total E-field inside a cavity is inaccurate due to the singularity of the EFIE. To verify this statement with the box, the total E-field due an incoming normal incident field with magnitude $1V/m$ is evaluated within a cubical box designed using the equal area rule with $\frac{\Delta}{a}$=6.283 and $L = 29.3cm$. The characteristics of the normal incident wave are given in Table 3.1.

For a perfectly conducting box, the total field within its interior would be zero at all frequencies. In the case of this study, the box designed is a model made of wire grids and therefore, the total field within its interior would not be zero. Analysis of

the total Ex-field magnitude plotted in Figure 3.6 reveals a total field with magnitude near zero at lower frequencies until $770MHz$ where the magnitude starts to increase and suddenly peaks to $9.5V/m$ at $777.04MHz$ before it decreases back down to near zero. The readings of the total field around $777.04MHz$ are inaccurate, given that the incoming field intensity is only $1V/m$. As a result of these observations, frequencies near to the resonance value of $777.04MHz$ are not considered in this study. The term 'box effectiveness' is used throughout the thesis to represent the ability of the box to prevent electromagnetic fields from leaking through its surface.

Wave description		
Incidence	Incidence Angle (degrees)	Magnitude(V/m)
Normal	$\theta = 0, \phi = 0$	1

Table 3.1. Description of the field used to excite the box.

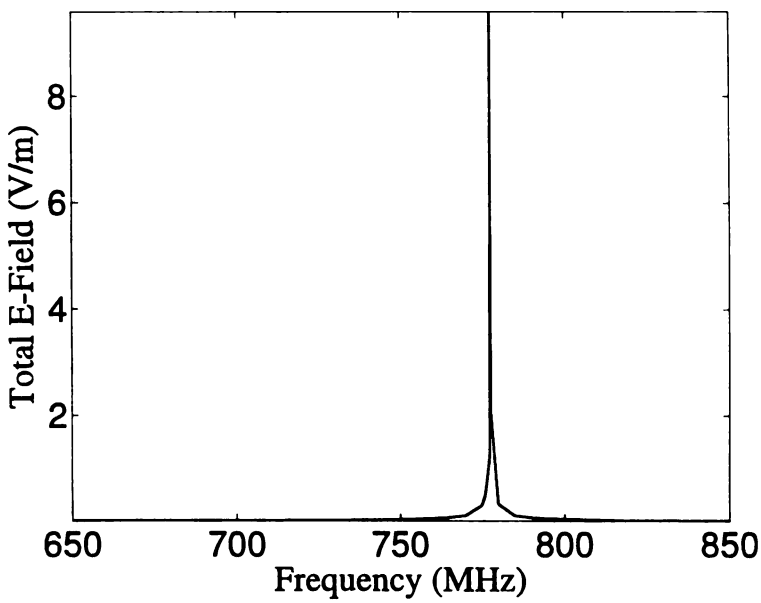

Figure 3.6. Total E-field of box designed using the EAR

To determine the value of the ratio $\frac{\Delta}{a}$ that provides the most box effectiveness, various boxes with identical segment length but varying radii are created and analyzed at frequencies ranging from 625MHz to 750MHz with frequency steps of 25MHz. Each box is loaded with a quarter wavelength monopole at the base and the entire structure is illuminated by the incident plane wave as described in Table 3.1. The current on each monopole is recorded for every box with and without the top surface for both normal and oblique polarization of the incident field. The box effectiveness (S) is evaluated in dB using,

$$S = 20 * log_{10}\frac{I_O}{I_C}, \tag{3.6}$$

where I_O is the current on the first segment of the probe, recorded for the box with no top surface and I_C is the current recorded for the box completely closed.

Considering the radius calculated from the equal area rule with a=$\frac{\Delta}{2\pi}$=0.155cm for $\Delta = 0.975cm$ as a reference point, 19 different boxes with radii ranging from $0.144cm - 0.162cm$ are designed and simulated at $750MHz$. The plot of the box effectiveness for normal polarization of the incident field is displayed in Figure 3.7 Analysis of this plot reveals a maximum reduction of $64dB$ obtained for a $\frac{\Delta}{a}$ ratio of 6.372 while the equal area rule ratio of $\frac{\Delta}{a}$=6.283 yields a maximum reduction of $62.18dB$.

Further simulations of the boxes at $725MHz$ reveal that a smaller ratio of $\frac{\Delta}{a}$ is needed for optimum shielding. Figure 3.8 shows a shift of the maximum box effectiveness provided by $\frac{\Delta}{a}$=6.372 to $\frac{\Delta}{a}$=6.17. The shielding obtained at $725MHz$

has a maximum value of $74dB$. This shift implies that boxes with smaller ratios of $\frac{\Delta}{a}$ are needed for analysis at lower frequencies.

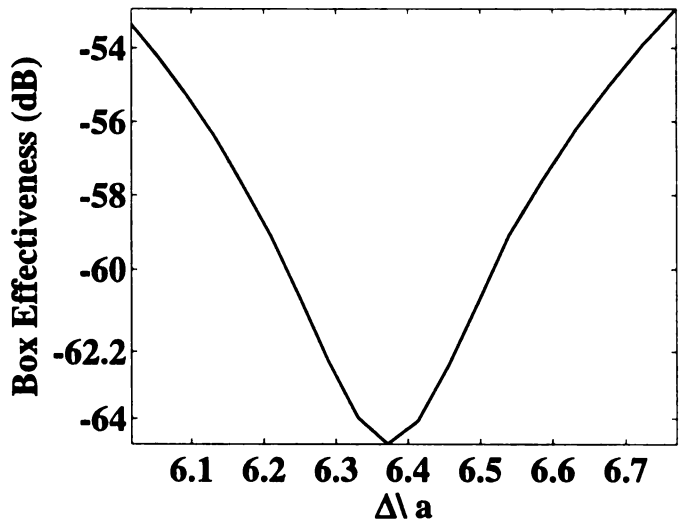

Figure 3.7. Box Effectiveness with different ratios of $\frac{\Delta}{a}$ at $750MHz$.

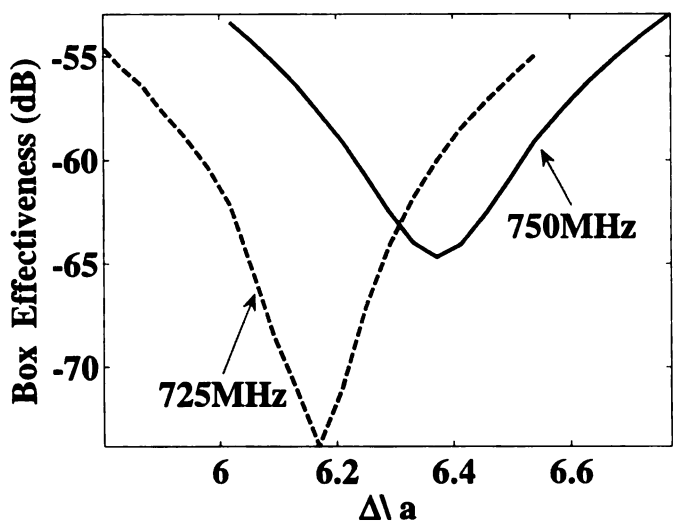

Figure 3.8. Box Effectiveness with varying $\frac{\Delta}{a}$ at 750MHz and 725MHz.

With regards to that observation, 42 boxes with varying $\frac{\Delta}{a}$ are simulated and their frequency response plotted in Figure 3.9 - Figure 3.12. As expected, as the frequency is lowered, the ratio of $\frac{\Delta}{a}$ has to be lowered as well in order to obtain optimum shielding. At every frequency considered, shielding of $60dB$ or more is obtained, with an outstanding shielding of $93dB$ found at $700MHz$ for $\frac{\Delta}{a}$=5.94. Considering $60dB$ to be an acceptable shielding value, it can be concluded that the wire grid model can adequately represent continuous conducting surfaces provided the right ratio of $\frac{\Delta}{a}$ is selected. The equal area rule did not provide the best box effectiveness but was essential as a reference point to determine better ratios as the frequency of interest is varied.

In order to determine the usable frequency range of each of the six boxes, a frequency sweep of each box is performed for a vertical incident E-field. Figure 3.13 shows a plot of the box effectiveness of each box as the frequency is varied. Still considering $60dB$ to be an acceptable box effectiveness value, close observation of Figure 3.13 shows that each box has a usable bandwidth of $50MHz$. Even though there are six boxes with $50MHz$ bandwidth, the overall bandwidth considering all six boxes is only $160MHz$ due to the overlapping.

The performance of each box for an incident field with oblique incidence is also evaluated and plotted as shown in Figure 3.14-Figure 3.19 but, as observed in [42], the box effectivenesses of all boxes designed are tremendously decreased for oblique incidence compared to normal incidence. Table 3.3 provides the characteristics of the normal and oblique waves used.

A list of the selected $\frac{\Delta}{a}$ ratios along with their respective box effectiveness for each of the six frequencies considered is provided on Table 3.2.

selected boxes characteristics				
Frequency (MHz)	*Radius* (mm)	Δ/a	a/λ	*Shielding* (dB)
750	1.53	6.37	0.0037	64.693
725	1.58	6.17	0.00381	73.819
700	1.64	5.94	0.00382	92.291
675	1.69	5.76	0.00380	73.904
650	1.74	5.60	0.00377	67.750
625	1.78	5.47	0.00370	63.233

Table 3.2. Best $\frac{\Delta}{a}$ ratios and their respective box effectiveness.

Wave description		
Incidence	Incidence Angles(degrees)	Magnitude(V/m)
Normal	$\theta = 0, \phi = 0$	1
Oblique	$\theta = 30, \phi = 60$	1

Table 3.3. Description of the two waves used to excite the boxes.

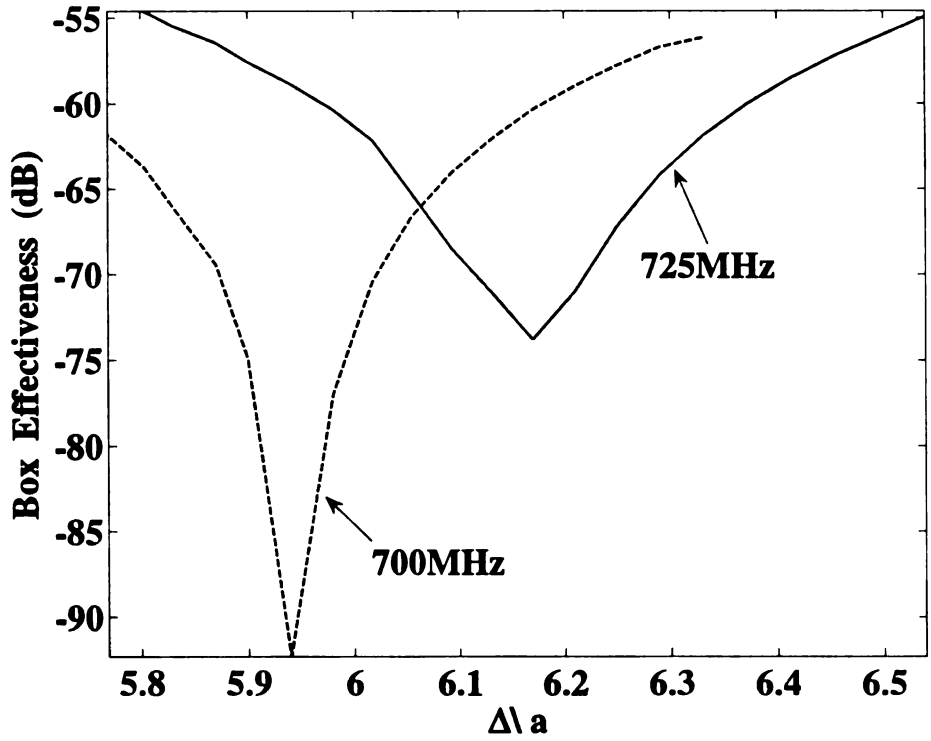

Figure 3.9. Box Effectiveness with varying $\frac{\Delta}{a}$ at 725MHz and 700MHz.

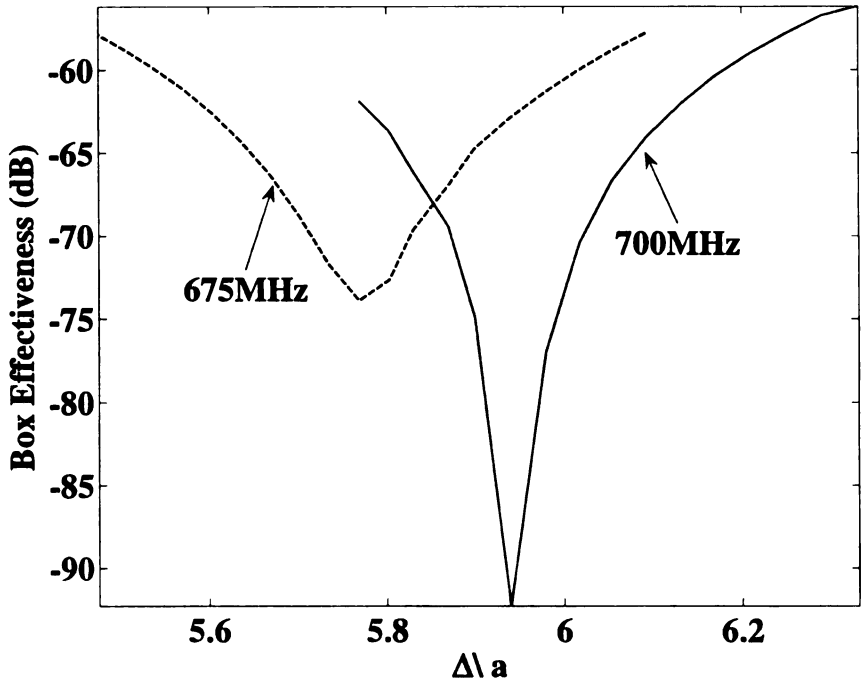

Figure 3.10. Box Effectiveness with varying $\frac{\Delta}{a}$ at 700MHz and 675MHz.

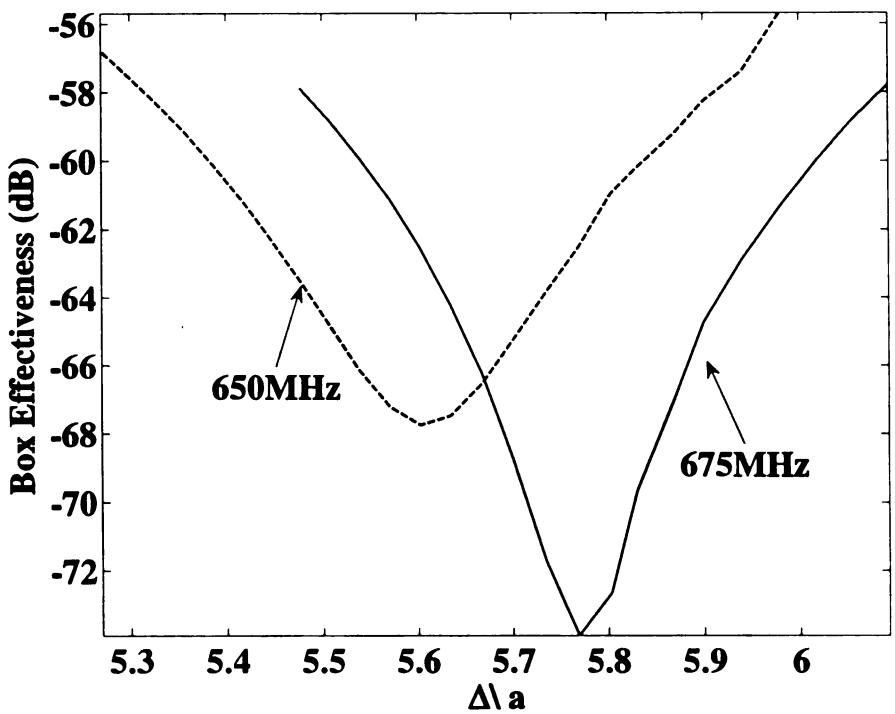

Figure 3.11. Box Effectiveness with varying $\frac{\Delta}{a}$ at 675MHz and 650MHz.

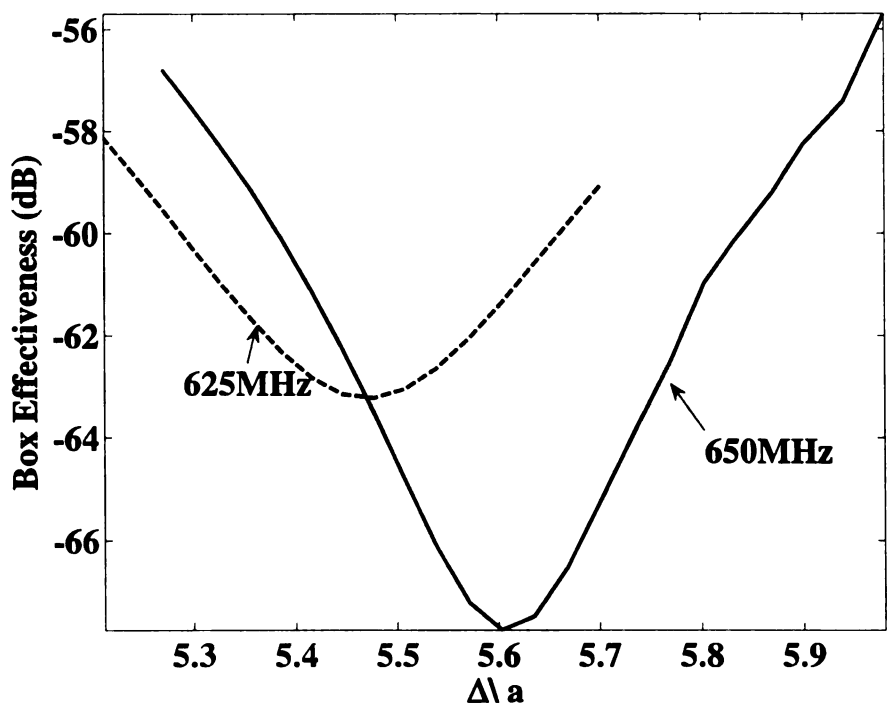

Figure 3.12. Box Effectiveness with varying $\frac{\Delta}{a}$ at 650MHz and 625MHz.

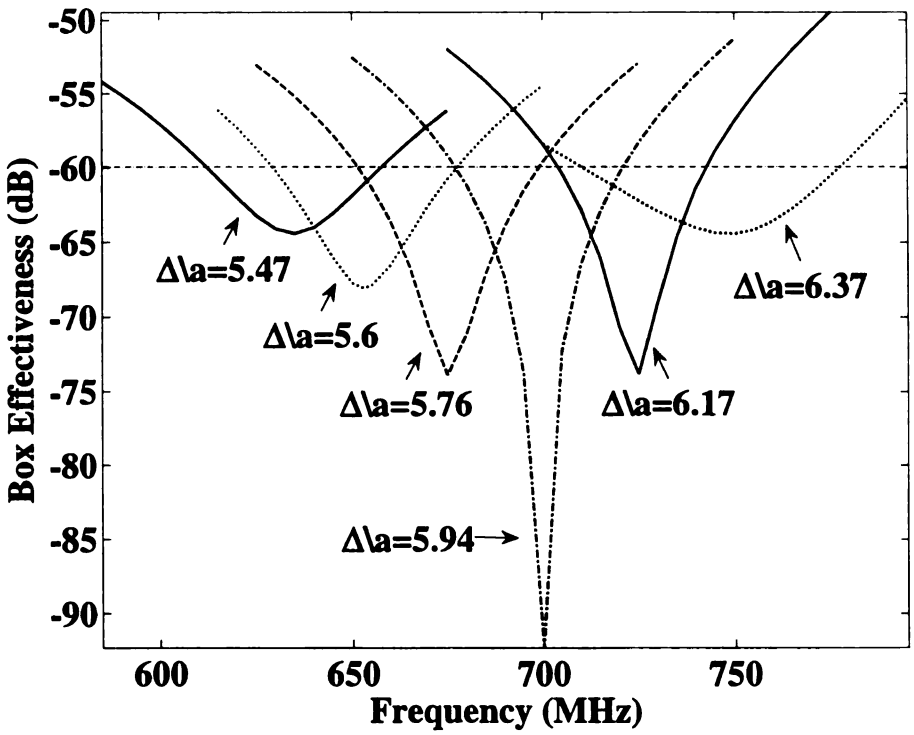

Figure 3.13. Box Effectiveness

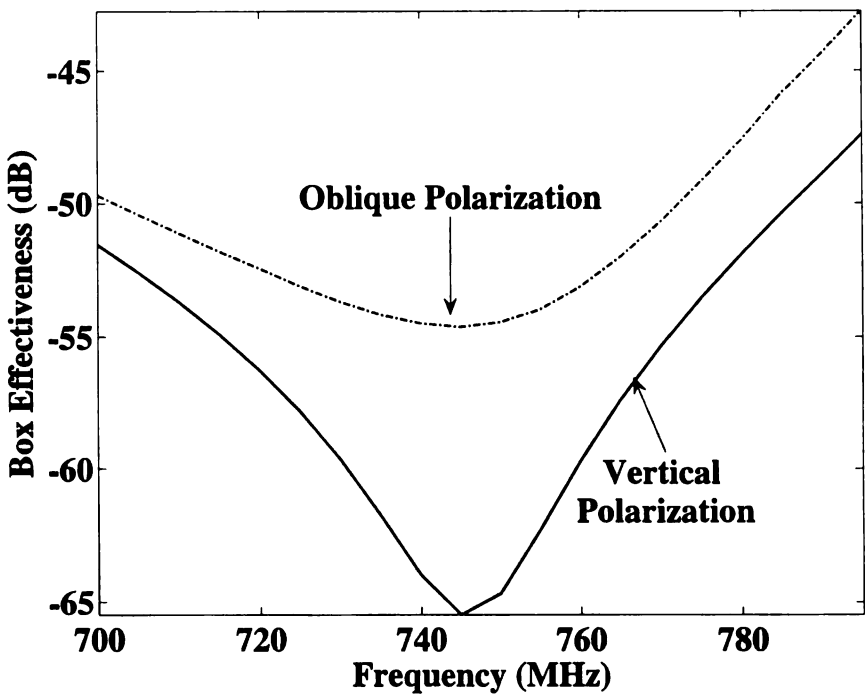

Figure 3.14. Box effectiveness for $\frac{\Delta}{a}$=6.37 for both normal and oblique waves

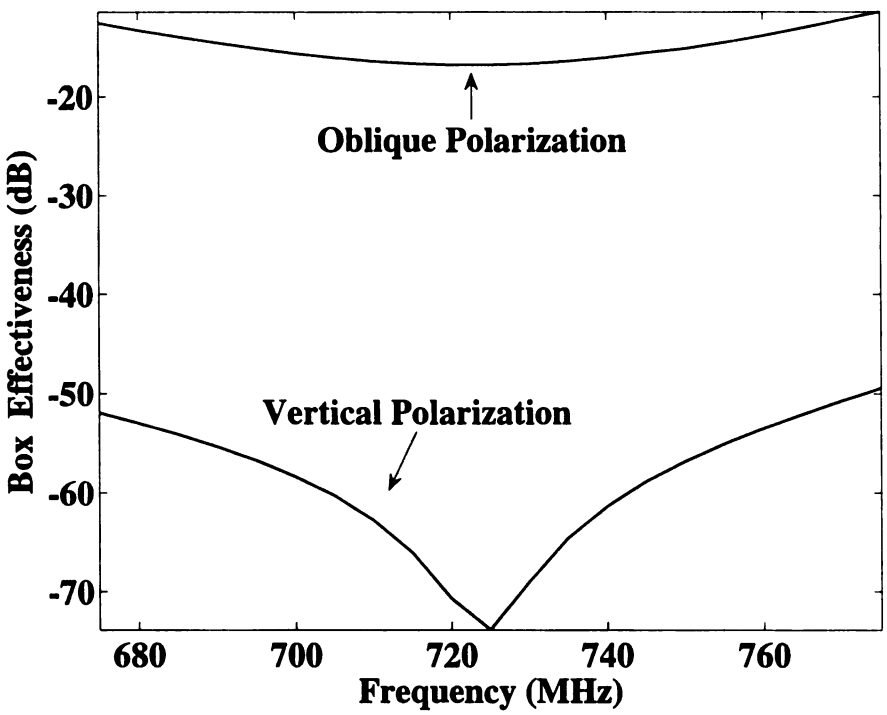

Figure 3.15. Box effectiveness for $\frac{\Delta}{a}$=6.17 for both normal and oblique waves

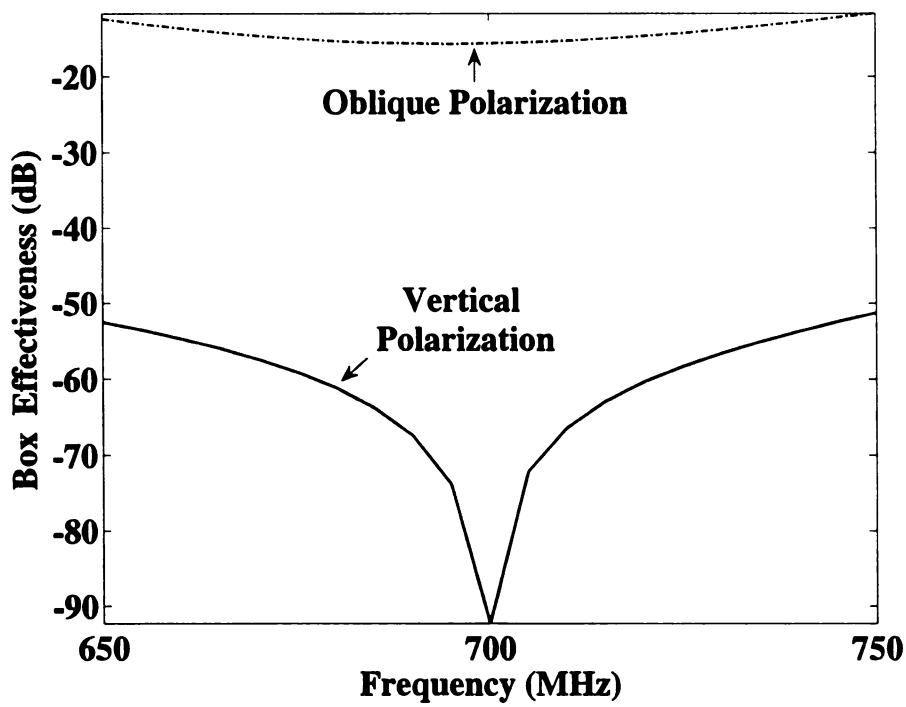

Figure 3.16. Box effectiveness for $\frac{\Delta}{a}$=5.94 for both normal and oblique waves

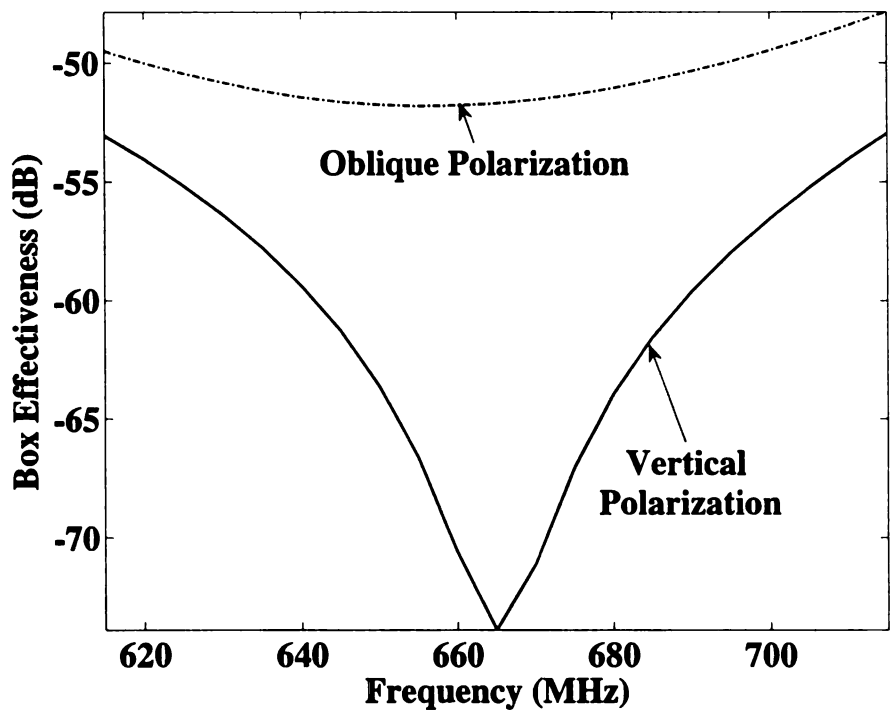

Figure 3.17. Box effectiveness for $\frac{\Delta}{a}$=5.76 for both normal and oblique waves

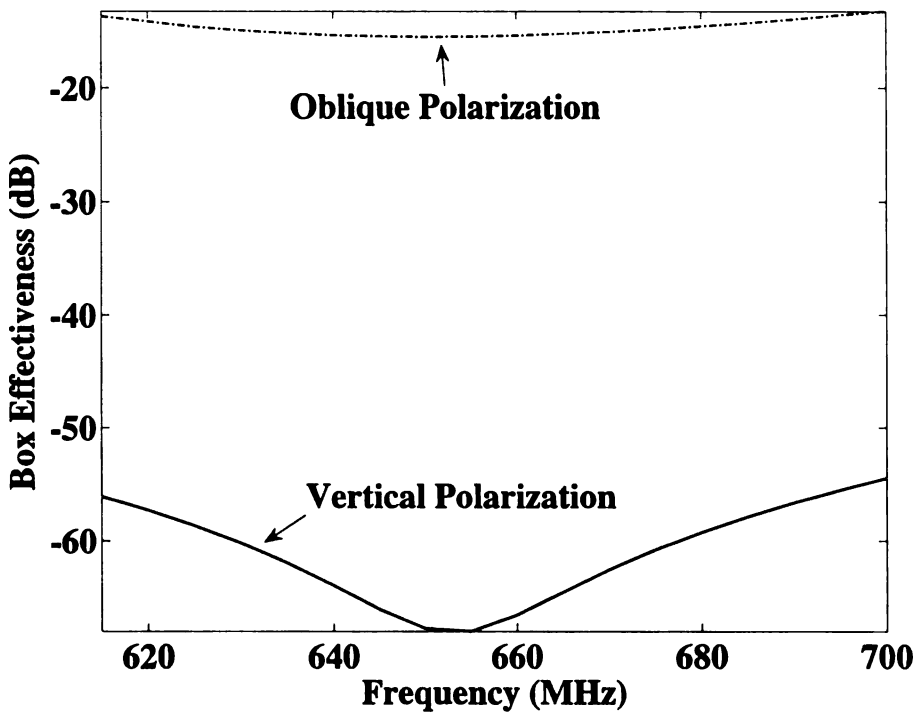

Figure 3.18. Box effectiveness for $\frac{\Delta}{a}$=5.6 for both normal and oblique waves

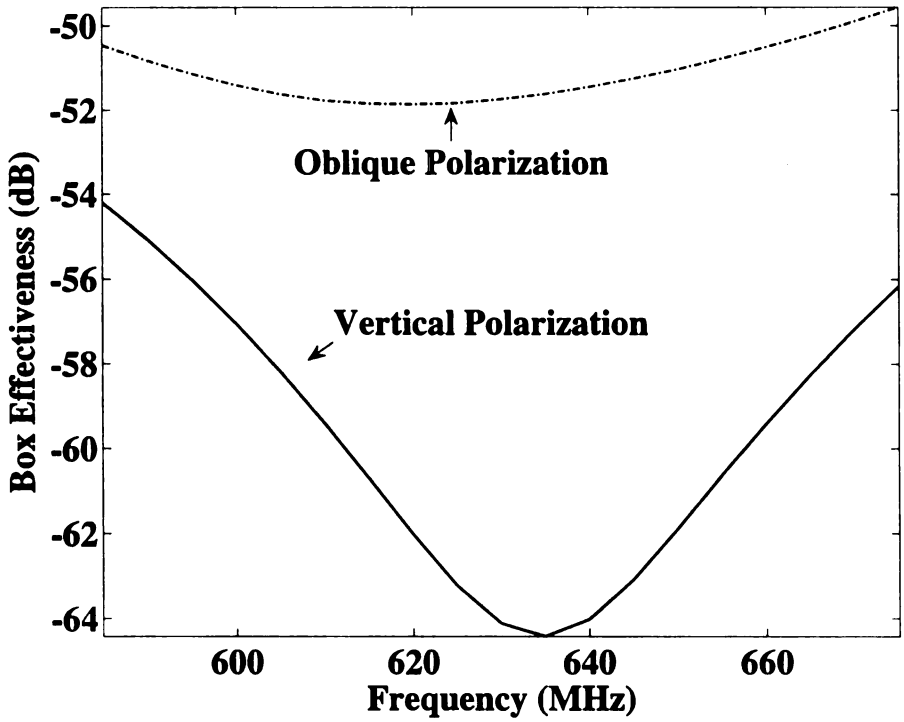

Figure 3.19. Box effectiveness for $\frac{\Delta}{a}$=5.47 for both normal and oblique waves

3.4 Conclusion

In this chapter, an overview of the numerical electromagnetic code, version 4, along with the design of the boxes used in STEMS simulations are presented. A discussion of the design constraints to be observed while using the electromagnetic simulation source code NEC4 is presented in section 3.2, while details of the design and simulation results of the boxes used to analyze the STEMS are presented in section 3.3. The next chapter presents in detail the design and simulation results of the STEMS template.

CHAPTER 4

STEMS TEMPLATE DESIGN AND SIMULATION RESULTS

4.1 Introduction

As a proof of concept of STEMS, intensive designs and simulations were conducted at Michigan State University. The selected STEMS template layout is created using a NEC geometry editor called 4NEC2 [46] and the input file is imported into GA-NEC for encoding and optimization. An overview of GA-NEC along with the optimization scheme and the switch model is given in section 4.2. A brief overview of the first STEMS considered is provided in section 4.3 while section 4.4 presents the details of the final design along with a discussion of the simulated results.

4.2 GA-NEC Overview and Switch Model

4.2.1 GA-NEC Overview

GA-NEC is a visual basic front end optimizer for NEC4. Dr. John Ross [34] created the software package by developing a genetic algorithm optimization tool in Visual Basic that uses the NEC4 executable file as a basic shell. To reduce the run time of the executable file, Dr. Ross replaced the original linear algebra solver (FACTR) with a much faster routine call LAPACK [35].

GA-NEC enables the optimization of NEC4 models by providing a framework through which three different tasks are performed. First, the NEC4 input file is created or imported through a netlist display and the parameters to be optimized

within the input file are encoded into binary chromosomes. Then, a fitness function is defined and the NEC4 output file is used to determine the fitness of the parameters to be optimized. Finally, a genetic algorithm is executed as a means to perform the optimization. A detailed description of a genetic algorithm is presented in section 4.2.2.

4.2.2 Genetic Algorithm

As discussed in section 2.7, GAs are robust self-evolving computational schemes that are used as optimization tools. They are search algorithms based on the principles of genetics and natural selection that follow the concept of a Darwinian evolution where only the fittest survive. The process of a genetic algorithm can be explained through the concept of natural evolution of beings.

In nature, the physical characteristics of an individual can be determined through analysis of its chromosomes. Within a given population, individuals with chromosomes that have the highest fitness have a higher probability to survive longer and produce offspring. As a result, subsequent generations of that population will be composed of individuals with genetic material inherited from the parents with the highest fitness.

This process is mimicked in GAs where every parameter is encoded into chromosomes and the fitness of each chromosome is evaluated through a defined fitness function. The individuals with the highest fitnesses are then selected to produce offspring that will continue on to the next generation. Applied to STEMS, every switch configuration is encoded into a chromosome as a binary string of '0's and '1's. A one

is used to represent a switch that is turned on, while a zero is used for a switch turned off. This implies that for a STEMS, the binary string or chromosome contains all the information needed to set the states of the switches.

A block diagram of the steps involved in a genetic algorithm is shown in Figure 4.1 and an explanation of each step is provided in section 4.2.2.1 to section 4.2.2.7.

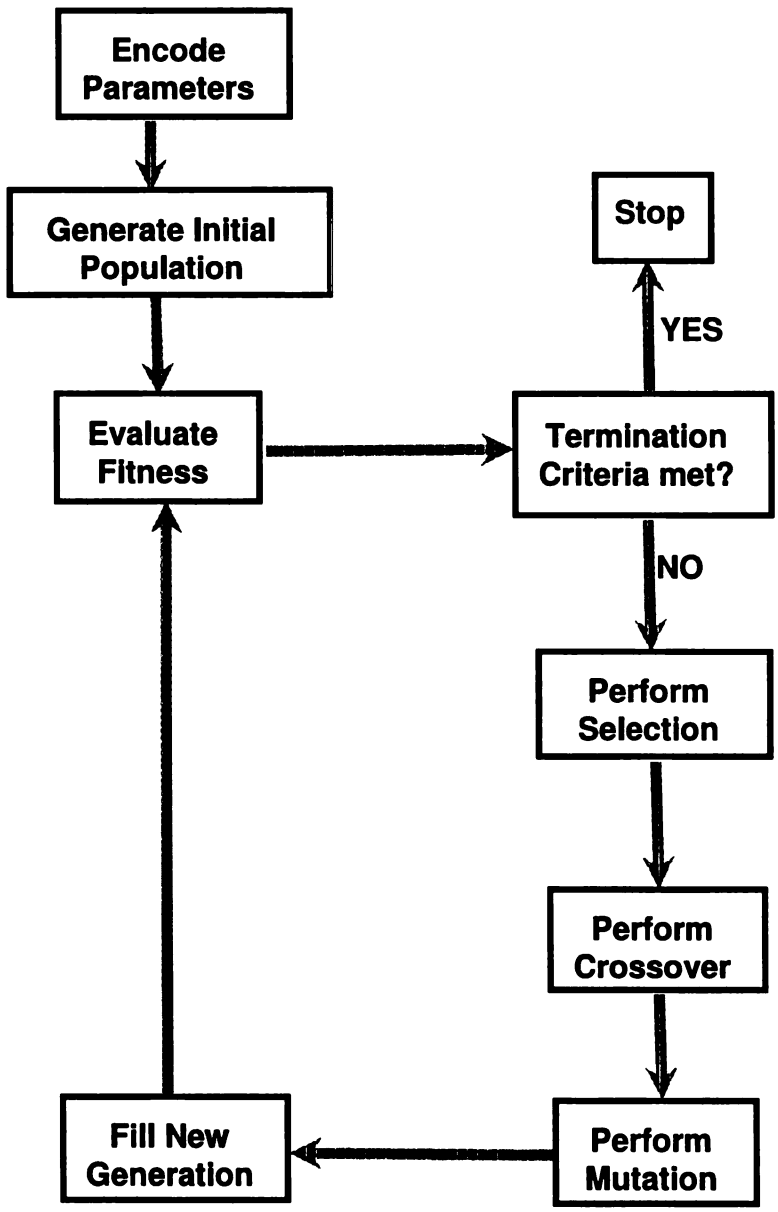

Figure 4.1. Block Diagram of a basic genetic algorithm

4.2.2.1 Encoding Parameters

As discussed in section 4.2.1, the parameters to be optimized need to be encoded into chromosomes. The lengths of the chromosomes determine the search space and longer chromosomes are needed for more complex problems. In the case of STEMS, the chromosome length is equal to the number of switches used on the template.

4.2.2.2 Initial Population

The initial population represents the first set of chromosomes to be considered for evaluation. This first set is usually generated randomly but a pre-existing pool can also be used as the starting set.

4.2.2.3 Evaluating the Fitness

In order to determine the fitness of the chromosomes within the population, a fitness function is defined. Each chromosome is then decoded and the fitness function is evaluated.

4.2.2.4 Mating Pool selection

The mating pool is composed of selected chromosomes also referred to as parents, that pass on their genetic information to the next generation. Selection of the mating pool can be done through various methods among which are elitist, thresholding, roulette wheel and tournament selection:

- Elitist: the chromosomes are ranked based on their fitness value and a predetermined number of chromosomes, counting from the fittest, are selected.
- Thresholding: a preselected fitness value or a ratio between a chromosome fitness and the average fitness is used as selection criteria.

- Roulette wheel: chromosomes with higher fitness values have higher probabilities to be selected compared to chromosomes with lower fitness values. The roulette wheel method allows for more diversity in the mating pool.

- Tournament: two or more chromosomes are selected randomly from the population and the chromosome with the highest fitness is selected for the mating pool. This process is repeated until the mating pool is filled.

4.2.2.5 Crossover

After the selection process is completed, the selected chromosomes or parents are paired and crossovers are performed with reference to a crossover probability P_{cross}. Crossover can be done at one or multiple points between two or multiple chromosomes. A simple one point crossover between two chromosomes can be described as follows. Consider a pair C_1 and C_2. Crossover is performed by randomly selecting a crossover point and each of the two chromosomes are split into two strings at that specific point. The strings are then swapped, creating two new chromosomes, or offspring, O_1 and O_2 as shown below.

Assume the parents:

$$C_1 = X_0X_1X_2X_3X_4X_5.....X_n, \tag{4.1}$$

$$C_2 = Y_0Y_1Y_2Y_3Y_4Y_5.....Y_n, \tag{4.2}$$

A crossover performed between points 4 and 5 will produce the following offspring:

$$O_1 = X_0X_1X_2X_3X_4Y_5.....Y_n, \tag{4.3}$$

$$O_2 = Y_0Y_1Y_2Y_3Y_4X_5.....X_n. \tag{4.4}$$

4.2.2.6 Mutate and Fill Next Generation

Once crossover is completed, random mutations are performed with mutation probability P_{mut}. Mutation is carried on by toggling a random bit within the binary string of the chromosome. For instance, a chromosome with binary string $\{11\bar{1}111\}$ will become the binary string $\{11\bar{0}111\}$ if mutation is performed on the third bit of its string. After the mutation process, the generation of offspring then becomes the new generation of parents and their fitness is evaluated once again.

4.2.2.7 Stopping Criteria

Often, the GA is stopped after a set number of generations has been evaluated. More often, a stopping condition can be imposed when a chromosome with a fitness value higher than a preselected value is found.

4.2.3 Switch model

Switches are not available in the current version of NEC4 but a switch model can be created in GA-NEC through the use of resistors by applying the basic concepts of circuits. Resistors are electrical components used to limit or regulate the flow of electrical current. The current through a resistor is inversely proportional to its resistance; therefore, the current flow through a wire segment can be controlled by loading the wire with a resistor. A low resistance allows for a current flow while a

very high value of resistance stops the current through the wire. The same behavior is observed for switches. When the switch is on, the current flows and when the switch is turned off the flow stops. In other words, an 'on' switch state is modeled by applying a low resistance while an 'off' switch state is obtained using a high resistance. In GA-NEC the high and low values of each resistor are encoded to 0 and 1. When a switch state is generated by the GA, the string of 0s and 1s are decoded back to their nominal values (0=low resistance; 1=high resistance) and each resistor is then set to its corresponding value. Through this thesis, the two values used for the resistors are 0.01Ω for low and 100000000.01Ω for high resistance.

4.3 Initial Design Approach and Observations

The STEMS template described in this thesis is the result of various studies performed on a different design configuration. The initial STEMS that was considered is a planar surface made of rectangular wire loop and switches, created with reference to the SSA mentioned in section 2.8. Its template is a square surface of side length 40cm, made of 28 wire loops and 34 switches as shown in Figure 4.2. The wires are designed with the same radius $a = 1.9mm$ and segment length $\Delta = 12.5mm$ following the guidelines mentioned in section 3.2. The layout and dimensions (width, length) of the loops were arbitrarily chosen and are shown in Table 4.1.

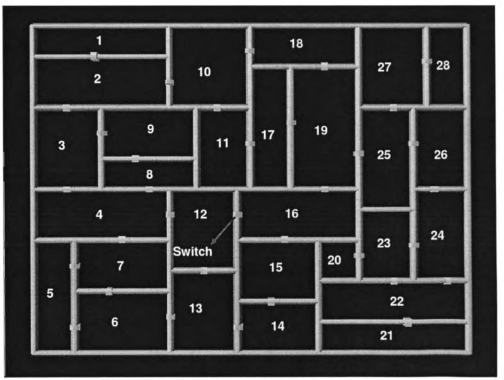

Figure 4.2. 4NEC2 screen shot of a the first wire STEMS

Wire Characteristics	
Wire loop	Lengths (mm)
1	37.5, 125
2	62.5, 125
3	62.5, 100
4	62.5, 125
5	37.5, 137.5
6	75, 87.5
7	15, 62.5
8	37.5, 87.5
9	62.5, 87.5
10	75, 100
11	50, 100
12	62.5, 100
13	62.5, 100
14	62.5, 100
15	62.5, 112.5
16	62.5, 125
17	37.5, 150
18	50, 100
19	62.5, 150
20	37.5, 50
21	37.5, 137.5
22	50, 137.5
23	50, 87.5
24	50, 112.5
25	50, 125
26	50, 100
27	62.5, 87.5
28	87.5, 37.5

Table 4.1. Wire STEMS loop dimensions.

To analyze the wire STEMS, an open box and a probe are also designed. The box is a cubical box with side length of 40cm and the probe is a quarter wavelength monopole (10.7cm) connected to the middle of one of the plates of the box as shown in Figure 4.3. The probe is also loaded with a 50Ω resistor on its first segment. The whole structure is then excited at $700MHz$ with a normal incident plane wave with its electric field polarized along the x-direction and of magnitude $1V/m$, and the current induced on the loaded segment of the probe is recorded as I_O. The characteristics of the incident plane wave are given in Table 4.2 while the open box and probe characteristics are given in Table 4.3. The wire STEMS is then used to seal the opening of the box containing the probe and the structure is excited once again at $700MHz$ with the same plane wave. To determine the shutter effectiveness S_e, which is the ability of the STEMS to create an open or closed surface, the value of the current on the loaded segment of the probe is recorded. This current value, termed as I_S, is used with the open box current I_O in Eq4.5 to find S_e. To either maximize S_e (STEMS open) or minimize S_e (STEMS closed) simulations are run using GA-NEC with the parameters of the GA given in Table 4.4. Initial results of the simulated wire STEMS showed good results when trying to create an open surface but very poor results were observed for the closed surface case with with values of S_e no less than -30dB.

$$S_e = 20 * log_{10}\frac{I_S}{I_O}, \tag{4.5}$$

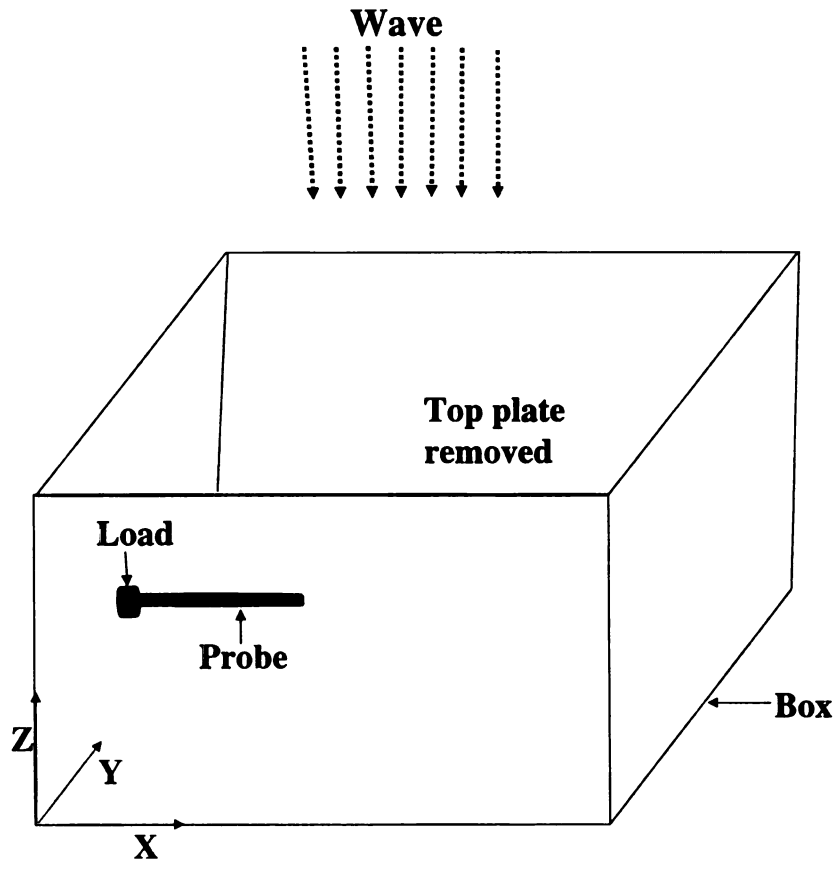

Figure 4.3. Figure showing the location of the probe and load inside the box

Wave description		
Incidence	Incidence Angles(degrees)	Magnitude(V/m)
Normal	$\theta = 0, \phi = 0$	1
Oblique	$\theta = 30, \phi = 60$	1

Table 4.2. Description of the two waves used to excite the boxes.

Cubical Box		
Length(mm)	Wire Radius(mm)	Segment Length (mm)
400	1.9	12.5
Probe		
Length(mm)	Wire Radius(mm)	Segment Length (mm)
107	0.56	10.7

Table 4.3. Characteristics of the probe and box.

GA parameters	
Population Size	100
Generations	50
Crossover Probability	0.7
Mutation Probability	0.1
Selection type	*Elitist*
% of population replaced	90

Table 4.4. Parameters used to set the genetic algorithm.

Different wire configurations were also analyzed, but all failed to create an efficient closed surface. A possible explanation of the poor performance of the wire STEMS is the large spacing between wires, ranging from 15mm to 150mm. In Figure 4.2, it is observed that the smallest area or hole is 15mm x 62.5 mm for wire set 7 while the biggest is observed for wire set 19 with an area of 62.5mm x 150mm is. These spacings are too wide for waves at $700MHz$ and hence explain the inability of the wire STEMS to find a switch configuration capable of creating a closed surface.

As a second attempt to create STEMS a slot version of the wire STEMS is created. Initial simulations of the slot STEMS revealed promising results with reference to the effectiveness of the slot STEMS to open or close itself to incoming plane waves. Details of the slot STEMS template and a thorough discussion of the simulation results are provided in section 4.4.

4.4 Slot STEMS Design and Simulation Results

4.4.1 Slot STEMS Template

With reference to the observations made in section 4.3, a slotted surface is designed as a means to create a self tuning electromagnetic shutter. The new model is a square surface of side length 27.3cm made of 12 conducting patches and 32 switches. The 4NEC2 model of the surface is as shown in Figure 4.4. The conducting patches are created using a wire grid model with each grid having a segment length of $\Delta = 9.75mm$ which also corresponds to the width of the slots between the patches. The radius of the wires are frequency dependent and the appropriate radius is used at each frequency of interest with reference to the results of section 3.3. A discussion of

the simulated results of the slot STEMS is provided in section 4.4.2

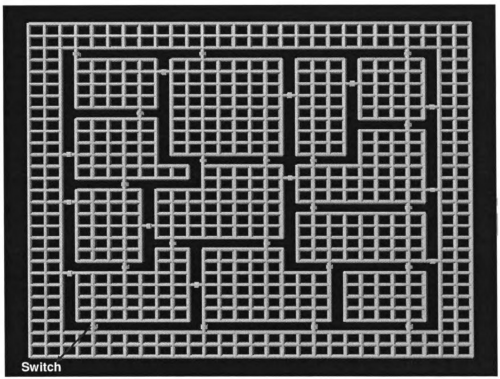

Figure 4.4. 4NEC2 screen shot of the slot STEMS

4.4.2 Slot STEMS Simulation Results

The details of the GA-NEC simulations of the slot STEMS are provided in this section. The procedure used to determine the shutter effectiveness S_e of the wire STEMS discussed in section 4.3 is also used in this section. Six different frequencies are selected to analyze the behavior of the STEMS and the parameters used to set up the GA are given in Table 4.5.

Recall that in section 3.3, 42 boxes with different $\frac{\Delta}{a}$ ratios are simulated at six different frequencies with the goal of determining the optimum $\frac{\Delta}{a}$ ratio that provides the best shielding effectiveness at each frequency. The same six frequencies are used in this section and for every frequency, the best $\frac{\Delta}{a}$ ratio found in section 3.3 is used to determine the radius and segment length of the wires used to design the STEMS. In other words, six frequencies are considered for analysis and for every frequency, a new STEMS template and a new box are designed. A description of the wires selected to design the slot STEMS at each frequency is provided in Table 4.6.

For every frequency, the structure (STEMS + open box +probe) as shown in Figure 4.5 is excited with a normal and an oblique linearly polarized plane wave that are described in Table 4.7. To evaluate the shutter effectiveness S_e of the STEMS for each incident wave, the current on the first segment of the probe is determined for the open box first. Then, the open box is sealed with the STEMS template and GA-NEC is ran using the parameters of Table 4.5. To seek a STEMS template configuration capable of creating a closed surface, the GA fitness function is set to minimize the current on the first segment of the probe while and an open surface is sought by

setting the GA fitness function to maximize the current. For each case, the STEMS shutter effectiveness is determined by using Eq4.5.

For every case, the STEMS is optimized at each of the six frequencies to create an open or closed surface using GA-NEC with the GA parameters given in Table 4.5. The best switch configuration found at each frequency for each case is then used to obtain the STEMS shutter effectiveness S_e over a frequency range of 100MHz centered at the frequency it has been optimized. The goal of the optimization is to find the state with the lowest value of S_e for the closed case and the highest value of S_e for the open case.

Discussions of the results obtained at each frequency for both incident plane waves are given in sections 4.4.2.1-4.4.2.6 while section 4.4.2.7 presents an analysis of the shutter effectiveness evaluated at 200 different locations within the box using the best switch configuration found at 700MHz. Table 4.8 through Table 4.11 show the best switch configuration found at each frequency for every case studied. Figure 4.6 references the corresponding location and number of all 32 switches used on the STEMS template. Note that:

- 'normal incidence angle' is used to reference the wave incident with $\theta = 0°$, $\phi = 0°$
- 'oblique incidence angle' is used to reference the wave incident with $\theta = 30°$, $\phi = 60°$
- 'closed STEMS' is used to reference the STEMS optimized to create a closed surface

- 'open STEMS' is used to reference the STEMS optimized to create an open surface

GA parameters	
Population Size	70
Generations	50
Crossover Probability	0.7
Mutation Probability	0.1
Selection Type	*Elitist*
Generation Gap	0.9

Table 4.5. Genetic algorithm set-up for slot STEMS.

Wire description		
Frequency(MHz)	Wire radius(mm)	Wire segment(mm)
750	1.53	9.75
725	1.58	9.75
700	1.64	9.75
675	1.69	9.75
650	1.74	9.75
625	1.78	9.75

Table 4.6. Slot STEMS wire segments and radii characteristics.

Wave description			
Incidence	Tilt *Angle* (degrees)	Incidence *Angle* (degrees)	*Magnitude* (V/m)
Normal	0	$\theta = 0, \phi = 0$	1
Oblique	0	$\theta = 30, \phi = 60$	1

Table 4.7. Description of the normal and oblique incident waves.

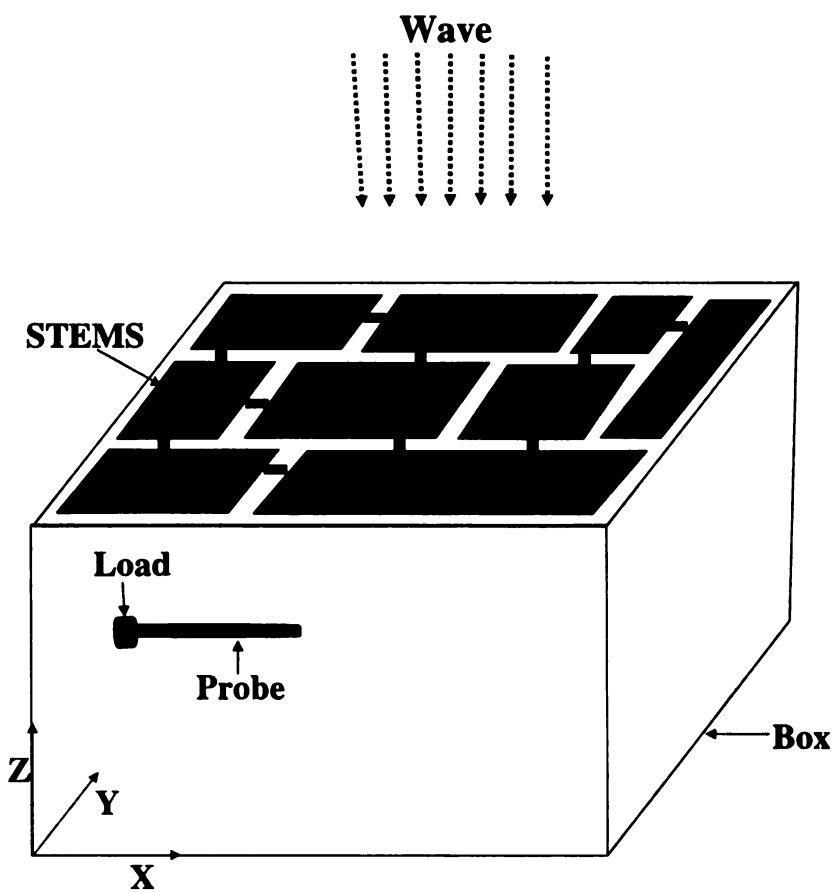

Figure 4.5. Drawing of a slot STEMS on a box with a loaded probe

Normal: closed STEMS						
switch number	625MHz	650MHz	675MHz	700MHz	725MHz	750MHz
1	1	0	0	1	1	1
2	0	0	0	0	0	0
3	0	1	0	0	1	0
4	1	0	0	0	1	0
5	0	1	1	0	1	1
6	0	1	0	1	0	1
7	1	0	0	0	0	0
8	1	0	0	0	1	0
9	0	0	1	0	0	1
10	0	1	0	0	1	0
11	0	0	0	0	0	0
12	1	1	1	1	1	1
13	0	1	0	0	0	0
14	0	1	1	0	0	1
15	0	1	1	1	1	1
16	0	0	0	0	0	0
17	0	0	0	0	0	1
18	0	0	1	1	0	0
19	0	1	1	1	0	0
20	1	1	1	1	1	1
21	0	1	0	0	1	1
22	1	0	1	1	1	0
23	0	0	1	1	1	0
24	1	0	1	0	0	0
25	1	1	0	0	1	0
26	1	1	0	0	0	0
27	1	0	0	1	1	1
28	0	1	0	1	1	0
29	1	1	1	1	1	0
30	0	0	0	1	0	1
31	1	0	0	1	0	1
32	0	0	0	0	0	0

Table 4.8. Closed STEMS best switch configurations: normal incidence angle.

oblique: closed STEMS						
switch number	625MHz	650MHz	675MHz	700MHz	725MHz	750MHz
1	1	1	0	0	1	0
2	0	1	1	0	0	0
3	1	0	0	0	0	1
4	0	1	1	0	0	0
5	0	1	1	1	0	1
6	0	0	0	0	0	0
7	0	1	0	1	0	0
8	0	0	0	0	1	0
9	1	0	1	0	0	0
10	0	0	1	0	0	0
11	1	1	0	0	1	1
12	1	0	0	1	0	1
13	1	0	1	0	0	0
14	1	1	1	1	0	1
15	1	0	1	1	0	1
16	1	1	1	0	0	0
17	0	0	1	0	1	0
18	1	0	0	1	0	1
19	1	1	0	1	0	0
20	0	1	1	1	1	1
21	1	0	1	1	0	1
22	0	1	0	0	1	0
23	1	1	1	1	1	1
24	0	0	0	0	0	0
25	1	1	0	0	0	0
26	0	0	0	0	1	0
27	1	1	1	1	1	1
28	0	0	1	1	0	1
29	1	0	1	1	0	1
30	0	0	1	0	1	0
31	0	0	1	1	1	1
32	1	0	1	1	1	1

Table 4.9. Closed STEMS best switch configurations: oblique incidence angle.

Normal: open STEMS						
switch number	625MHz	650MHz	675MHz	700MHz	725MHz	750MHz
1	1	0	0	0	1	1
2	0	0	0	0	0	0
3	1	1	1	0	1	1
4	1	1	1	1	1	0
5	0	0	0	1	1	1
6	1	0	1	1	0	1
7	1	1	0	0	1	1
8	1	0	1	0	0	1
9	0	0	0	1	1	0
10	1	1	0	1	1	1
11	1	1	0	1	0	1
12	0	0	0	1	1	0
13	0	0	1	1	0	0
14	0	1	0	1	0	1
15	0	0	1	1	0	1
16	1	0	1	1	0	0
17	1	0	0	0	0	1
18	1	0	1	1	0	1
19	1	1	0	0	0	0
20	1	0	0	0	0	1
21	0	1	1	0	1	1
22	0	1	0	0	1	1
23	0	1	1	1	0	0
24	0	1	0	1	0	1
25	0	0	0	0	0	1
26	0	0	1	0	1	0
27	1	1	0	0	1	0
28	1	0	0	1	1	1
29	1	0	1	0	0	1
30	1	0	1	0	0	0
31	1	1	0	0	1	1
32	1	1	1	0	0	1

Table 4.10. Open STEMS best switch configurations: normal incidence angle..

Oblique: open STEMS						
switch number	625MHz	650MHz	675MHz	700MHz	725MHz	750MHz
1	1	0	0	0	1	0
2	1	1	0	0	0	1
3	1	0	1	1	0	1
4	1	1	1	1	1	1
5	1	0	1	1	1	0
6	1	1	1	0	1	0
7	0	1	0	1	0	0
8	1	1	1	0	1	1
9	1	1	1	1	1	0
10	1	0	0	1	1	1
11	1	1	0	0	0	1
12	1	0	0	0	0	0
13	1	1	1	1	1	0
14	0	0	0	0	1	1
15	1	0	0	0	1	1
16	1	1	1	1	1	1
17	1	1	1	0	1	1
18	1	1	1	1	1	1
19	1	1	0	1	0	1
20	1	1	1	0	0	0
21	1	0	1	1	0	0
22	0	1	1	0	1	1
23	1	0	0	0	1	0
24	1	1	1	0	1	1
25	1	0	0	1	1	0
26	0	0	0	1	1	1
27	1	1	0	1	1	1
28	0	1	1	0	0	1
29	1	1	0	1	1	0
30	1	1	1	0	1	1
31	0	0	1	0	1	1

Table 4.11. Open STEMS best switch configurations: oblique incidence angle..

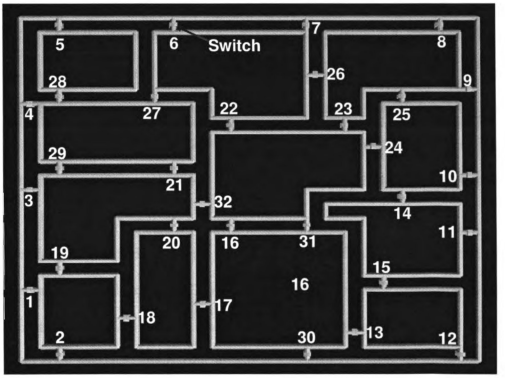

Figure 4.6. Switch location on STEMS template

4.4.2.1 Results at 625MHz

The first frequency analyzed is 625MHz. For a vertical incidence angle, the open box current is recorded to be $I_{boxopen} = 2.314E-03$ (A) while the optimized STEMS produced a current $I_{STEMS} = 1.2798E-06$ (A) for the closed closed STEMS. Using Eq4.5, this yields a shutter effectiveness of S_e=-65.144dB. The frequency sweep of the optimized template as shown in Figure 4.7 reveals an even lower S_e at 625.5MHz with S_e=-73.69dB. When optimized to create an open surface, GA-NEC found a state with a shutter effectiveness of S_e=1.23dB, obtained with 13 of the 32 switches turned on. The frequency sweep of the open STEMS, also displayed in Figure 4.7, shows a frequency range of 595MHz to 640MHz with a shutter effectiveness of 0 or higher. At 625MHz, the difference between closed and open STEMS shutter effectiveness is found to be 66.27dB.

For the oblique incidence angle, the best switch configuration found over the 50 generations run for the closed STEMS has 15 switches on and 17 switches off with a shutter effectiveness S_e=-43.dB. The frequency sweep as shown in Figure 4.8 shows that the same switch configuration produces a shutter effectiveness $S_e = -58.597B$ at 624MHz. This represents a difference of $15dB$ for just a 1MHz shift in frequency. An interesting result is also obtained for the the open STEMS where the frequency sweep of the best switch configuration produces a shielding effectiveness greater than $0dB$ from 585MHz to 670Mhz, shown in Figure 4.8 as well.

The histogram of the best switch states found for all 4 cases as shown in Figure 4.9 reveals that switches 1, 27 and 29 are off each time and none of the 32 switches

is used for all 4 cases. These results do not necessarily mean that switches 1, 27 and 29 can be deleted from the template because a different environment might require a different switch configuration that involves 1, 27 and 29. Also, the results found by the GA are not necessarily the best of the bunch. With a population of 70 and a total of 50 generations, the GA only evaluates 3500 states out of the possible 4.2950 billion states. There are still over 4.294 billion unexplored states and a definitive answer cannot be given unless all states are evaluated.

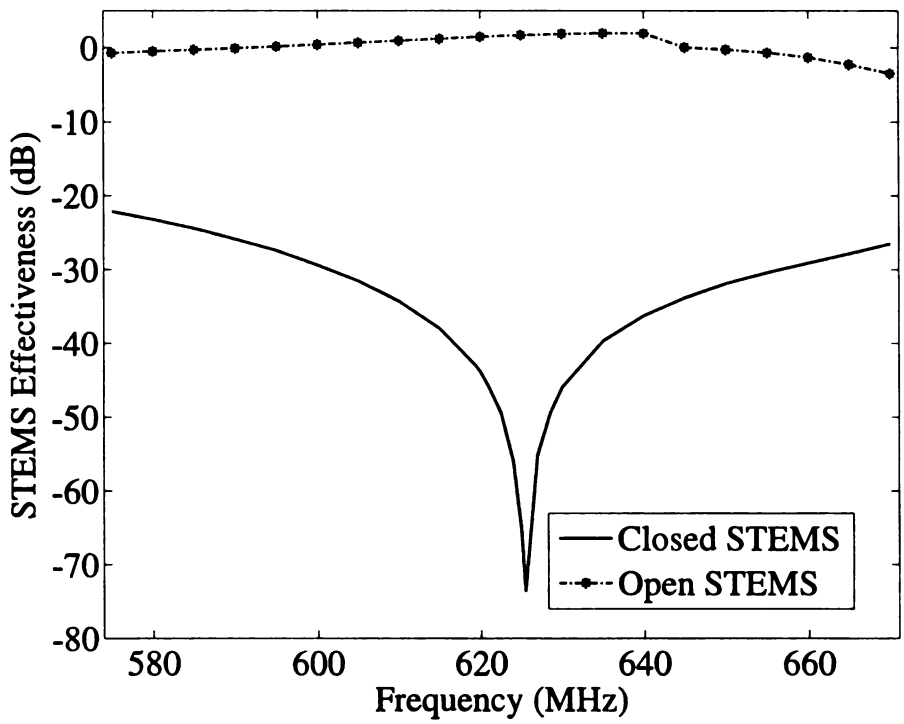

Figure 4.7. Frequency sweep of STEMS optimized at 625MHz: normal incidence

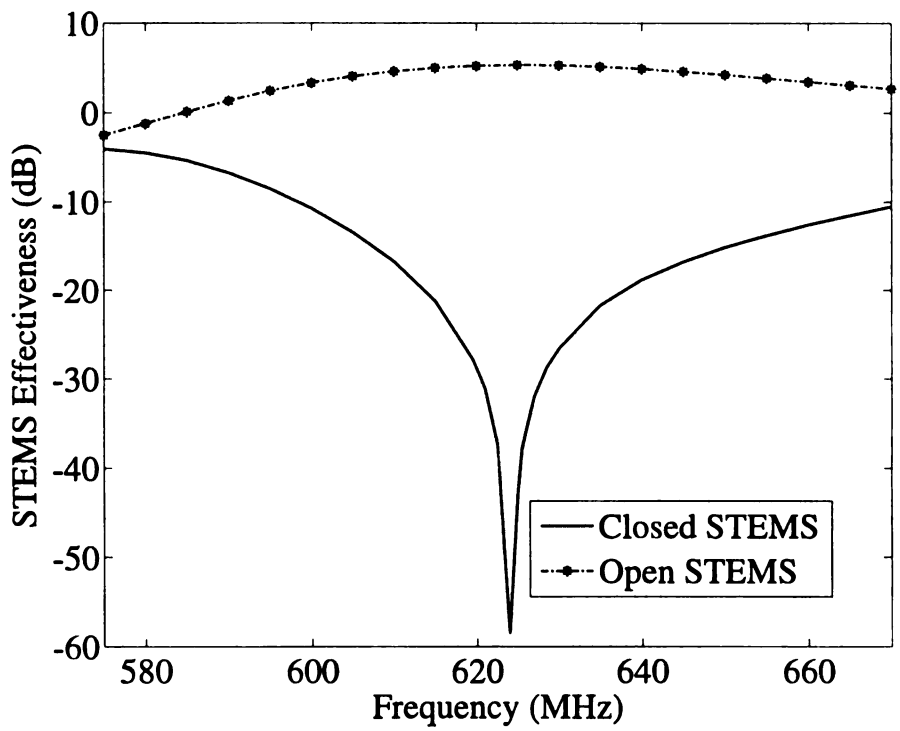

Figure 4.8. Frequency sweep of STEMS optimized at 625MHz: oblique incidence

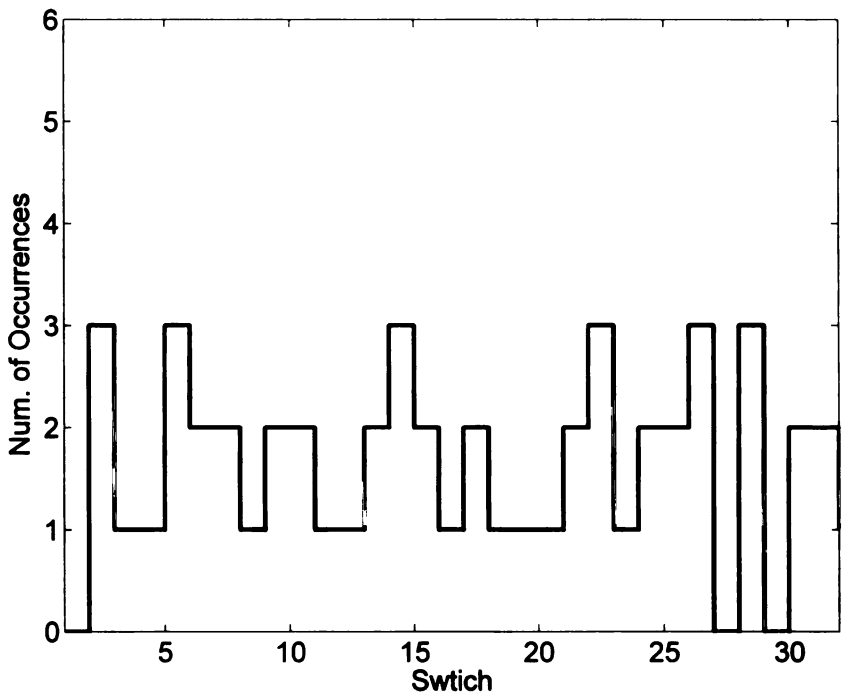

Figure 4.9. Histogram of the best switch states found for all 4 cases at 625MHz

4.4.2.2 Results at 650MHz

At 650MHz, for a normal incidence angle, the best state found for the closed STEMS yields a shutter effectiveness of S_e=-60.6937dB. Similar to the results at 625MHz, the frequency sweep of best state as shown in Figure 4.10 reveals a shutter effectiveness S_e=-77dB obtained at 649MHz. This is an even bigger difference in the value of S_e for only a 1MHz shift, compared to the result at 625MHz. A frequency sweep of the best state found for the open STEMS case is also shown in Figure 4.10. This state produces a shutter effectiveness of $1.179dB$ and a frequency range of 645MHz to 665MHz with value of S_e greater than 0.

For the oblique incidence angle as shown in Figure 4.11, the open STEMS frequency sweep shows a positive S_e from 600MHz to 675MHz with its highest value of $4.58dB$ found at 655MHz. A value of S_e=4.44dB is found at the frequency of interest which is 650MHz. The best S_e values for the closed STEMS is obtained at exactly 650MHz with S_e=-44.7266dB

The histogram of the best switch states found for all 4 cases as shown in Figure 4.12 also reveals that none of the 32 switches is used for all 4 cases but this time, only switch 19 is turned off for all 4 cases. Only 7 switches are turned on only once compared to 11 switches for 625MHz.

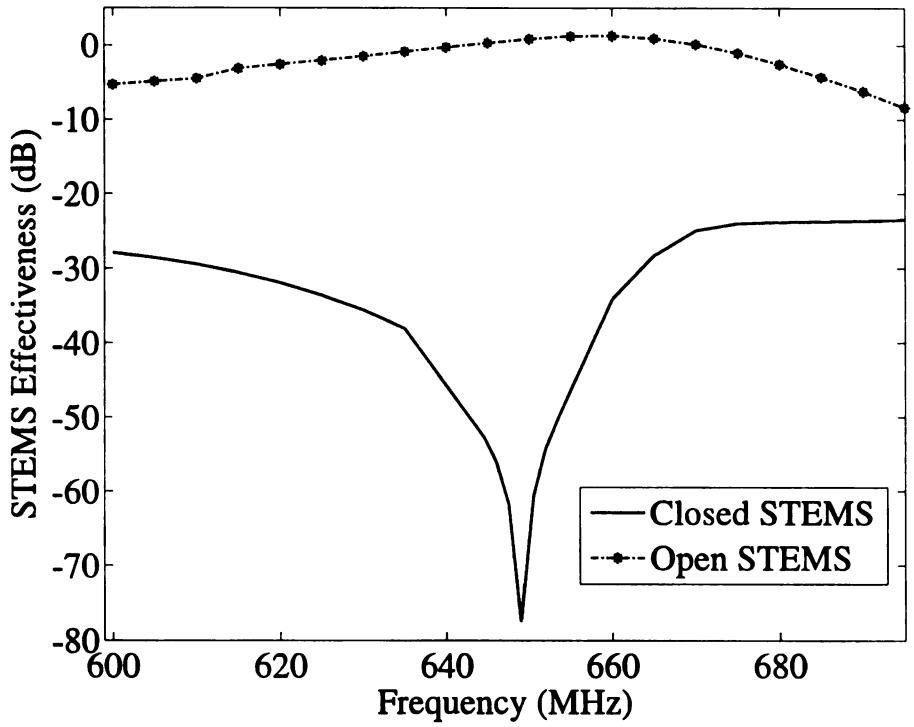

Figure 4.10. Frequency sweep of STEMS optimized at 650MHz: normal incidence

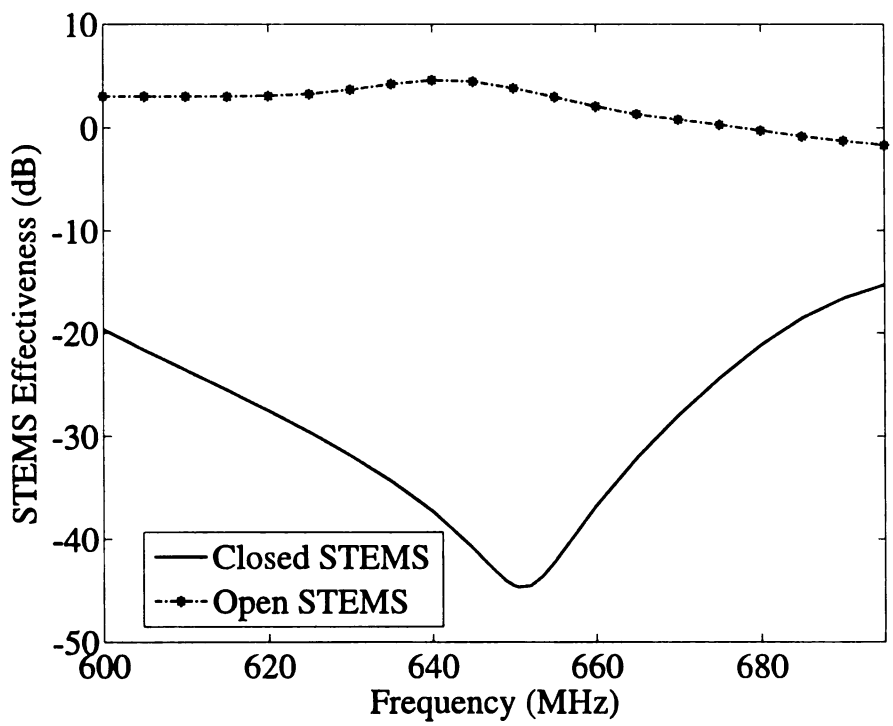

Figure 4.11. Frequency sweep of STEMS optimized at 650MHz: oblique incidence

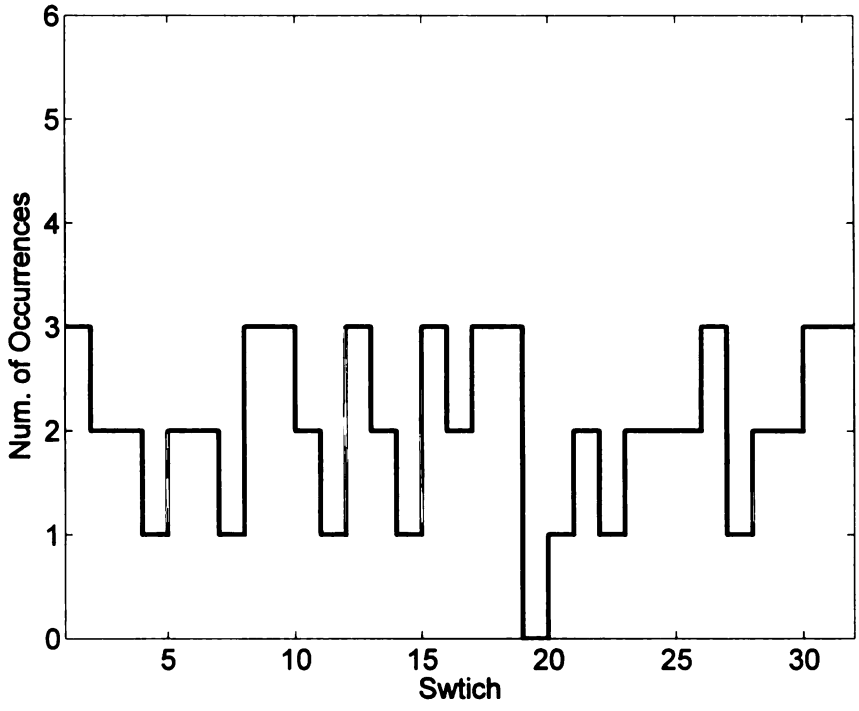

Figure 4.12. Histogram of the best switch states found for all 4 cases at 650MHz

4.4.2.3 Results at 675MHz

Figure 4.13 show the frequency sweep of the closed and open STEMS at 675MHz for a normal incidence angle. Unlike 625MHz and 650MHz, the GA was unable to find a switch state that yields a value of S_e greater than 0 when set to create an open surface. The best state found has a shutter effectiveness of S_e= -1.652dB for the open STEMS and S_e=-54.6269dB for the closed STEMS.

The oblique incidence angle produced the worst results for the closed STEMS case with S_e=-14.376 found with a switch configuration that had only 13 of the 32 switches turned on. As shown in Figure 4.14, the frequency sweep revealed a better shutter effectiveness with S_e=-21.23dB at 690MHz. More simulations are still being performed to find a better state. The optimization for the open STEMS on the other hand produced a state with S_e=5.67dB as also shown in Figure 4.14.

Unlike the precedent frequencies, the histogram of the best switch states found for all 4 cases as shown in Figure 4.15 shows that all switches are used at least once and switches 1, 7, 11 and 26 are always turned on.

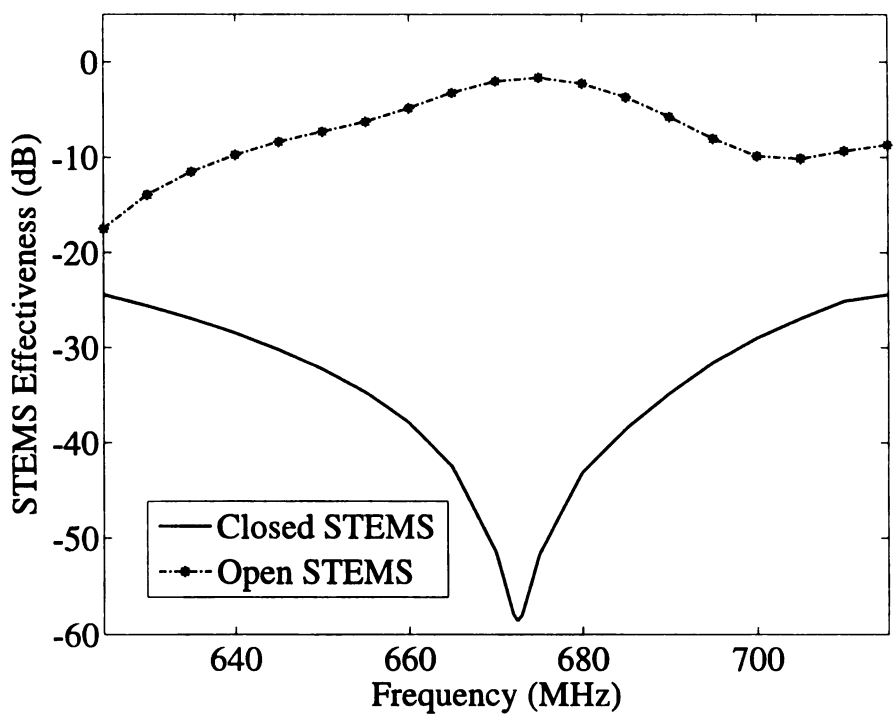

Figure 4.13. Frequency sweep of STEMS optimized at 675MHz: normal incidence

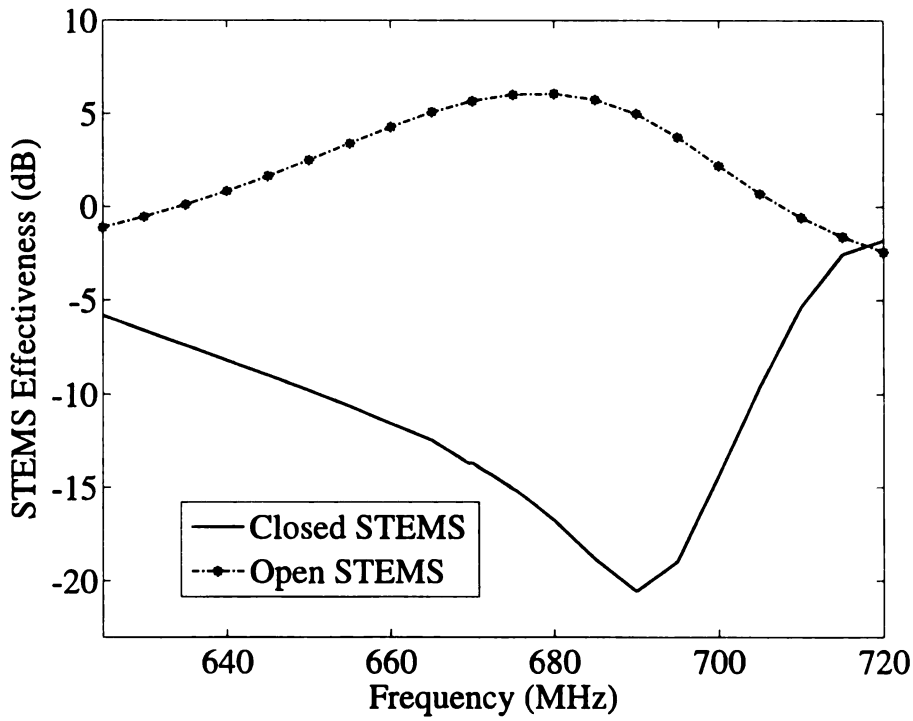

Figure 4.14. Frequency sweep of STEMS optimized at 675MHz: oblique incidence

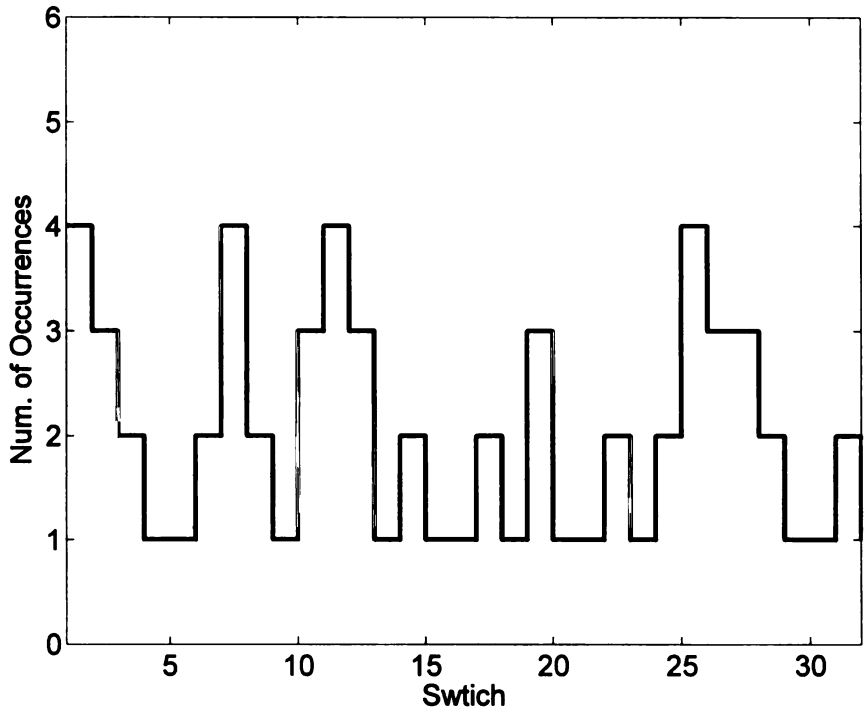

Figure 4.15. Histogram of the best switch states found for all 4 cases at 675MHz

4.4.2.4 Results at 700MHz

Analysis at 700MHz for a normal incidence angle produced states capable of creating an open and closed STEMS as shown in Figure 4.16. For the closed STEMS case, the best shutter effectiveness is found to be S_e=-67.4928dB while for the open STEMS case, the best switch configuration produces a shutter effectiveness of S_e=0.709dB.

Figure 4.17 shows an interesting plot of S_e for a frequency sweep of the oblique incidence angle case. It is observed that the sweep of the open STEMS best configuration shows a positive value of S_e for all frequency points evaluated between 650MHz and 745MHz with a value of S_e=8.285dB found at 700MHz. The plot of S_e for the frequency sweep of the closed STEMS shows the best value of S_e=-43dB found exactly at the optimized frequency.

The Histogram of the best states for all 4 cases is shown in Figure 4.18. This figure shows that 18 switches are tuned on only once and no switch is on for all 4 cases.

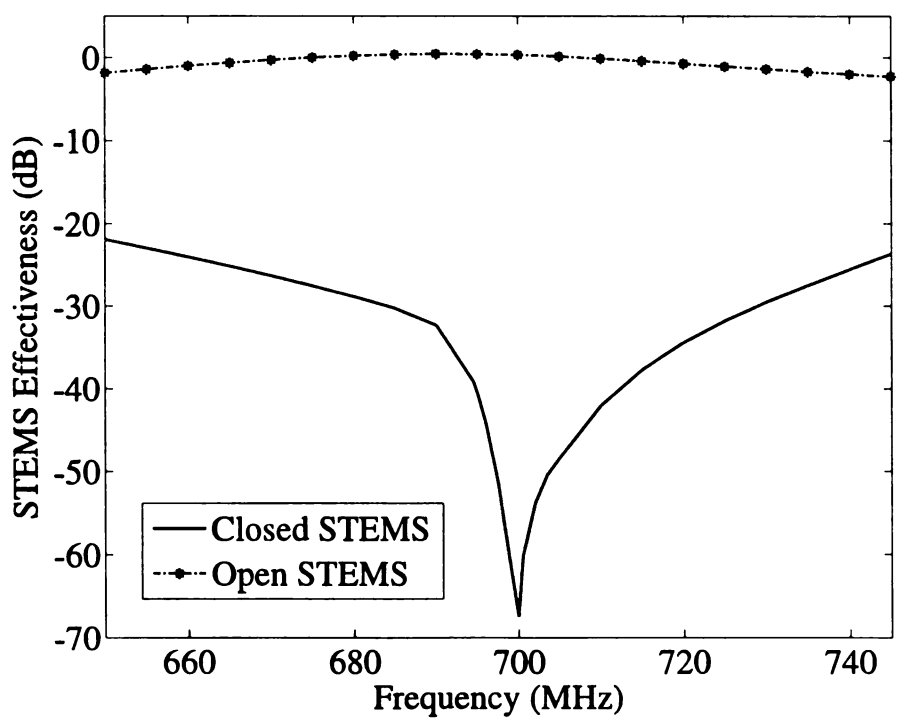

Figure 4.16. Frequency sweep of STEMS optimized at 700MHz: normal incidence

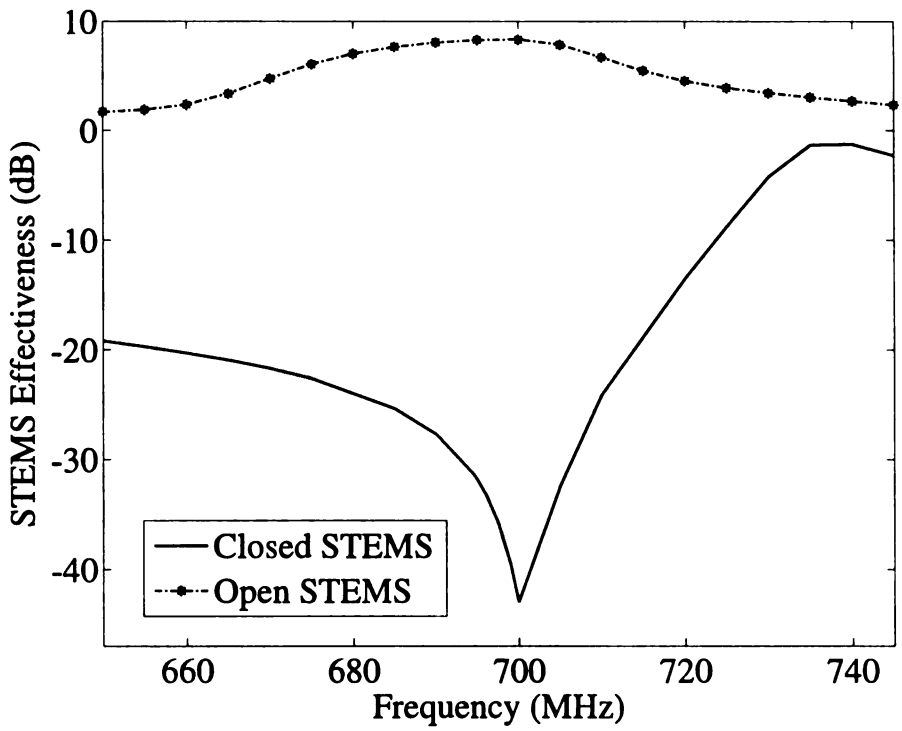

Figure 4.17. Frequency sweep of STEMS optimized at 700MHz: oblique incidence

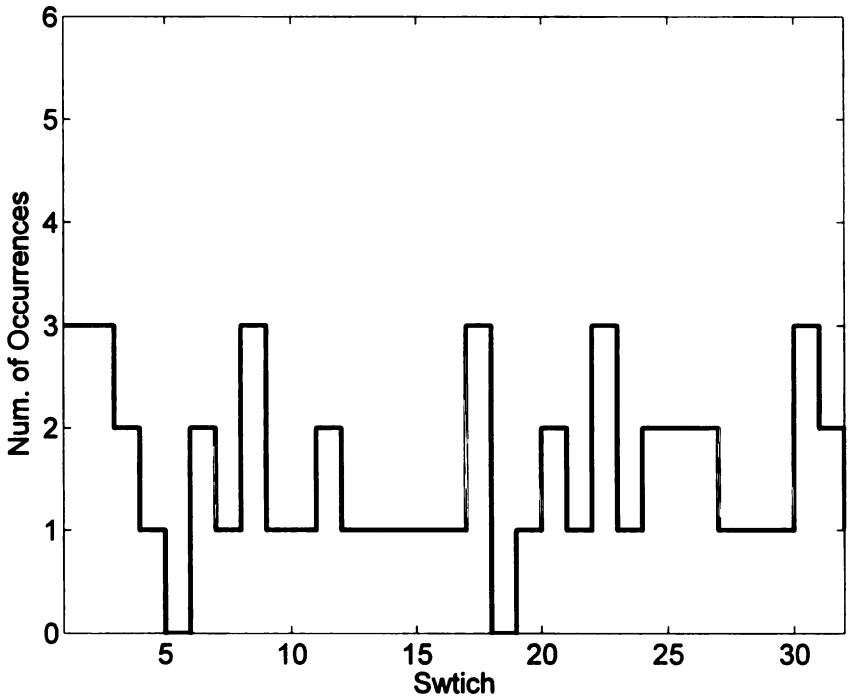

Figure 4.18. Histogram of the best switch states found for all 4 cases at 700MHz

4.4.2.5 Results at 725MHz and 750MHz

For a normal incidence angle, the best state found for the closed STEMS has a shutter effectiveness of S_e=-46.6479dB at 725MHz and -32dB at 750MHz. The open STEMS optimization, returned S_e=1.048dB at 725MHz and S_e=1.665dB at 750MHz. Figure 4.19 and Figure 4.21 show respectively the plot of the frequency sweep of the best states found 725MHz and 750MHz.

For an oblique incidence angle, the GA produced S_e=-54dB at 725MHz and S_e=-36dB at 750MHz for the closed STEMS and S_e=6.39dB at 725MHz and S_e=8.2294dB at 750MHz. The plot of S_e for the frequency sweep of the best states found at 725MHz and 750MHz are respectively shown in Figure 4.20 and Figure 4.22

The histogram of the best switch states for all 4 cases at 725MHz as shown in Figure 4.23 shows that switches 1, 22 and 27 are turned off while switches 2 and 19 are turned on in all cases. Figure 4.24 shows the histogram of the best switches at 750MHz where switches 14 and 32 are turned off in all cases while 14 and 23 are turned on for all 4 analysis.

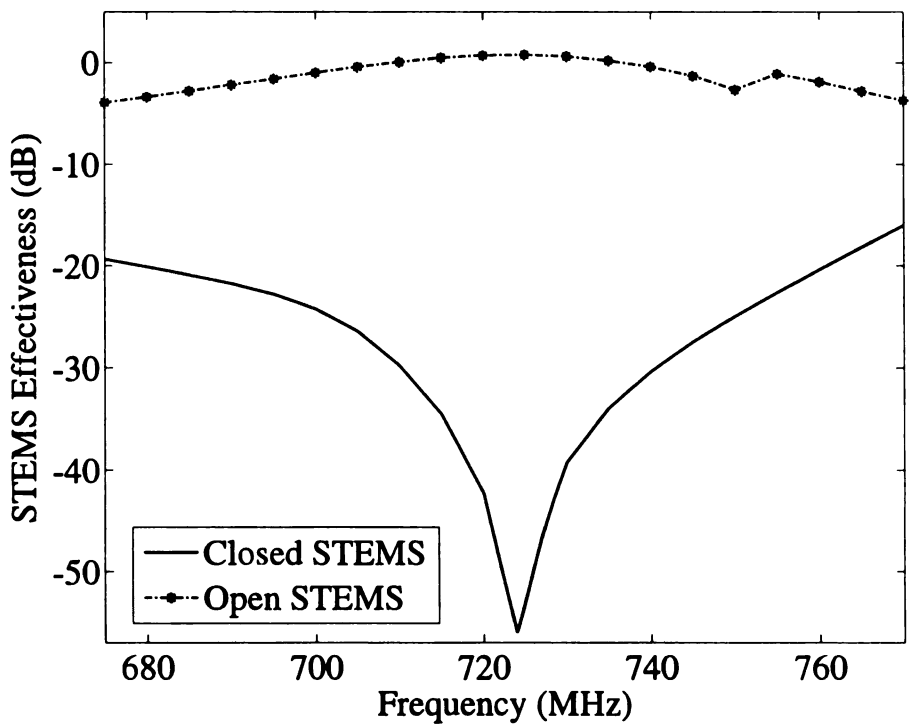

Figure 4.19. Frequency sweep of STEMS optimized at 725MHz: normal incidence

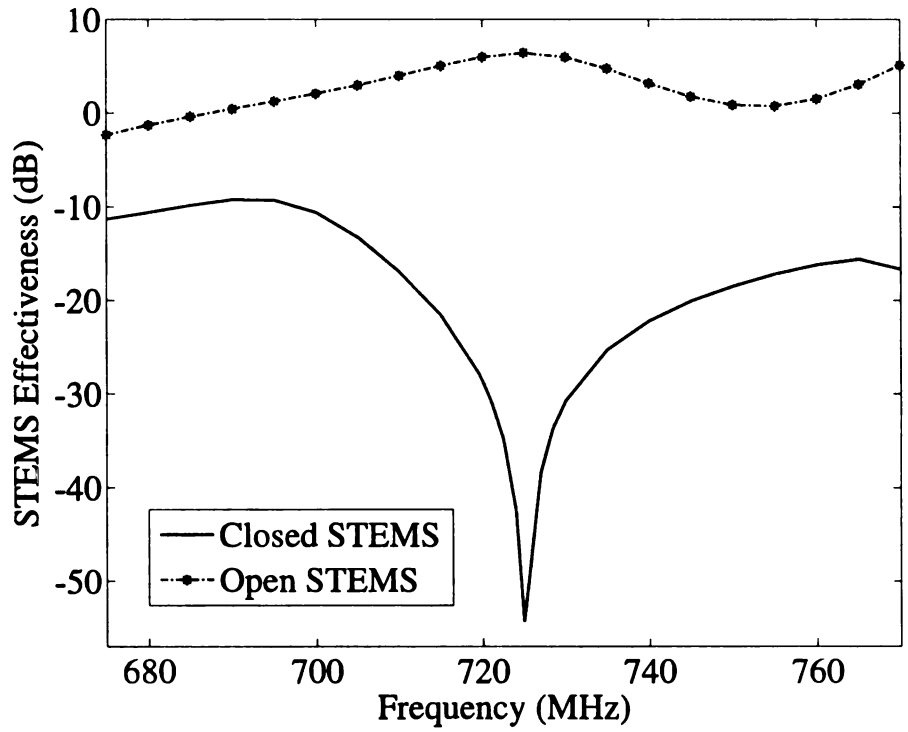

Figure 4.20. Frequency sweep of STEMS optimized at 725MHz: oblique incidence

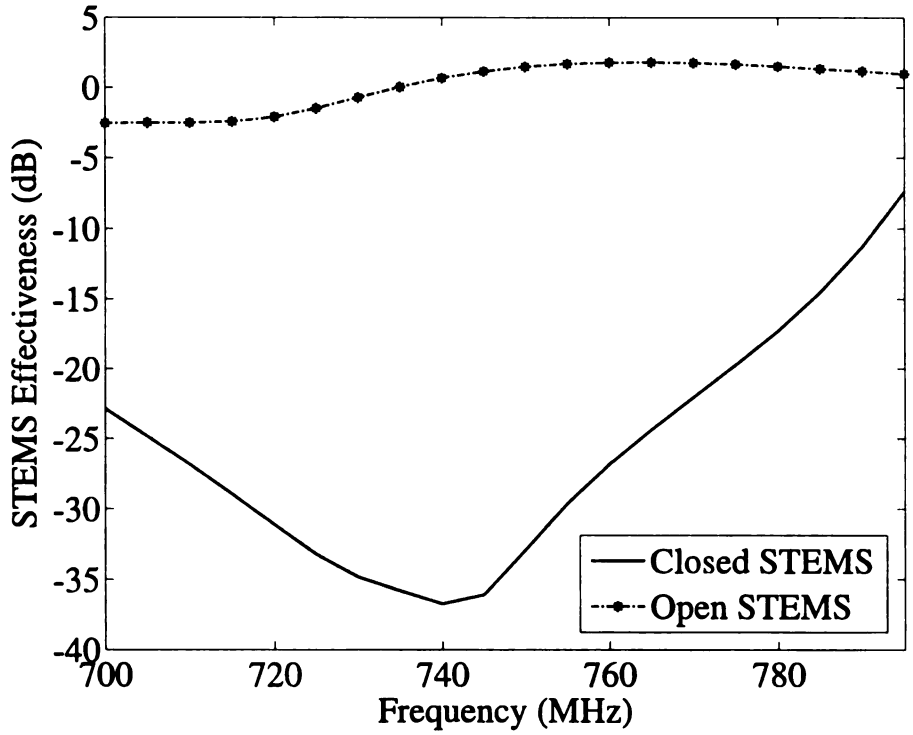

Figure 4.21. Frequency sweep of STEMS optimized at 750MHz: normal incidence

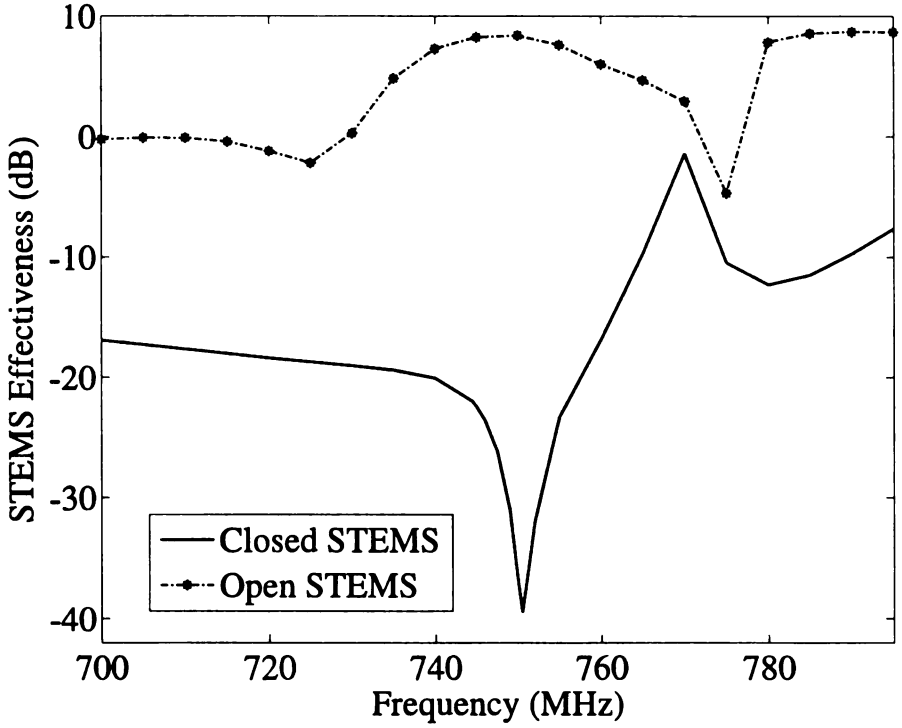

Figure 4.22. Frequency sweep of STEMS optimized at 750MHz: oblique incidence

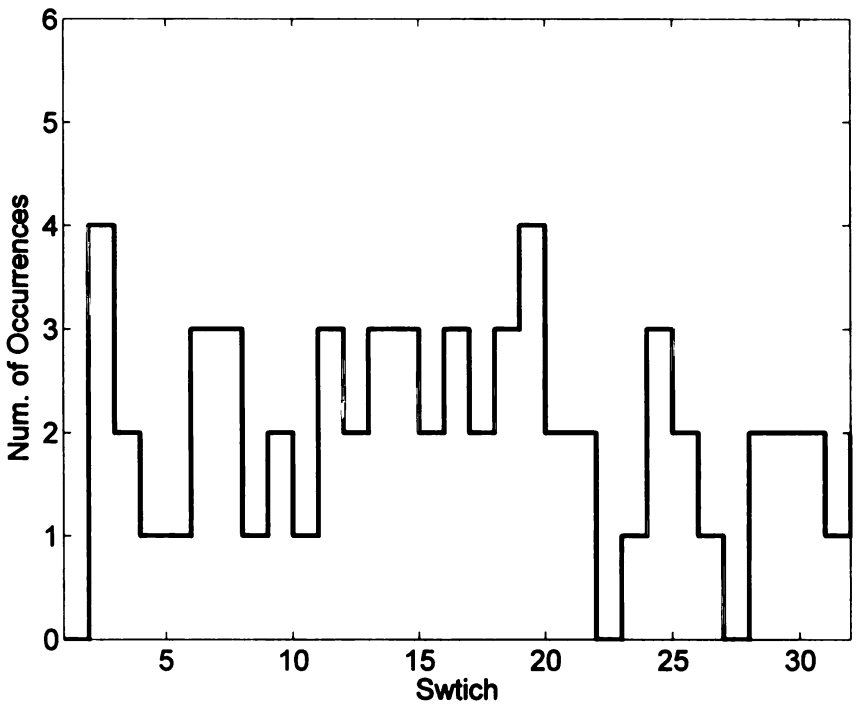

Figure 4.23. Histogram of the best switch states found for all 4 cases at 725MHz

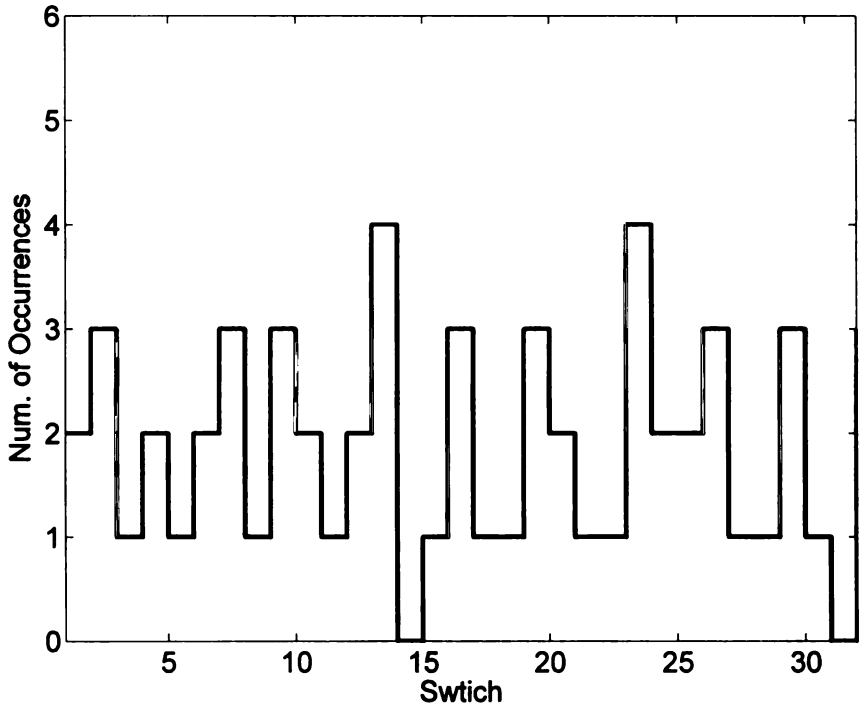

Figure 4.24. Histogram of the best switch states found for all 4 cases at 750MHz

4.4.2.6 Study of shutter effectiveness with reference to location within the box

The shutter effectiveness of the STEMS is optimized based on the ratio of the current on the loaded segment of the probe. This represents a single observation point inside the box. In order to determine the effect on the shutter effectiveness of a given template configuration due to changes of location within the box, a new study is performed. In this study, the best switch configurations found for a normal incidence wave at 700MHz for the open and closed STEMS are used.

Given the open box of Figure 4.3 without the probe and the load, 200 points are selected and the open box is excited with the normal incident wave described in Table 4.7. Using NEC4, the total electric field at each point is evaluated. The box is then sealed with the STEMS and the switches are set to the states found to be the best at creating a closed surface for the normal incidence wave. The total electric field at the location of the same 200 points is evaluated once more. The process is repeated by changing the configuration of the switches to the states found to be the best at creating an open surface.

Let S_f be defined to be the ratio of the total field for the box sealed with the STEMS to the total field of the open box. Using that definition, the value of S_f for the open and closed STEMS is evaluated at each of the 200 point and plotted. Figure 4.25 shows a plot of S_f for a closed STEMS. In that figure, it can be seen that there is very little change (2.3dB) of the value of S_f as the line is moved from (Y=0, Z=0) to (Y=-0.05, Z=-0.05). The biggest variation (17dB) is recorded when moving along

the X axis from one end of the box to the other. The same observation applies to the open STEMS $S_f$as shown in Figure 4.26 where the maximum variation of S_f from (Y=0, Z=0) to (Y=-0.05, Z=-0.05) is only 1.5dB. There is less variation in this case as the location is moved along the X axis from one end of the box to the other, with a maximum difference of 1.7dB, compare to the 17dB obtained for the closed STEMS

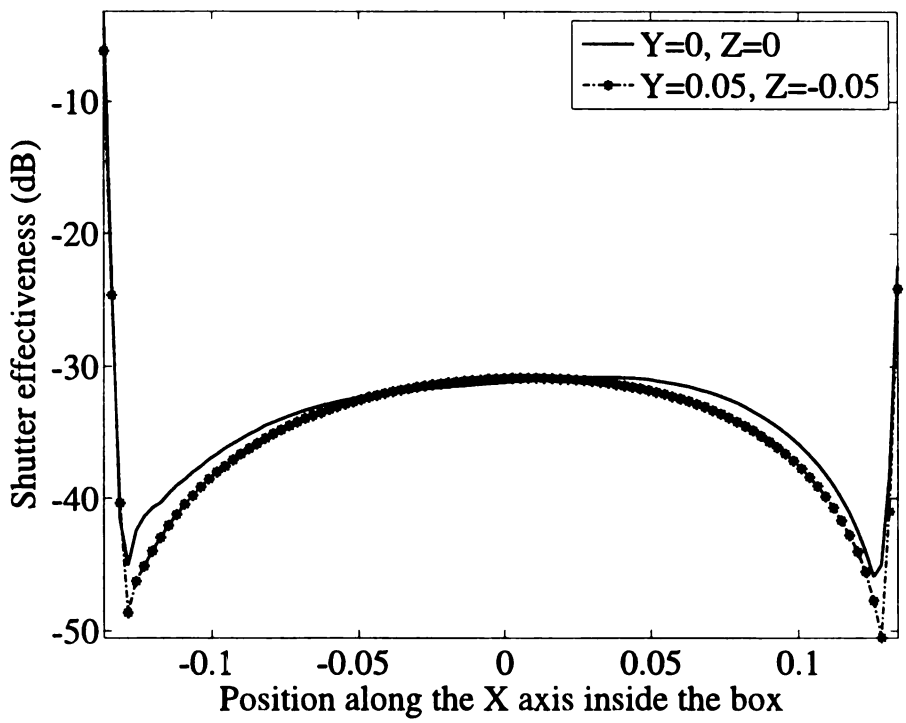

Figure 4.25. Total field within the box based on location for closed STEMS

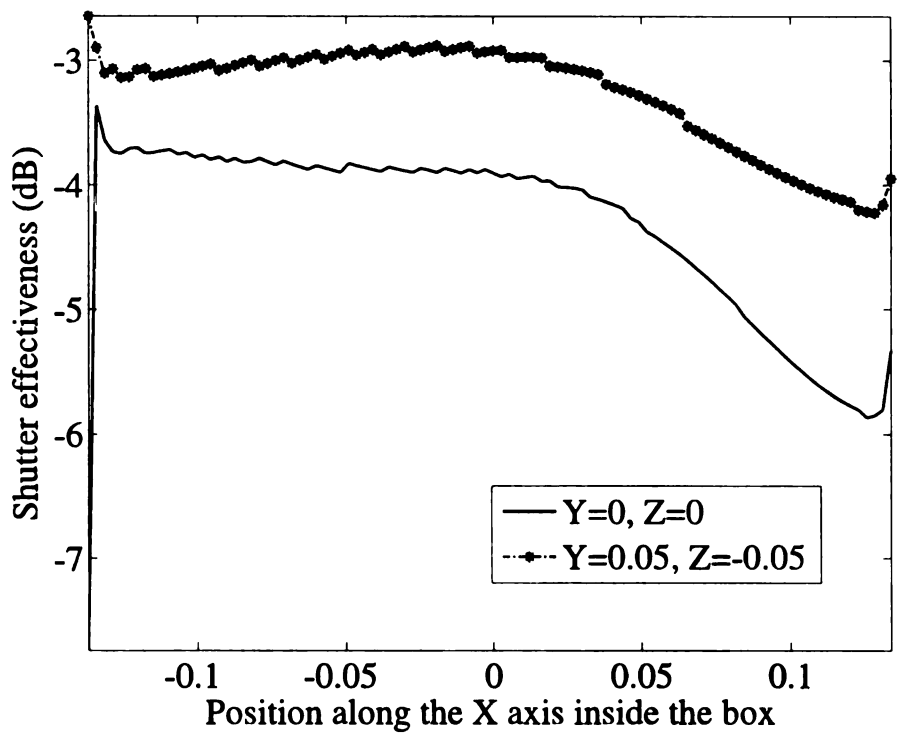

Figure 4.26. Total field within the box based on location for open STEMS

4.5 Conclusion

In this chapter, an overview of GA-NEC along with the optimization scheme and the switch model is given in section 4.2. A brief overview of the first STEMS considered is provided in section 4.3 while section 4.4 presents the details of the final design along with a discussion of the simulated results. The next chapter discusses measurement results of a prototype STEMS fabricated at Michigan State University

CHAPTER 5

MEASUREMENT SET-UP AND AND RESULTS

In this chapter, the fabrication, measurement set-up and measured results of a prototype STEMS are presented. The template of the prototype is made of 12 patches with 32 switches. In section 5.2, the design and fabrication of the STEMS prototype are presented. Details of the fabricated conducting box and monopole antenna are given in section 5.3. The experimental set-up for measuring the STEMS shutter effectiveness is detailed in section 5.4. The results of the measured shutter effectiveness using a random search code and a genetic algorithm are discussed in section 5.5.

5.1 Design and fabrication of STEMS prototype

To fabricate the STEMS prototype, a layout of the template geometry is first realized using ORCAD10.0. The template is laid out as a single layer, square surface of side 27.3cm with 12 surface patches. This layout is selected to be identical to the simulated STEMS of section 4.4. The initial slot width of 9.75mm used in section 4.4 is changed to 7.62mm so that the spacing between surface patches is equivalent to the spacing between the two end pins of the switches that are placed on the template.

To enable the placement of the switches on the template, small areas of copper with diameter 1.5mm are placed on the surface. The diameter of 1.5mm is selected to provide sufficient area to solder the switch pins to the copper. Figure 5.1 shows a sketch of the STEMS template and a screen shot of a copper pad as drawn in orcad is shown in Figure 5.2. Table 5.1 provides the dimensions of the patches used

to create the STEMS surface. The layout of the finished surface was then sent to the Michigan State University ECE Shop where the STEMS template is realized by milling out copper at the location of the slots on an FR4 epoxy circuit board of thickness 1.25mm. This board was selected based on availability.

The type of switch selected for the purpose of this project is a Coto technology SIP REED relay switch series 9011-05-10. This type of switch is selected because it is the same type used on a prototype of the SSA antenna mentioned in section 3.7. A photograph of the switch is shown in Figure 5.3 and its characteristics are presented in Table 5.2.

The switches are soldered on the milled FR4 eproxy board by first drilling through holes of 0.52mm in diameter at the location of the copper pads. The switches are then placed on the bottom layer of the FR4 Eproxy board in such way that the pins go through the holes to the top layer that has the patches and copper pads. The two outer pins of the switches are soldered to the patches while the two inner pins get soldered to the copper pads as shown in Figure 5.4 . Wires are then soldered to the inner pins and connected to the header of a six-inch 64-line ribbon cable. The ribbon cable header is epoxied to the edge of the top layer of the FR4 Eproxy to avoid movements from the wires. A photograph of the switches on the bottom layer is shown in Figure 5.5 while Figure 5.6 shows a photograph of the top layer with the soldered pins, wires, surface patches and ribbon cable.

Prior to soldering the switches, their functionality is tested by conducting a continuity test. The continuity test is performed by measuring the resistance between the two end pins of the switches using an ohmmeter. When the two inner pins are

connected to a 5V supply, the reading of the resistance should be near 0Ω and when the inner pins are left unconnected, a value of -1 should be displayed on the screen of the ohmmeter, indicating an open circuit. A closed switch is characterized by the near 0Ω reading while an open switch is characterized by the value of -1.

To control the states of the switches, the ribbon cable is connected to a control board that serves as interface between the STEMS and the computer. The control board is used to provide the necessary current needed to power the switches. To drive the relays, Toshiba TD62783AP integrated circuits are used. The TOSHIBA TD62783AP are high-voltage source drivers that output 5V on each of the output pins. Each IC has 8 input pins, 8 output pins, 1 ground and 1 VCC pin. To power the 32 switches, 4 Toshiba TD62783AP are needed. The input of the Toshiba TD62783AP are connected to the computer via a 50 pin National Instrument cable connector and a 10 pin ribbon cable connector while the output pins are connected to the switches using a 64 pin ribbon cable connector. A protoboard PB104 is used to implement the control board; a photograph of the finished board is shown in Figure 5.7.

It should be noted at this point that the NEC4 model of the STEMS as discussed in section4.4 was not backed by any substrate. This is due to the fact that NEC4 does not support substrates. A prototype closer to the NEC4 model could have been fabricated using a mesh of wires backed by a foam material because of the near free space characteristics of the foam, but soldering the switches would have been a problem. Besides, the simulation study of chapter4 is performed only to get an insight into the concept of STEMS.

Patch characteristics	
Patch number	Width and Length (mm)
1	49.815, 40.065
2*a*	49.815, 49.815
2*b*	20.565, 10.815
3	59.565, 40.065
4*a*	69.315, 40.065
4*b*	20.565, 20.565
5	79.065, 69.315
6*a*	79.065, 40.065
6*b*	49.815, 20.565
7*a*	79.065, 40.065
7*b*	49.815, 20.565
8	79.065, 30.315
9	49.815, 40.065
10*a*	79.065, 30.315
10*b*	40.065, 30.315
11	79.065, 40.065
12	49.815, 40.065

Table 5.1. Patch Sizes.

Switch Characteristics
Nominal Voltage = 5V
Nominal Current = 10mA
Vmax = 6.5V
Vmin = 3.75V
Coil Resistance = 500Ω
Switching Cycle = 2222/s
Lifetime = 250 million cycles

Table 5.2. Properties of Coto technology SIP REED relay switch.

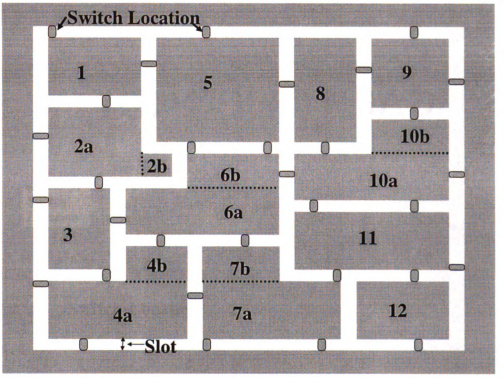

Figure 5.1. Design of the STEMS template.

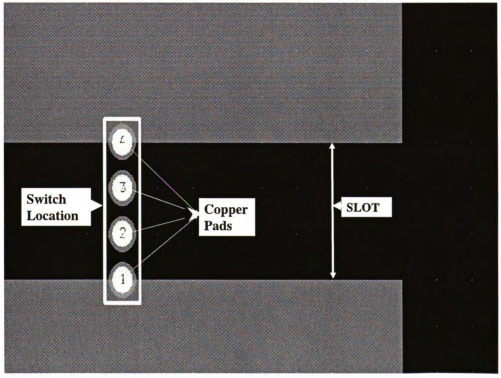

Figure 5.2. Screenshot of the location of a switch marked by copperpads.

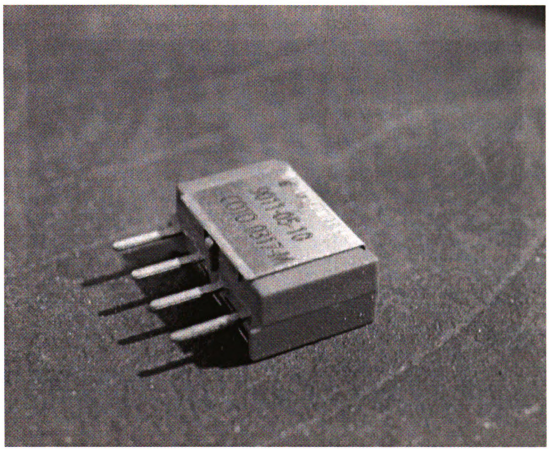

Figure 5.3. Coto technology SIP REED relay switch series 9011-05-10.

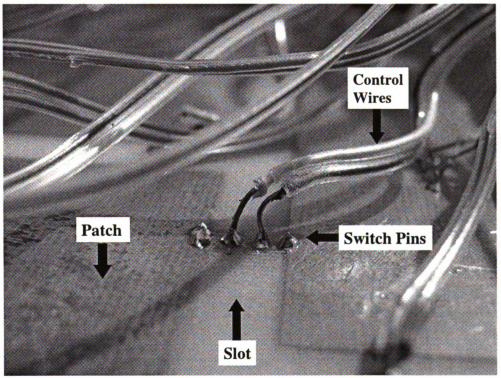

Figure 5.4. Photograph Showing the placement of each switch.

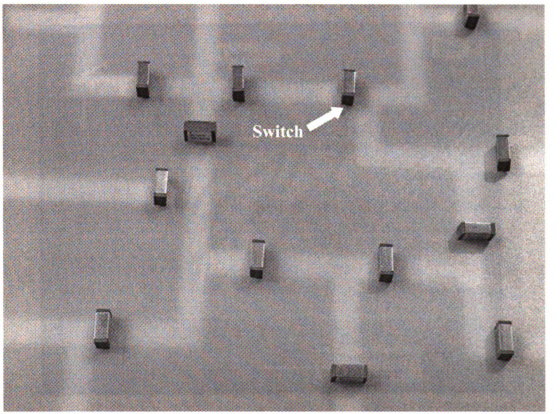

Figure 5.5. Bottom layer of the fabricated prototype with the switches.

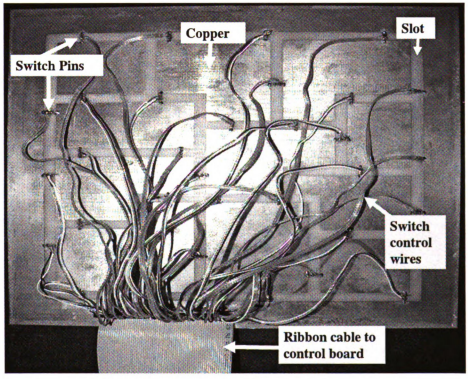

Figure 5.6. Top layer of the fabricated prototype.

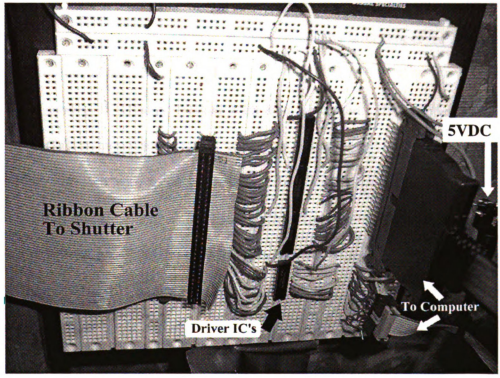

Figure 5.7. Photograph Showing the control board.

5.2 Open box and probe fabrication

As a means to measure the shutter effectiveness of STEMS, a conducting open box and various probes were also fabricated. Fabrication of the conducting open box was done at the Michigan State University Machine Shop using 5 aluminum sheets of equal dimensions (27.3 by 27.3cm). The open box was fabricated by first creating a frame out of aluminum rods. The aluminum sheets were then screwed to the frame to create an open box. To avoid gaps at the edges of the box, copper tape is applied over the contour of the edges of the box.

Three probes of different lengths were also fabricated. The probes are quarter wavelength monopoles fabricated by simply cutting wires of length equal to $\frac{\lambda}{4}$ then soldering each wire to an SMA connector. The wires have the same radius (a=0.645mm) and their lengths are 10cm, 8.82cm and 7.894cm. Their respective resonant frequencies are 750MHz, 850MHz and 950MHz to enable measurements from 700MHz to 1GHz. It is important to note that for the purpose of STEMS measurements, a new monopole antenna does not need to be fabricated each time that a new frequency is selected for measurement. The reason is that the STEMS shutter efficiency is calculated as a ratio of the current on the probe for the box open with the box sealed by the STEMS. A photograph of the fabricated box with a probe is shown in Figure 5.8

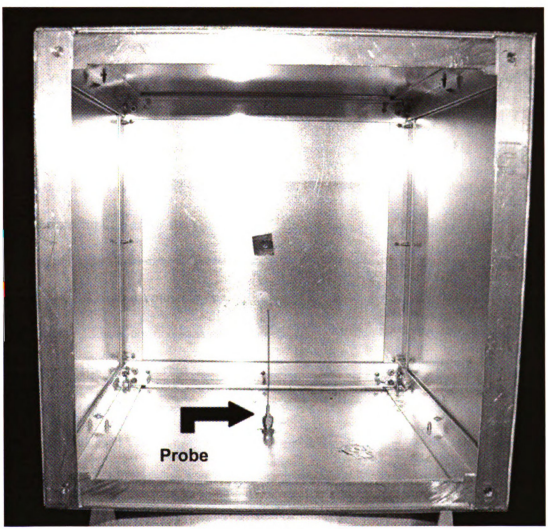

Figure 5.8. Fabricated box with a probe.

5.3 Experiment Set Up

The set-up for the experiment is done following the diagram shown in Figure 5.9. A Hewlett-Packard 8657A Signal Generator is used as a source to the transmit antenna which in this case is a broadband horn antenna (500MHz to 6GHz). The connection between the signal generator and the transmit antenna is done using a coaxial Type-N cable as shown in Figure 5.10. A photograph showing how the horn antenna is placed inside the anechoic chamber with reference to the box is shown in Figure 5.11.

The receiver as shown in Figure 5.12 is a Singer Stoddart NM-37/57 EMI/Field Intensity Meter that connects to the computer and the probe. The probe is connected to the front input port of the receiver through a coaxial Type-N cable. The computer used is a Fujitsu B-Series Lifebook laptop with a 700MHz Pentium 3 processor and 512MB of RAM that connects to the control board and the video log output port of the receiver. These connections are achieved using two national Instrument PCMCIA DAQ cards that are inserted into the computer. These cards are: DAQCard-DIO-24 and DAQCard-6024E as shown in Figure 5.13. The DAQCard-DIO-24 is a 24 bit input/output card that connects to the 50 pin header of the control board through a ribbon cable. The DAQCard-6024E is a 12 bit input/output card with a 16 channel in, 2 channel out analog to digital converter (ADC) that has a sampling rate of 200,000/s. Only 1 of the ADC channels along with 16 channel in of the DAQCard-6024E are used in this set up. The DAQCard-6024E connects to the 10 pin header of the control board and the video log output port of the receiver via a split ribbon cable that is shown is Figure 5.14

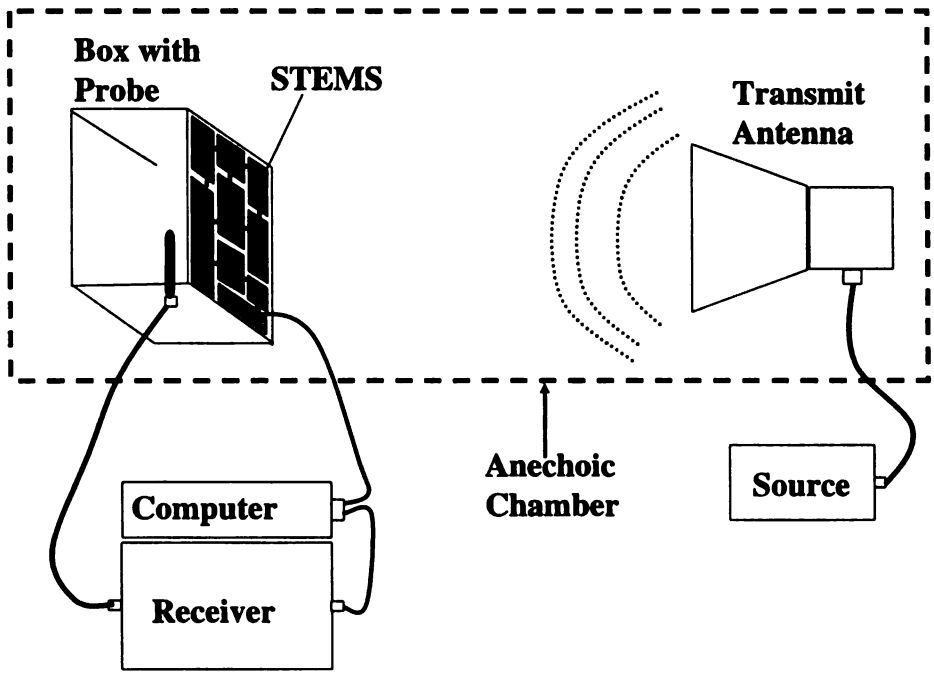

Figure 5.9. Diagram of the set-up used to measure the STEMS.

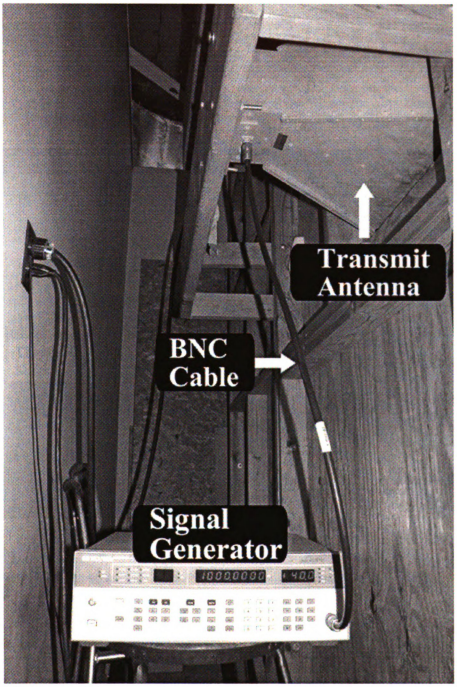

Figure 5.10. Signal generator connected to the transmit antenna.

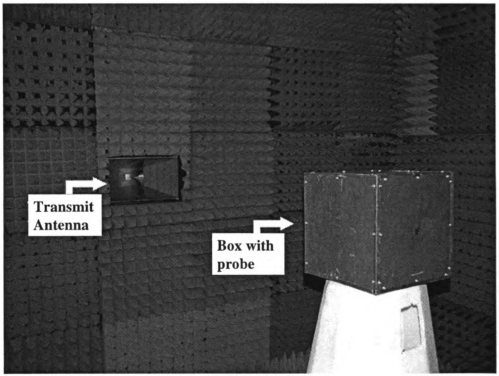

Figure 5.11. Box and transmit antenna inside the anechoic chamber.

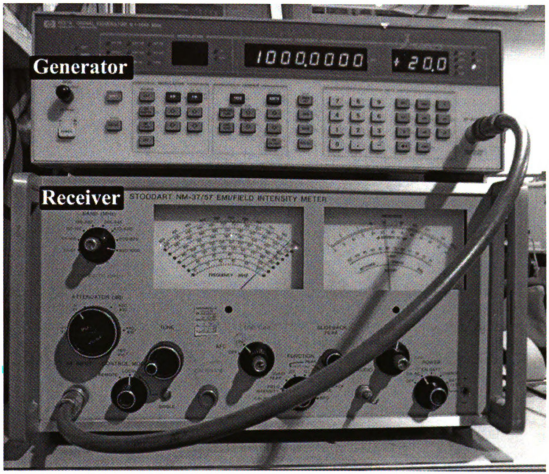

Figure 5.12. Photograph showing the receiver

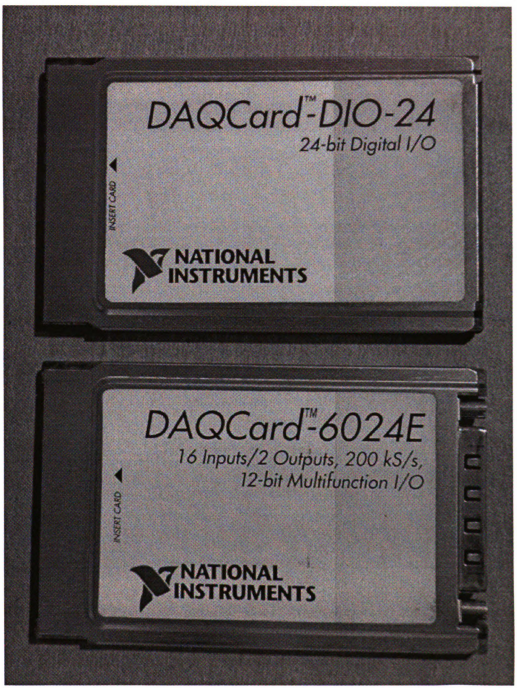

Figure 5.13. National Instrument Data Acquisition cards

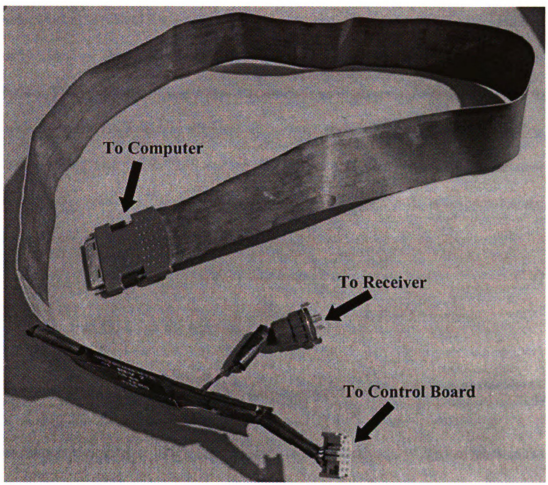

Figure 5.14. National Instrument split ribbon cable

5.4 Evaluating the STEMS shutter effectiveness

In order to evaluate the STEMS shutter effectiveness, the transmit antenna is first excited at the desired frequency X by the source with an amplitude of Y volts. Then the open box voltage is measured by the receiver through the probe within the box. A code written in Visual Basic (included in the appendix) is used to capture the reading of the receiver through the use of the analog to digital converter card, DAQCard-6024E. The open box voltage is saved in the code as reference voltage V_O and used to evaluate the STEMS shutter efficiency at the same specific frequency X. The open box is then sealed with the STEMS and the STEMS voltage, V_S, measured by the receiver is sent to the computer for evaluation. The shutter effectiveness S_e is evaluated using:

$$S_e = 20 * log_{10} \frac{V_O}{V_S}. \tag{5.1}$$

Notice that Eq-5.1 is the same as,

$$S_e = 20 * log_{10} \frac{I_O}{I_S}, \tag{5.2}$$

as defined in chapter 4. The reason is due to the relationship $V = R*I$ which requires $V_O = R*I_O$ and $V_S = R*I_S$. Here R is the 50Ω impedance of the receiver; therefore,

$$\frac{I_O}{I_S} = \frac{V_O}{V_S}. \tag{5.3}$$

It is important to point out that the system must be calibrated each time before any measurement is made at a given frequency. It was observed in a previous project

[47] that the voltage reported by the computer is not the same as the input voltage to the receiver. Therefore, the voltage at the receiver output V_{log} must be converted to give the input voltage V_O . Through experimentation, it was found that the conversion equation is:

$$V_O = 10^{\frac{V_{log} - AB}{\cdot}} \tag{5.4}$$

where A and B are variables that need to be determined for each frequency. A and B are found by connecting the input port of the receiver directly to the source. In this manner, the value of V_O ia be the same as the amplitude at which the source is set. Knowing V_O, Eq-5.4 can be solved by setting V_O to two different values and using the values obtain for V_{log} to solve for A and B.

5.5 Measurement results

To gain a better understanding of STEMS, several tests were performed on the built prototype. The first analysis performed on the prototype was a statistical study to determine the distribution of the STEMS shutter effectiveness for a random sample space of 50000 switch configurations. The next study performed was an optimization of the STEMS template using a genetic algorithm. The results obtained from the random search and genetic algorithm are compared to determine the most efficient approach for finding appropriate STEMS configurations.

To perform the random search and genetic algorithm analysis, the box and probe are set up in the far field region of the transmit antenna in such a way that the

fields from the transmit antenna are normally incident on the the STEMS as shown in Figure 5.15 with $\theta = 90°$ and $\phi = 0°$.

A third study of the STEMS behavior was performed where the STEMS was displaced 4Ft sideways from its original location, also shown in Figure 5.15. Even though the STEMS is still located within the anechoic chamber, the displacement by 4Ft creates a different environment where the waves from the transmit antenna are no longer normally incident on the STEMS. Hence, this technique enables the study of the STEMS for an oblique incidence angle given by ($\theta = 90°$ and $\phi = 41.6°$).

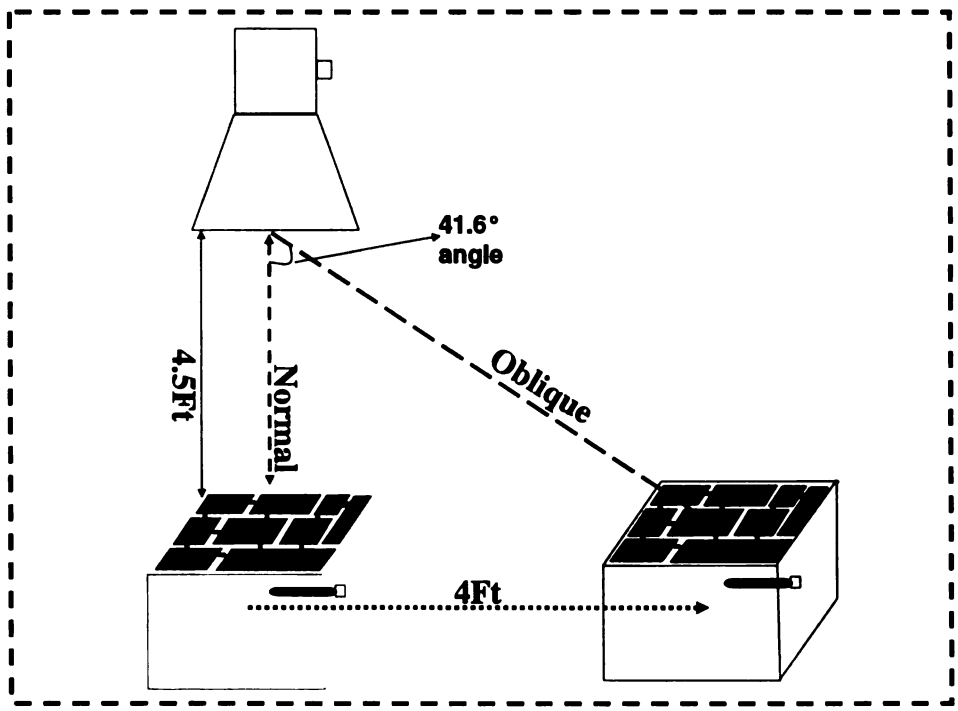

Figure 5.15. Box placement for normal and oblique measurements

5.5.1 Random Search

The first experimental test performed on the prototype STEMS is a statistical study of the STEMS shutter effectiveness for a random sample of 50000 switch configurations. With 32 switches used on the STEMS template, 50000 switch configurations represents only 0.001164% of the total 4.295 billion states. In order to carry out the evaluation of the 50000 random states, a simple Visual Basic code was written. Before all the states can be evaluated, the open box voltage is read and saved in the Visual Basic code. Then, the box is sealed with the STEMS template and all of the 50000 random switch configurations are evaluated one at a time.

The code reads from a file of random 8 bit binary strings. Each bit is assigned to a switch and the state of the switch is set with reference to the value of the binary bit. For each switch, if the assigned bit is a 1, the switch is turned on and if the bit is a 0, then the switch is left open. Since there are 32 switches on the STEMS template, the code reads four 8 bit strings at a time.

Once the states of all 32 bits are set, the voltage on the probe is read and the shutter effectiveness of the present state is evaluated with reference to the open box voltage by using Eq-5.1. The shutter effectiveness is evaluated for all 50000 random switch configurations and saved to a text file. The process starting with the measurement of the open box voltage was repeated for 13 evenly spaced frequencies selected between 700MHz and 1000MHz with a step size of 25MHz using the same 50000 swtich configurations. Once all 50000 states are evaluated, the histogram of the sample is plotted using a code written in Matlab. The random search and histogram

codes are included in the appendix.

The first frequency selected is 700MHz. As shown in Figure 5.16, the shutter effectiveness of all 50000 states measured varies between -44dB and -5dB. It is also observed that over 98% of all the states considered have a shutter effectiveness between -32.3dB and -8.9dB. A closer view of Figure 5.16 as shown in Figure 5.17 reveals that only 2 switch configurations have a sutter effectiveness of -40dB or lower, while only one state is found with S_e=-5dB. If -40dB is selected to be an acceptable shutter effectiveness to create a closed surface, only 2 switch configurations or 0.004% of the 50000 random sample would be able to provide the desired result. Likewise, if -6dB is selected as an acceptable value to create an open surface, only 5 out of the 50000 random sample would be able to perform as required. However, this implies that approximately $(5/50000) * 4295000000 = 429500$ of the STEMS configurations have at least this value. 429500 represents a big number of states. Thus, there is hope that a good search algorithm may be able to quickly find one of these states, or perhaps even a better state.

The second frequency considered is 725MHz. At this frequency, As shown in Figure 5.18, the distribution of the shutter effectiveness is between -26dB and -6dB with over 99% of the 50000 random states considered ranging between -24dB and -7dB. Figure 5.19 shows that the -6dB required to create an open surface is achieved by 3 states while none of the 50000 random sample was able to provide the requiered -40dB to create a closed surface.

The third frequency selected for measurement is 750MHz. The histogram at this frequency as shown in Figure 5.20 shows a pattern very different from those obtained

at 700MHz and 725MHz. The distribution of the shutter effectiveness is skewed toward lower values with 37571 states having a shutter effectiveness of -43dB or less. While there is an abundance of states capable of creating a closed surface, no state was found with a shutter effectiveness of -6dB or higher. A closer view of the distribution of the shutter effectiveness as shown in Figure 5.21 reveals that the highest S_e value obtained is -7dB, showing that none of the sample of 50000 states considered can be used to create an open surface.

The distribution of the shutter effectiveness at 775MHz is shown in Figure 5.22 and Figure 5.23. Analysis of these plots shows a distribution of the shutter effectiveness skewed toward higher values with 804 random states having a shutter effectiveness of -6dB or higher. This means that 1.61% of the 50000 states are able to create an open surface. On the other hand, Only 23 states have a shutter effectiveness lower than -40dB with the lowest value recorded to be -50.94dB.

At 800MHz, the distribution of the shutter effectiveness as shown in Figure 5.24 reveals 148 states with a positive value of S_e. These positive values signify that the voltage measured by the probe for all 148 different switch configurations have a value greater than the open box probe voltage. 14817 states out of the 50000 random states have a value of S_e greater than -6dB. This implies that 29.63% of the sample space considered can be used to create an open surface. Though over 25% of the sample space states are capable of creating an open surface, Figure 5.25 shows that only 1 switch configuration with S_e¡-40dB is capable of creating a closed surface.

At 825MHz, a distribution of the shutter effectiveness similar to that of Figure 5.24 is observed. As seen in Figure 5.26, over 97% of the 50000 random states considered

have a value of S_e ranging between -14.6dB and 4dB. 1075 switch configurations have a positive S_e value and 16142 have a value of S_e greater than -6dB. Unlike 800MHz, the lowest shutter effectiveness was recorded to be -26.1925dB. A closer view of the distribution of the shutter is shown in Figure 5.27.

The following frequency selected for measurement was 850MHz. This frequency produced the worst results with regards to creating a closed surface. As shown in Figure 5.28 and Figure 5.29. No state out of the 50000 random sample was able to produce a shutter effectiveness lower than -13.06dB. On the other hand, up to 43466 states with a shutter effectiveness greater than -6dB were found.

The next frequency of interest was 875MHz. Though none of the 50000 random states produced a shutter effectiveness capable of creating a closed surface, the histograms as shown in Figure 5.30 and Figure 5.31 show a better distribution compared with the distribution obtained at 850MHz. The lowest S_e found was -38.523dB, which is just -1.477dB short from the desired value of -40dB. 6128 states produced a shutter effectiveness greater than -6dB.

At 900Mhz, the histogram of the shutter effectiveness as shown in Figure 5.32 reveals the lowest value of S_e=-58.3022dB recorded among all frequencies measured so far. A closer view of the distribution of the shutter effectiveness as shown in Figure 5.33 shows 28 different states with a shutter effectiveness less than -40dB. 1579 states were also recorded to have a shutter effectiveness greater than -6dB. Unlike 875MHz and 850MHz, no state was recorded to have a positive value of S_e.

A 925 MHz, results similar to those recorded at 900MHz are observed. Figure 5.34 shows a distribution of the shutter effectiveness skewed toward higher values

of S_e with its highest recorded to be -3dB. The lowest value of S_e is found to be -54.0146dB. Of all 50000 states measured, 104 were found to have a value of S_e lower than -40dB while 890 states produced a value S_e greater than -6dB. A close view of the distribution of the shutter effectiveness is shown in Figure 5.33.

At 950MHz, a pattern similar to that of 925MHz is observed as shown in Figure 5.34. The lowest S_e recorded was found to be -56.37dB. One state produced a positive value of S_e=0.138dB and 9378 states have a value of S_e higher than -6dB. Only 122 states were recoded with S_e lower than -40dB. A close view of the distribution of the shutter effectiveness is shown in Figure 5.37.

The final 2 frequencies considered are 975MHz and 1000MHz. The distributions obtained for these two frequencies were very similar to 950MHz, 925MHz and 900MHz. As shown in Figure 5.38 and Figure 5.39 the distribution of the shutter effectiveness at 975MHz reveals that over 49232 states are between -30dB and 2dB with 1278 states having a value of S_e greater than -6dB. Only 56 states were recoded to have a shutter effectiveness of -40dB or lower. The distribution of the shutter effectiveness at 1000MHz is shown in Figure 5.40 and Figure 5.41. Though the lowest value of S_e in the 900Mhz to 1000MHz range was recorded at 1000MHz with S_e=-48.8005dB the highest value of S_e among all frequencies analyzed was recorded at 1000MHz with S_e=8.585dB. A close view of the distribution of the shutter effectiveness at 975MHz and 1000MHz are shown shown in Figure 5.37. At 1000MHz, 36 states have a value of S_e lower than -40dB while 13722 have a shutter effectiveness greater than -6dB.

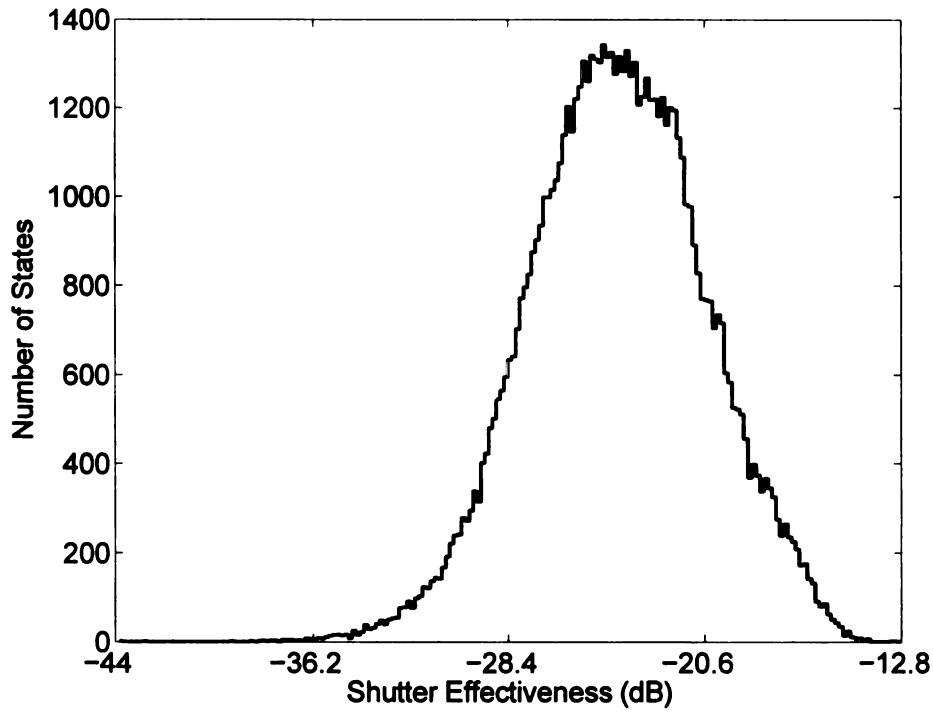

Figure 5.16. Distribution of S_e for a random sample of 50000 states at 700MHz

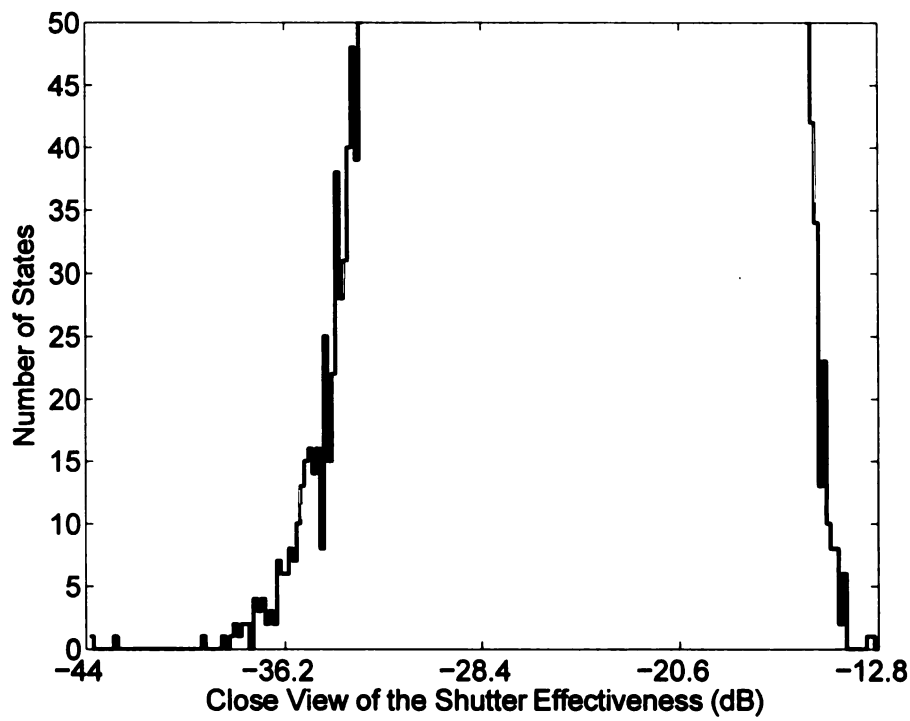

Figure 5.17. Close view of the distribution of S_e for the random sample at 700MHz

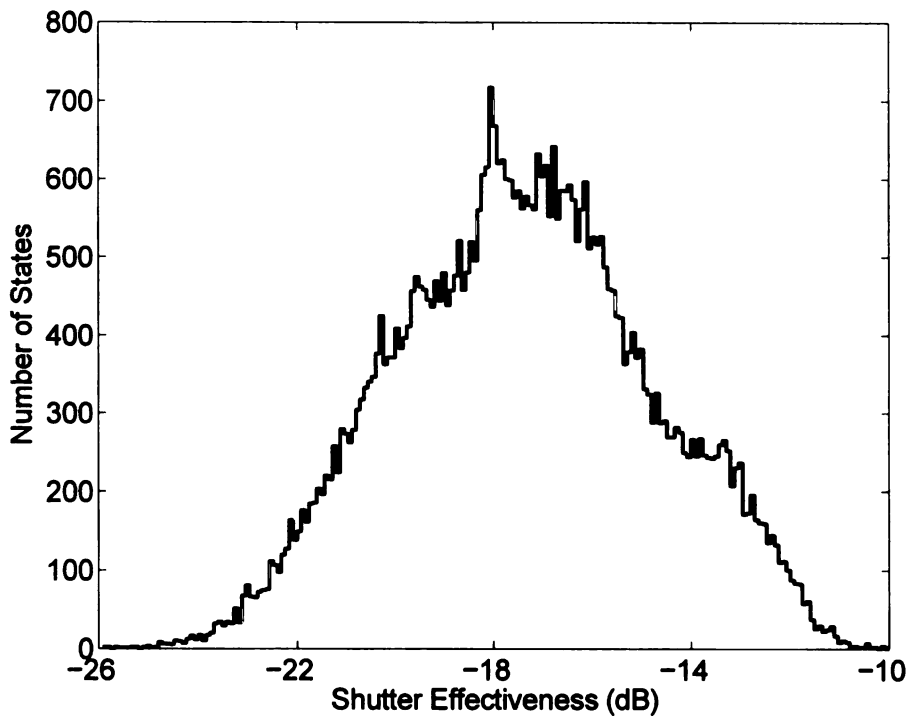

Figure 5.18. Distribution of S_e for a random sample of 50000 states at 725MHz

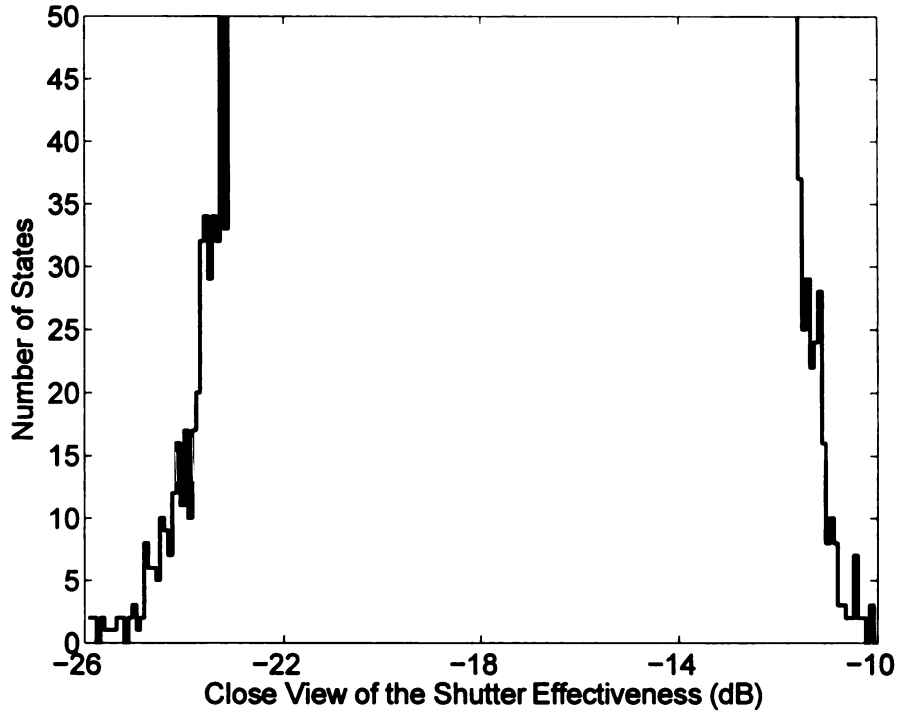

Figure 5.19. Close view of the distribution of S_e for the random sample at 725MHz

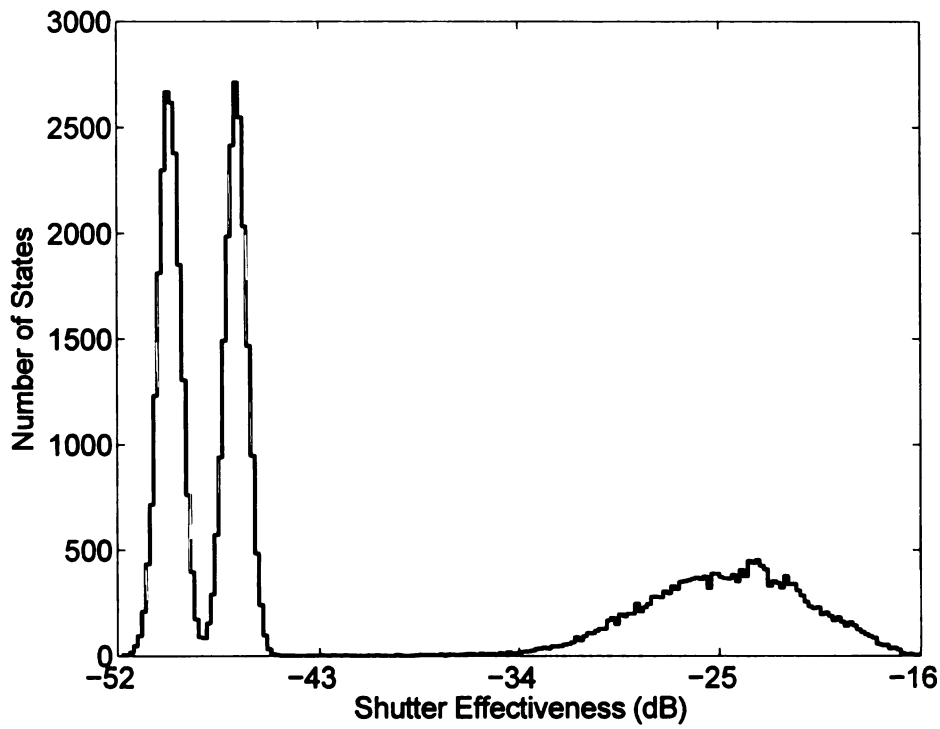

Figure 5.20. Distribution of S_e for a random sample of 50000 states at 750MHz

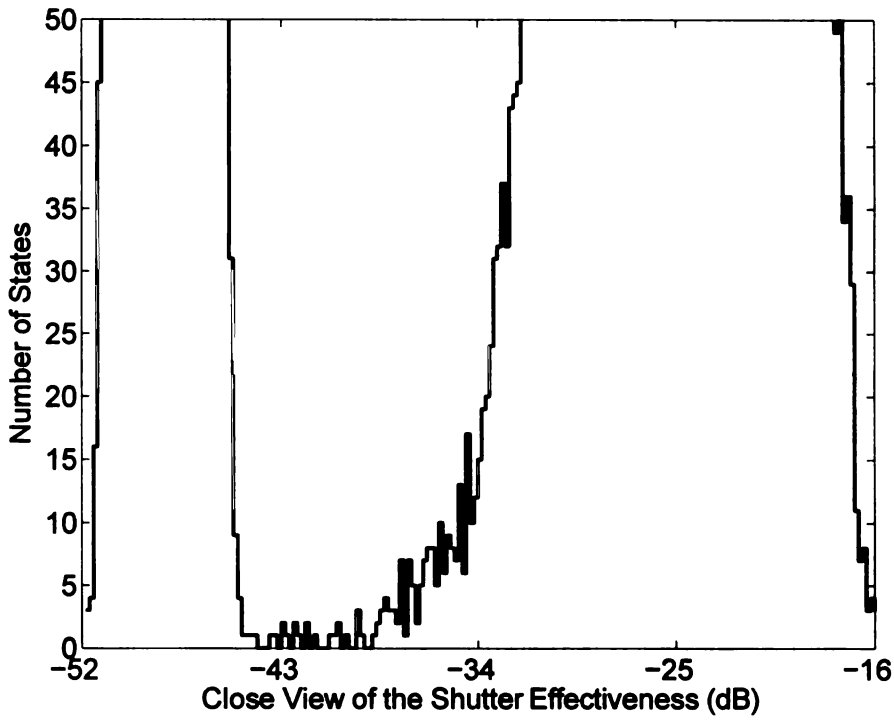

Figure 5.21. Close view of the distribution of S_e for the random sample at 750MHz

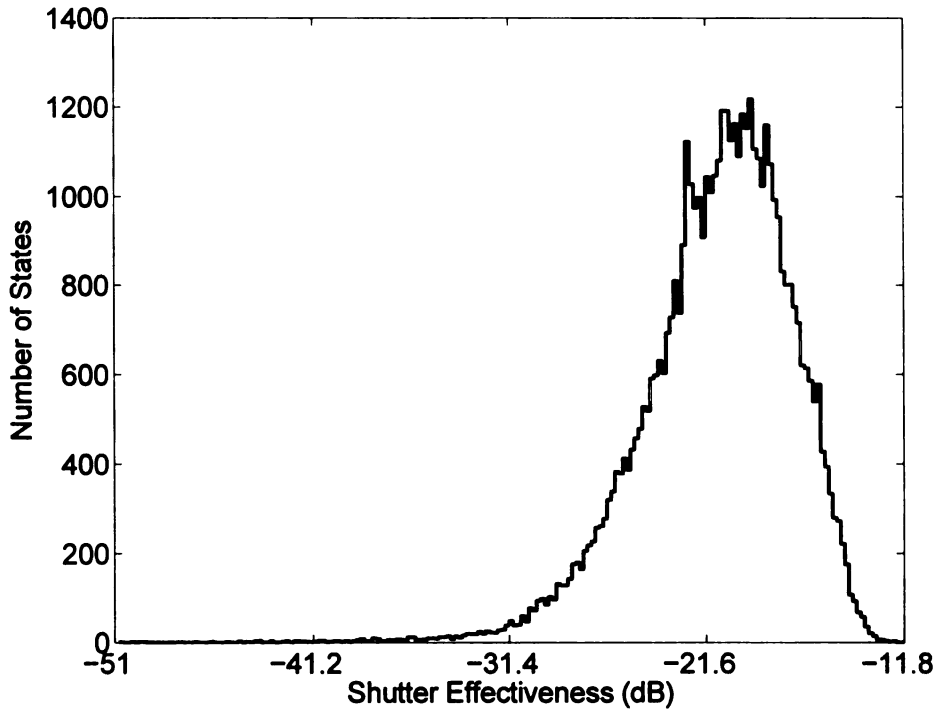

Figure 5.22. Distribution of S_e for a random sample of 50000 states at 775MHz

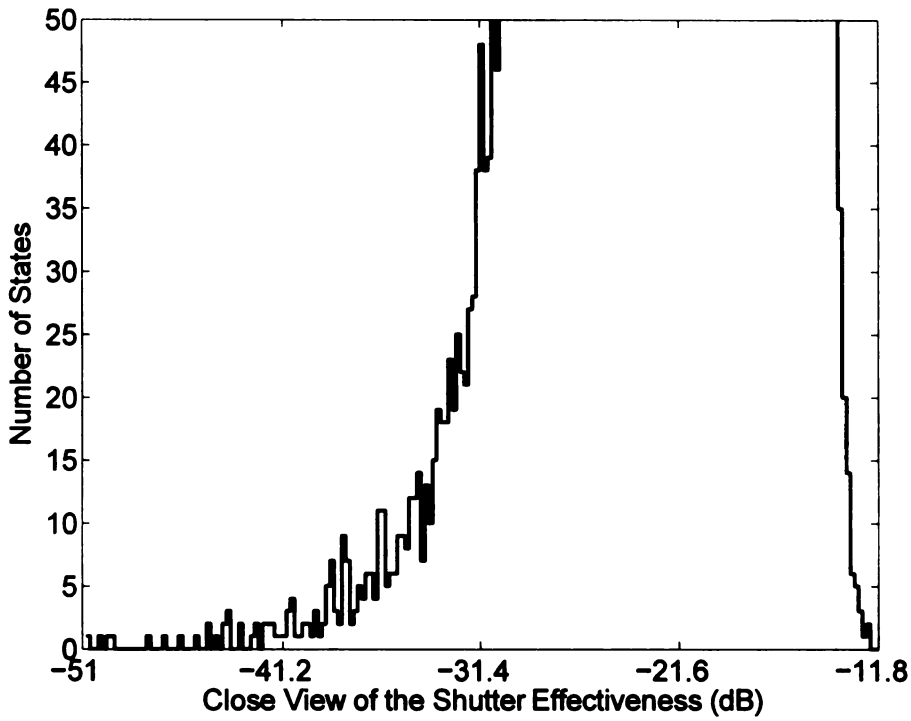

Figure 5.23. Close view of the distribution of S_e for the random sample at 775MHz

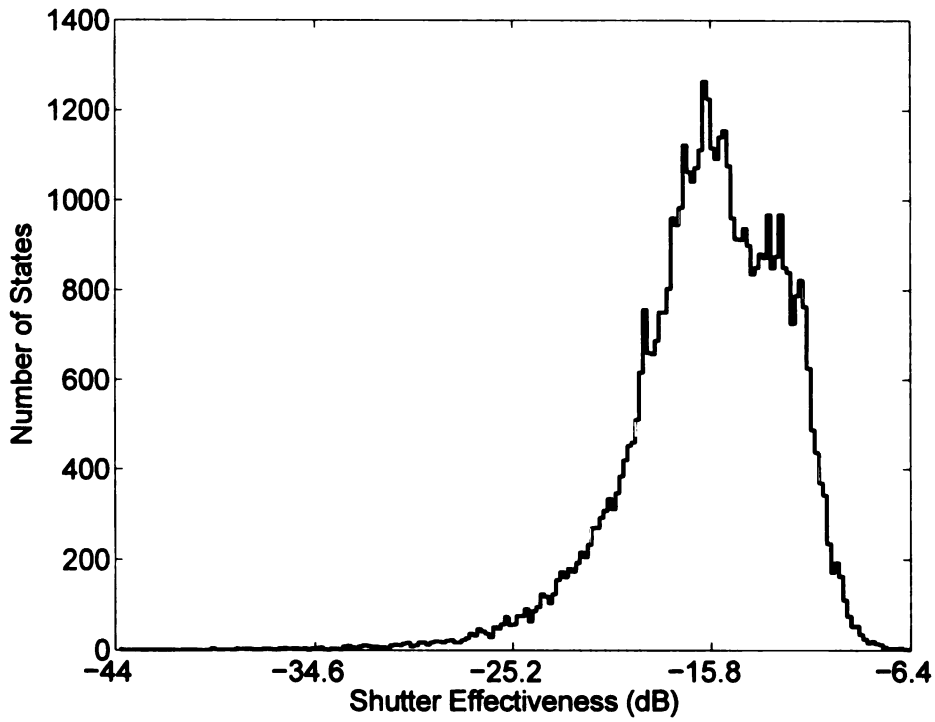

Figure 5.24. Distribution of S_e for a random sample of 50000 states at 800MHz

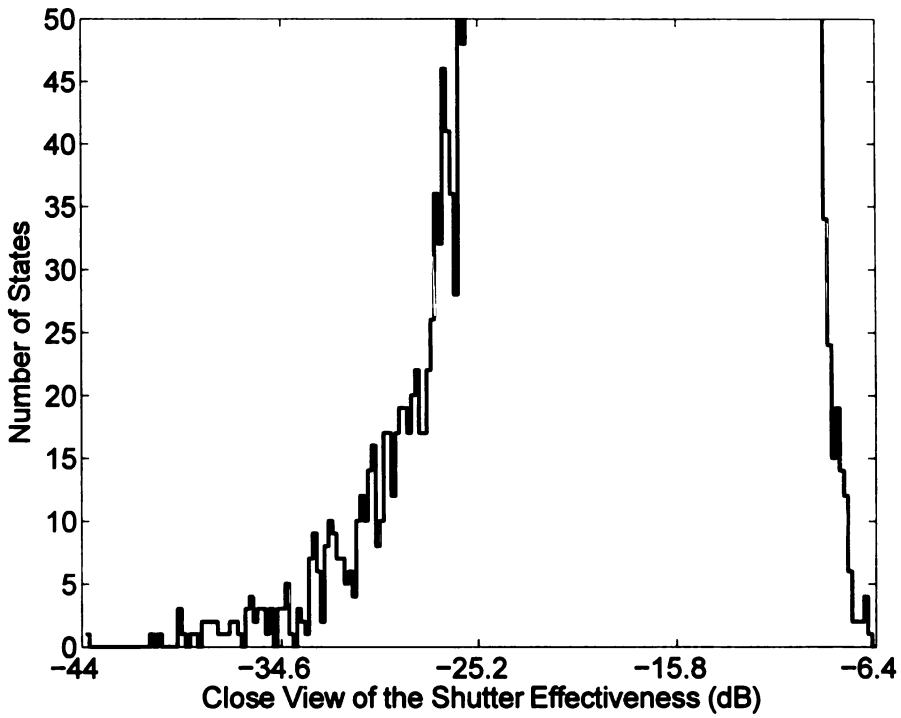

Figure 5.25. Close view of the distribution of S_e for the random sample at 800MHz

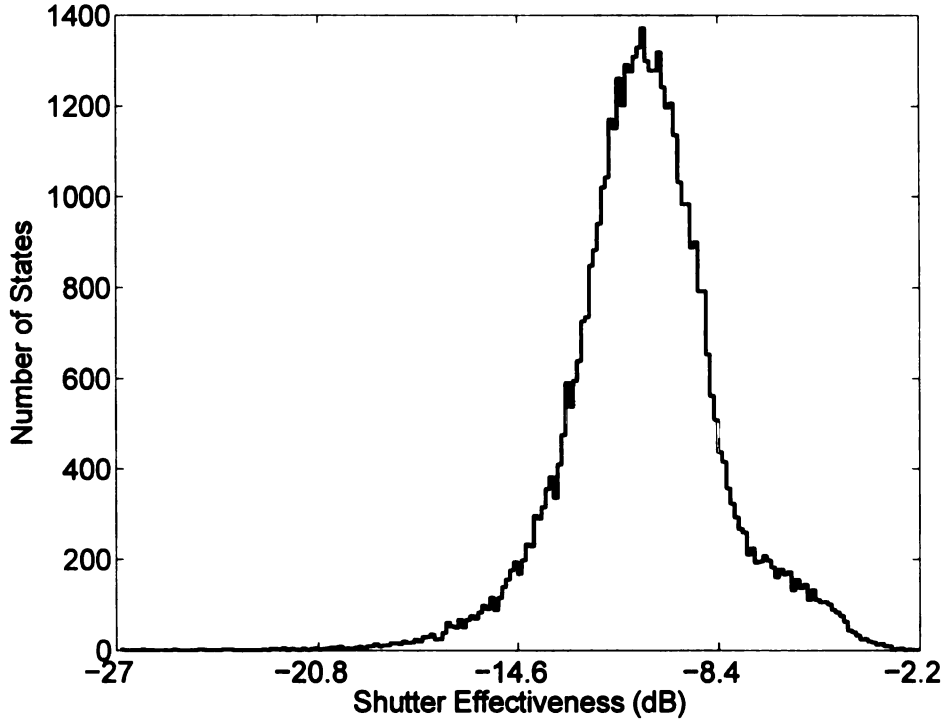

Figure 5.26. Distribution of S_e for a random sample of 50000 states at 825MHz

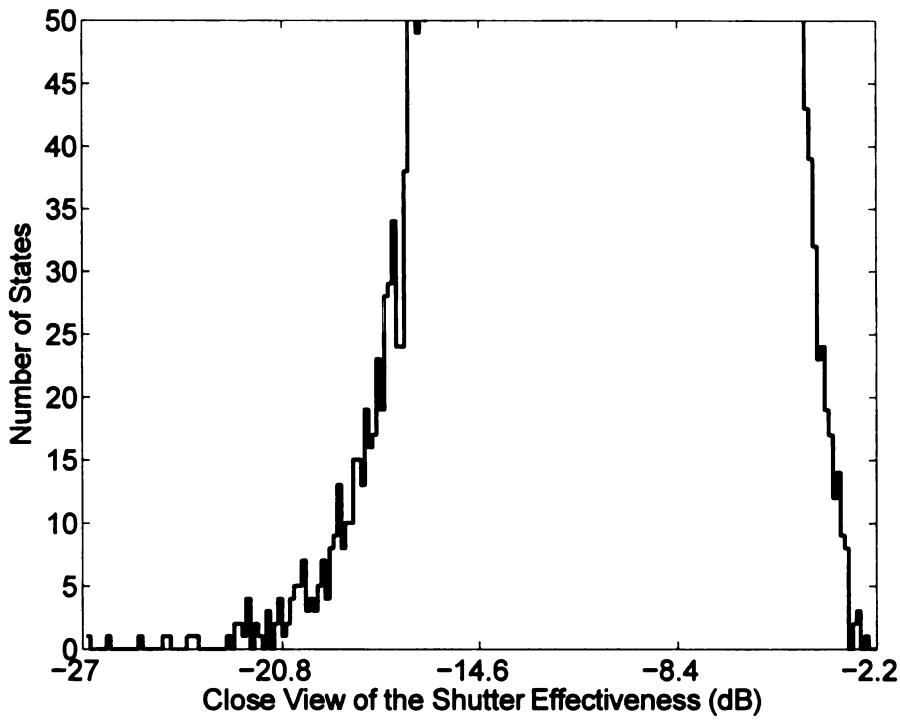

Figure 5.27. Close view of the distribution of S_e for the random sample at 825MHz

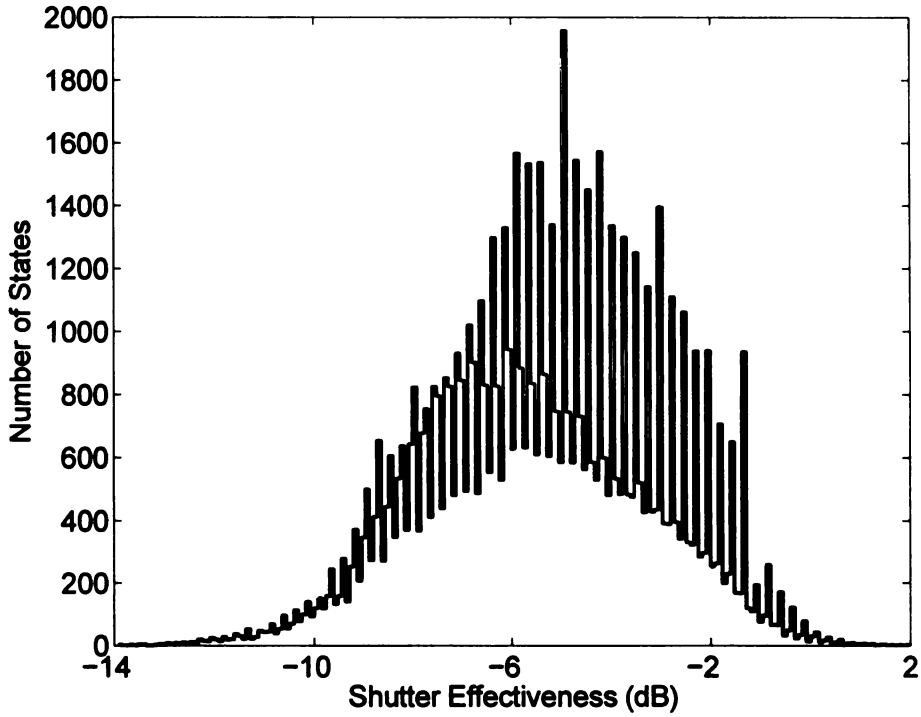

Figure 5.28. Distribution of S_e for a random sample of 50000 states at 850MHz

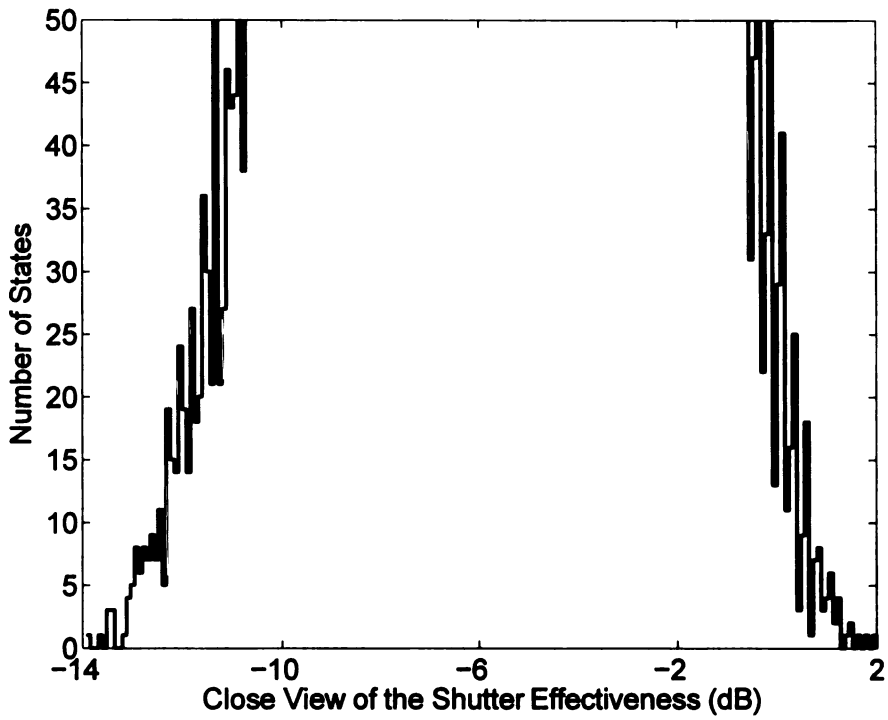

Figure 5.29. Close view of the distribution of S_e for the random sample at 850MHz

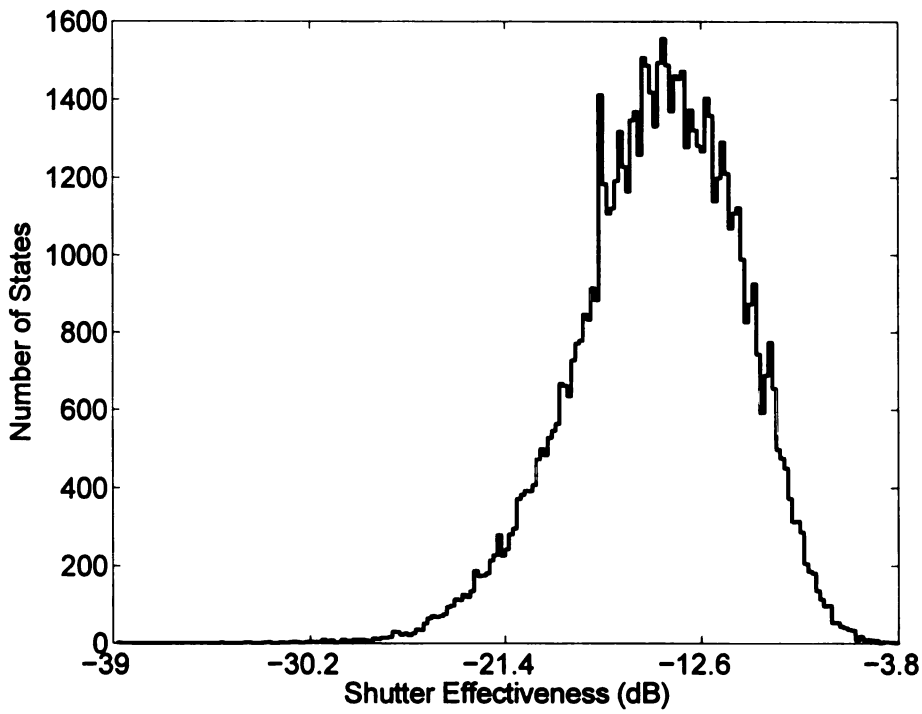

Figure 5.30. Distribution of S_e for a random sample of 50000 states at 875MHz

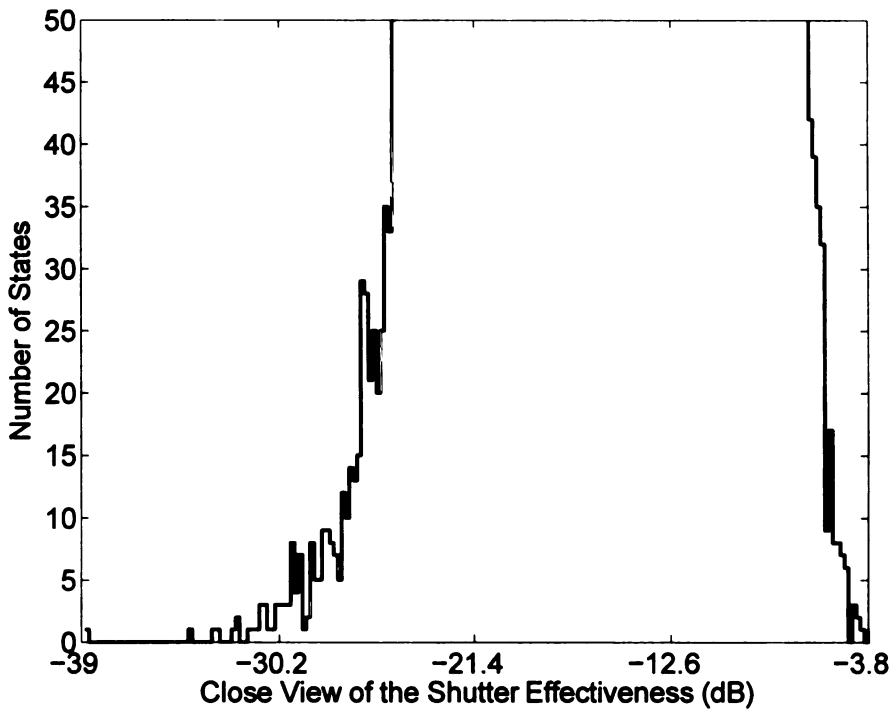

Figure 5.31. Close view of the distribution of S_e for the random sample at 875MHz

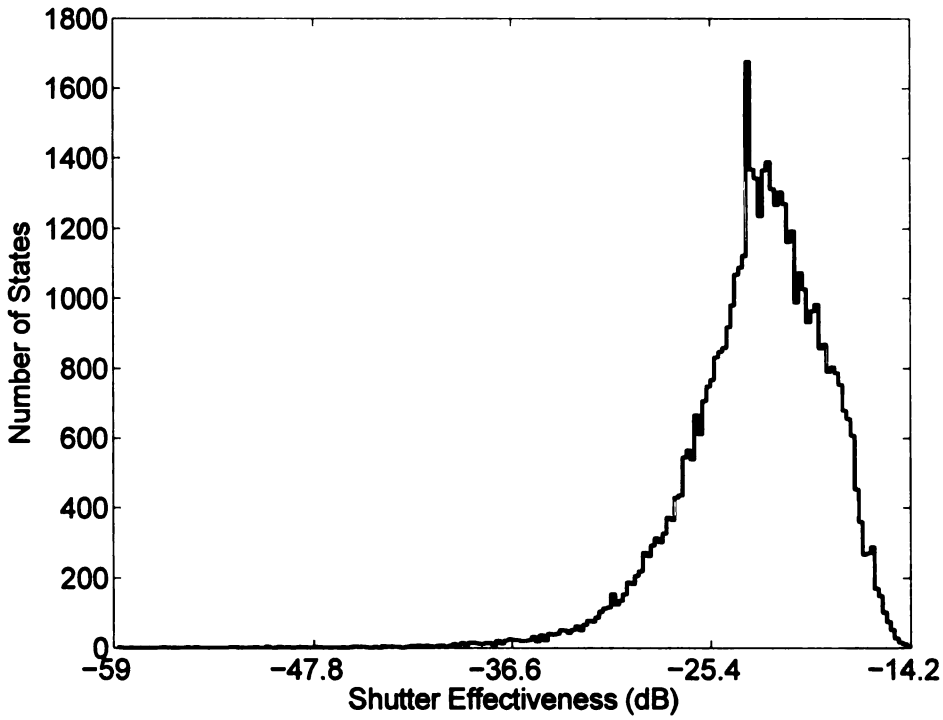

Figure 5.32. Distribution of S_e for a random sample of 50000 states at 900MHz

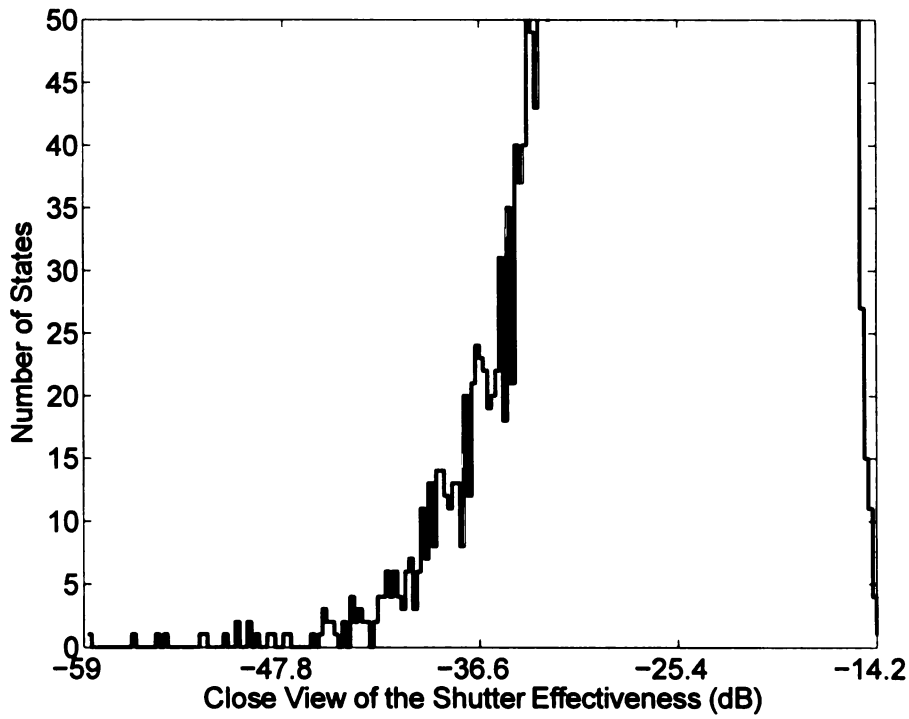

Figure 5.33. Close view of the distribution of S_e for the random sample at 900MHz

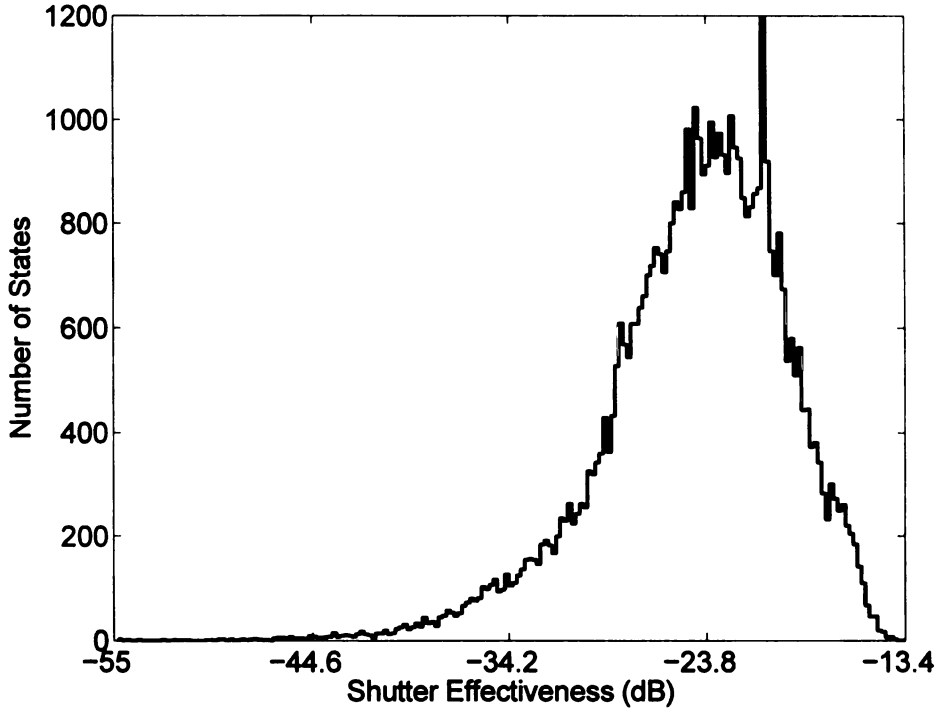

Figure 5.34. Distribution of S_e for a random sample of 50000 states at 925MHz

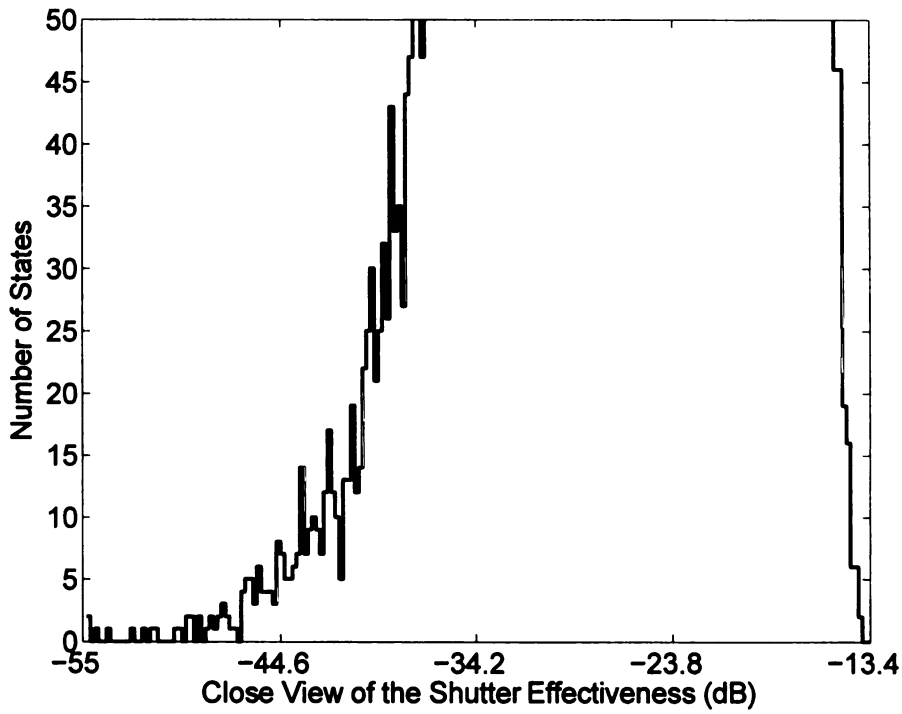

Figure 5.35. Close view of the distribution of S_e for the random sample at 925MHz

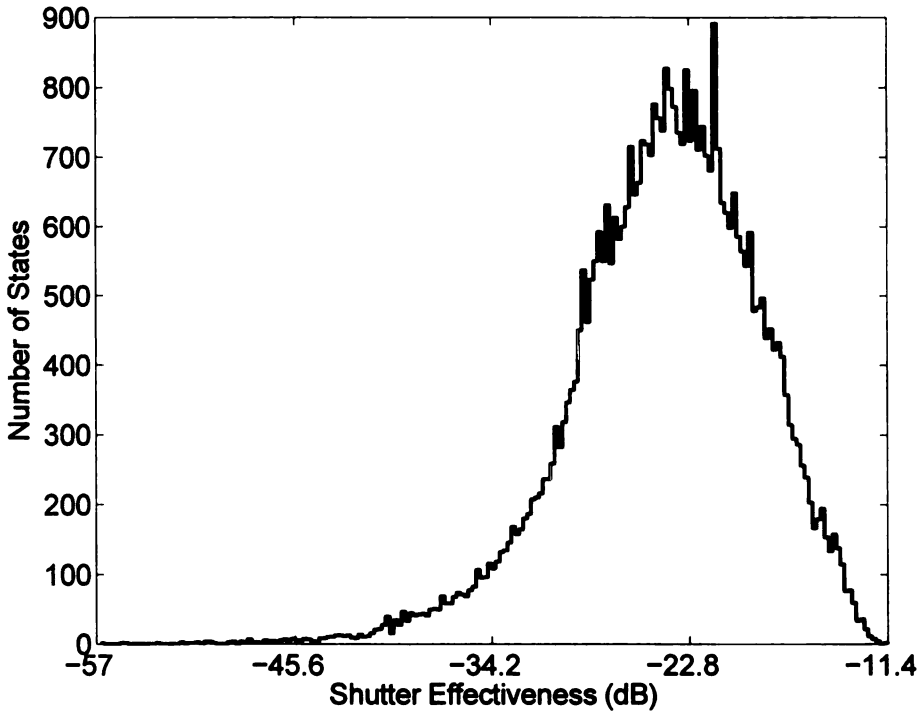

Figure 5.36. Distribution of S_e for a random sample of 50000 states at 950MHz

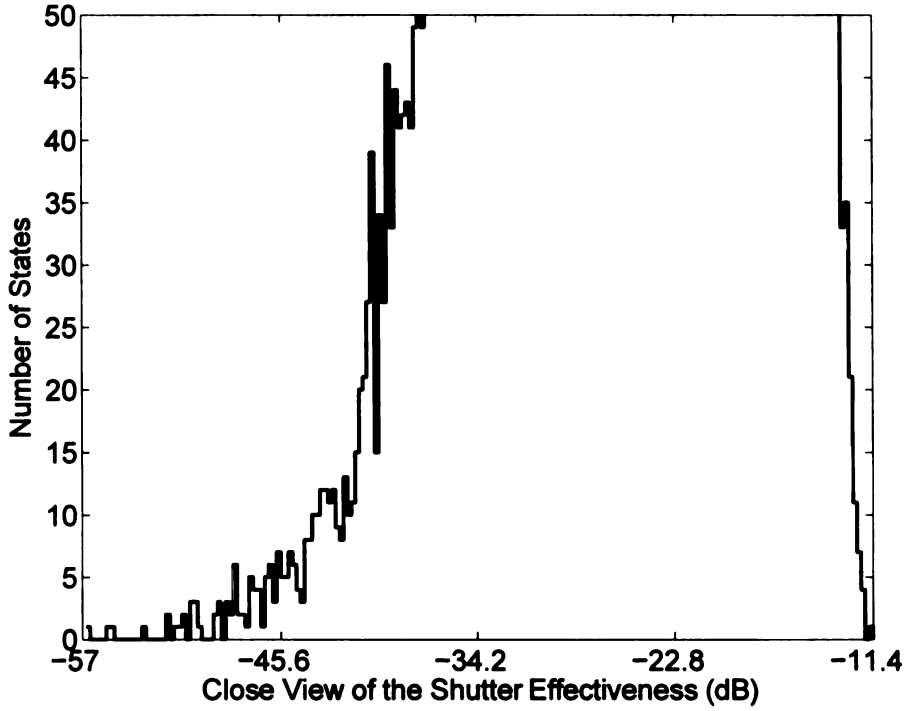

Figure 5.37. Close view of the distribution of S_e for the random sample at 950MHz

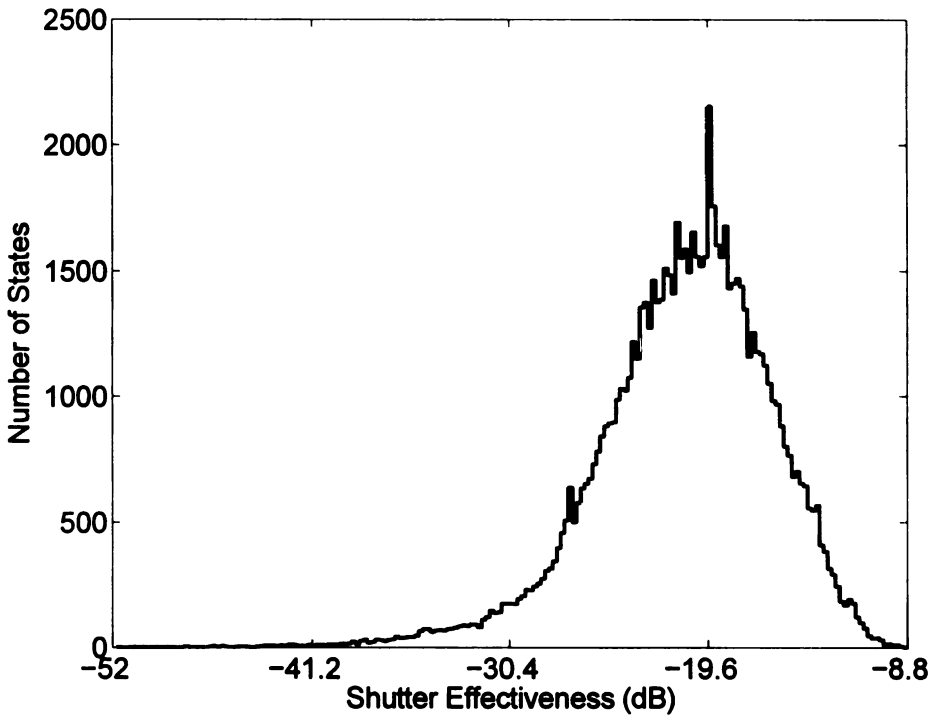

Figure 5.38. Distribution of S_e for a random sample of 50000 states at 975MHz

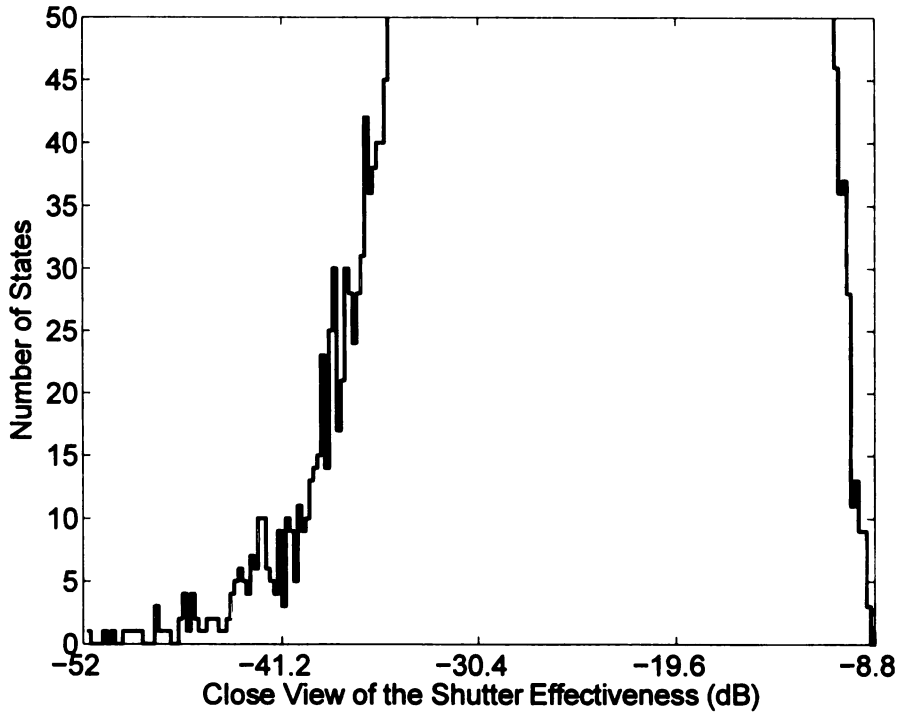

Figure 5.39. Close view of the distribution of S_e for the random sample at 975MHz

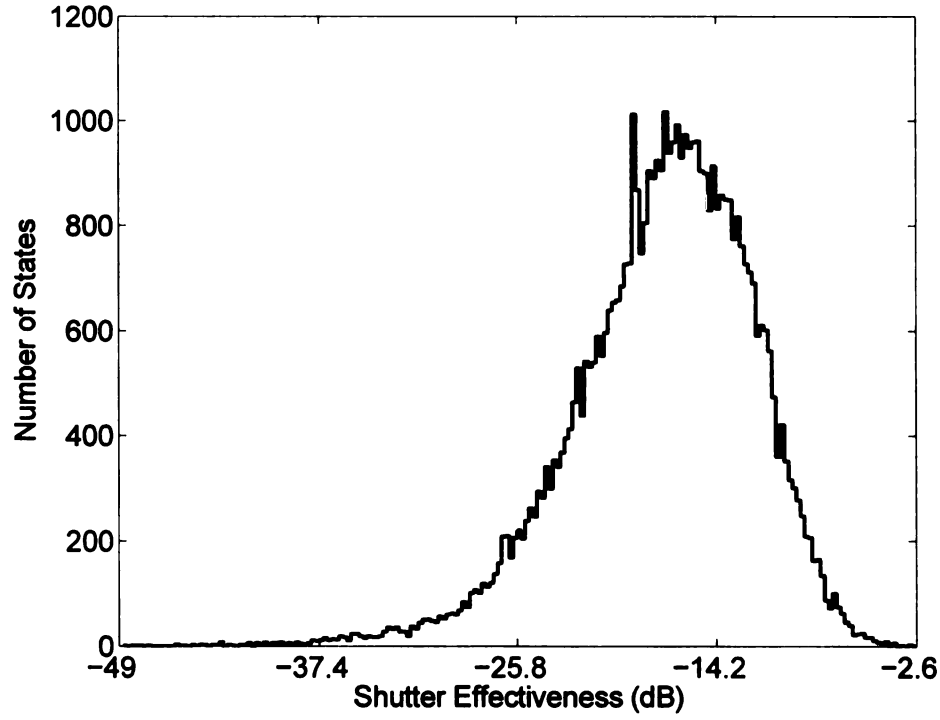

Figure 5.40. Distribution of S_e for a random sample of 50000 states at 1000MHz

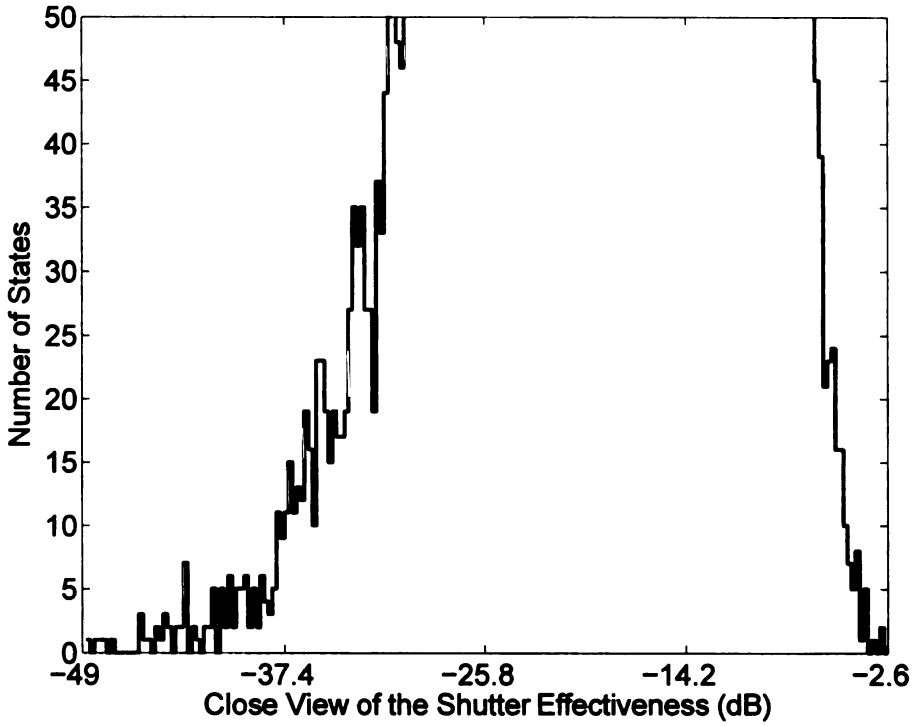

Figure 5.41. Close view of the distribution of S_e for the random sample: 1000MHz

Recall that a state is capable of creating a closed surface if it has a shutter effectiveness of -40dB or lower. Similarly, a state is capable of creating an open surface if it has a shutter effectiveness of -6dB or higher. A summary of the percentage of states capable of creating an open or closed surface for all the frequencies analyzed is shown in Figure 5.42 and Figure 5.43. From these plots, it can be observed that the random search failed to find a state capable of creating a closed surface at 725MHz, 825MHz, 850MHz and 875MHz. It found only 1 state at 800MHz and 2 states at 700MHz. These are results obtained for a sample space of 50000 states and the total measurement time per frequency for all 50000 states is 3hrs and 35mn. These results are not satisfactory because of the low probability of finding acceptable states.

Better results are obtained as far as finding states capable of creating an open surface. The random search only failed at 750MHz and barely made it at 700MHz and 725MHz. At the frequencies where no acceptable values where obtained, a bigger sample space of 100000 states was evaluated but still with no success. This does not imply that there are no states at those frequencies capable of creating a closed or open surface. With 32 switches, there are over 4.2 billion states and 100000 only represents a mere fraction of the total possible states. To avoid evaluating all 4.2 billion states, a more sophisticated search algorithm becomes needed to complete the task.

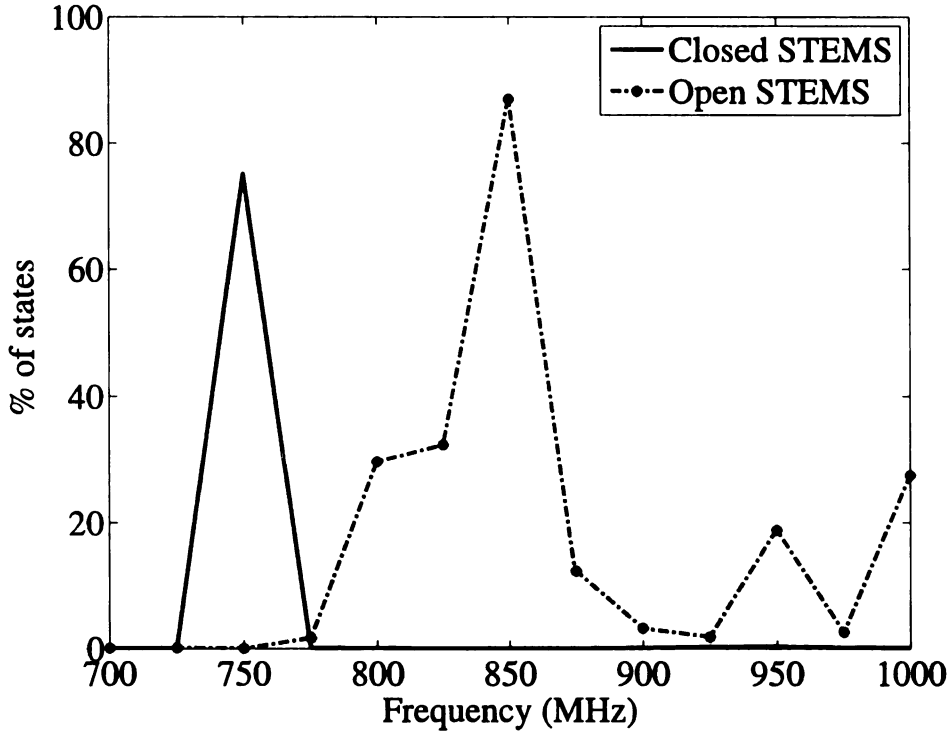

Figure 5.42. Percentage of states for a sample of 50000 states

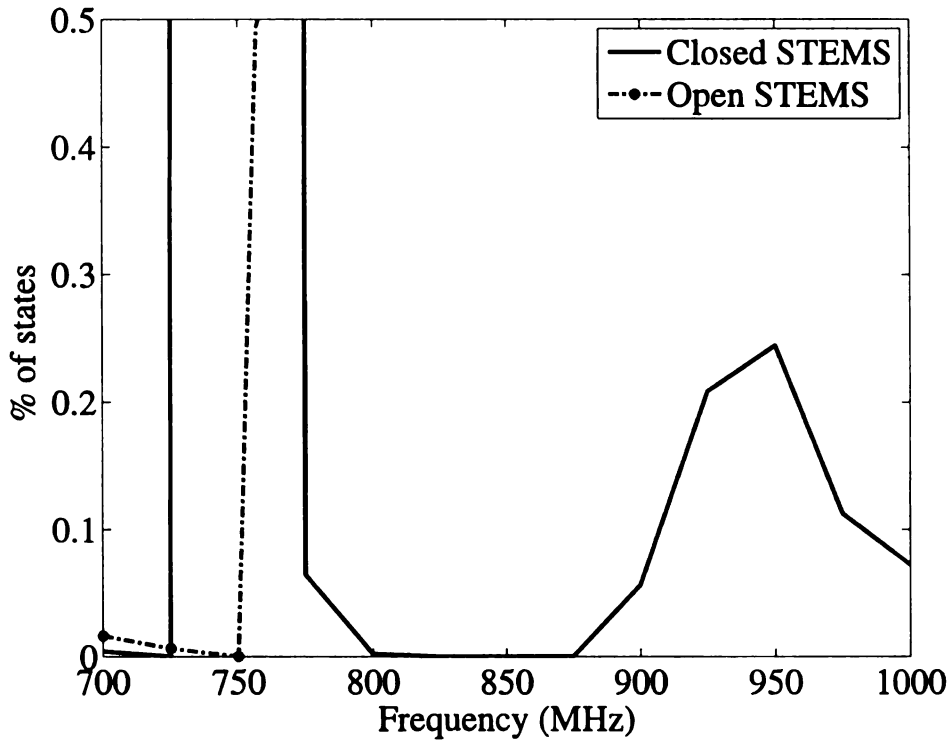

Figure 5.43. Close view Percentage of states for a sample of 50000 states

5.5.2 Genetic Algorithm

Upon completion of the random search, a genetic algorithm was run at the same 13 frequencies with the same experimental set up as that of the random search. The GA used is written in visual basic following the diagram of Figure 5.44. For each frequency, an initial population of 100 different switch configurations selected randomly is generated. Each of the 100 configurations is used to set the states of the switches on the template and the shutter effectiveness of each state is calculated using (5.1) and the value of the shutter effectiveness is used to determine the fitness of the configuration. The fitness is evaluated using a fitness function that was found through trial and error. The fitness function used is $F = \sqrt{0.5841} - V_{log}$, where V_{log} is the voltage at the video log output of the receiver.

Once the evaluation of the fitness of all switch configurations in the population is completed and the population is not the last generation, a selection of the switch configurations with the best fitness values are selected. The selection type used in the code is tournament among three switch configurations. Three switch configurations are selected randomly and their fitness values are compared. The switch configuration with the highest fitness is selected.

This process is repeated till the mating pool is filled. Once the mating pool is filled, mates are pared randomly and a 2 point crossover is performed with crossover probability P_C. After the crossover process, a single bit mutation is performed with probability P_m. After the mutation, a new generation is filled and the process is repeated until all the generations have been evaluated. The fitness function is set to

minimize or maximize $\sqrt{0.5841} - V_{log}$ depending on the goal of the GA. If the goal is to create a closed STEMS then the fitness function is set to minimize, and if the goal is to create an open STEMS then the fitness function is set to maximize.

All GA measurements are taken with the following parameters:

- Population=100
- Generations=80
- Crossover probability=0.7
- Mutation probability= Evolving
- Generation gap = 50%

The term evolving is used to represent a quantity that varies with time. The mutation probability starts with a value of 0.5 and changes after each generation to 0.5/(generation number). The generation gap represents the number of individuals within the population that are selected for crossover.

For every frequency evaluated the system is first calibrated and the open box voltage is recorded and saved in the Visual Basic code for reference.

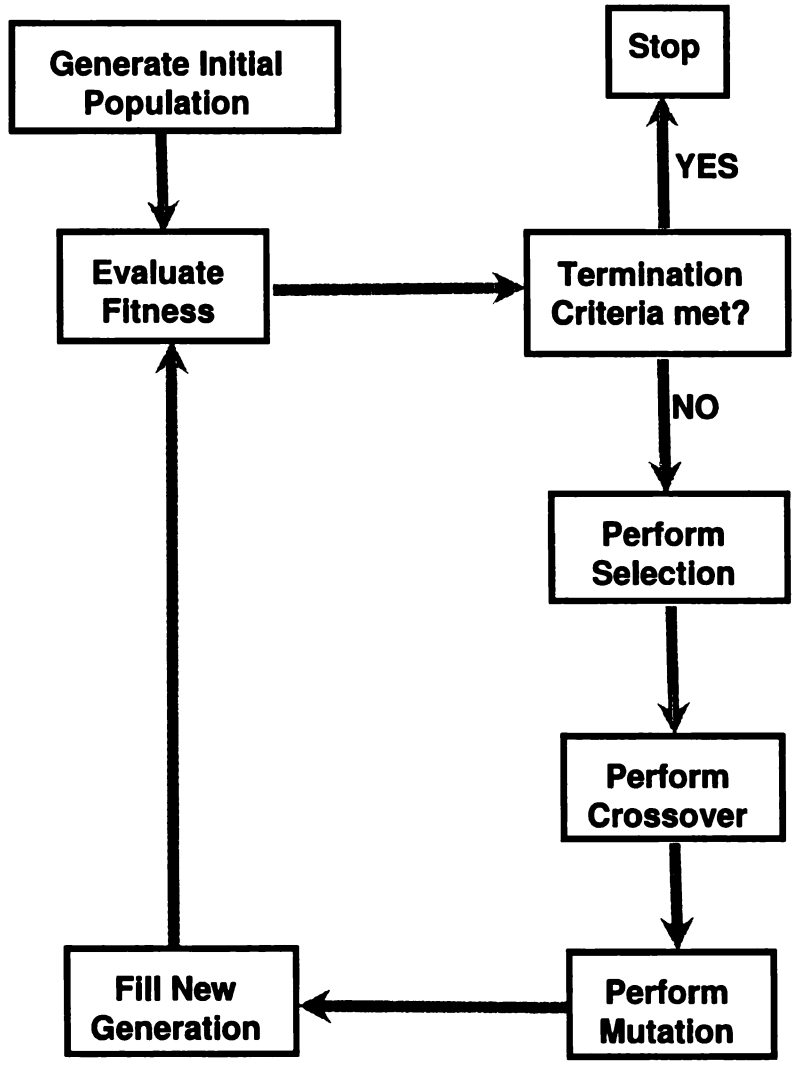

Figure 5.44. Diagram of the genetic algorithm used in the experiment

The first frequency selected for analysis is 700MHz. At that frequency, a value of -40.038dB was recorded for the closed STEMS while 0.9966dB was found for the open box. When the random search was ran, the best switch configuration for the closed STEMS produced -43.108dB and -4.5dB for the best switch configuration found for the open STEMS. Though the random search produced a lower value of the shutter effectiveness compared to the GA, it should be pointed out that the GA reached the value of -40.038 after 69 generations as shown in Figure 5.45. This implies that the GA was able to find an acceptable state within 6900 evaluations.

Figure 5.46 shows a plot of the best shutter effectiveness found for each generation that the GA is set to optimize for an open surface. The GA found an acceptable state right from its first generation and continued to produce better results till all the generation were exhausted. The best state is found at generation 77 with S_e=.995dB. generation 77 is 4 generations from the stopping point. With only 4 more generations to run, it could be implied that the GA had not yet converge and better value of the Shutter effectiveness could have been obtained is the number of generations was increased.

The second frequency selected for optimization is 725MHz. As shown in Figure 5.47, the GA set up to optimize for a closed surface was able to find an acceptable state after 70 generations. The random search was unable to find a state with a shutter effectiveness less than -40dB at 725MHz. The best value of the shutter effectiveness the random search found was -25.7702dB. The GA found a switch configuration with a shutter effectiveness less than -25.7702dB after only 20 generation and the best shutter effectiveness after all 80 generations was recoded to be -40.09dB.

The best state found when optimized to create an open surface had a shutter effectiveness of -1.86011dB while the best state produced by the random search had a shutter effectiveness of -6.0007dB. As shown in Figure 5.48, the GA was run only for 52 generations because it found the best switch configuration with the shutter effectiveness of -1.86011dB after only 12 generations or 1200 evaluation. The GA ran from generation 12 to generation 52 without finding any better states. At that point, it was concluded that the GA had converged and the run was stopped.

The next frequency at which the GA was run is 750MHz. As shown in Figure 5.49, the GA set up to optimize for a closed surface was able to find an acceptable state after only 12 generations. The best shutter effectiveness recorded after all 80 generations were evaluated was found to be -51.1512dB.

When optimized to create an open surface, the best state found had a shutter effectiveness of -1.7926dB after only 23 generations. The random search failed to find a state with a shutter effectiveness of -6dB or higher after all 50000 sample states were evaluated. The GA was stopped after 33 generations and a plot of the best shutter effectiveness found for each generation is displayed in Figure 5.50.

At 775MHz, the GA was able to find states capable of achieving the desired results. As shown in Figure 5.51, when set up to optimize for a closed surface, the best state found after all 80 generations were evaluated had a shutter effectiveness of -56.7673dB. The GA was able to find a switch configuration with a shutter effectiveness less than -40dB on its second generation. A plot of the best shutter effectiveness obtained for each generation when the GA is set up to create an open surface is shown in Figure 5.52. A shutter effectiveness higher than the desired value of -6dB was obtained after

only 7 generations and the best state found after all 80 generations was found to be -2.9389dB.

After 775MHz, 800MHz was selected for measurement. The GA set up to optimize for a closed surface was able to find an acceptable state after 40 generations. The best shutter effectiveness recorded after all 80 generations were evaluated was found to be -44.262dB and Figure 5.53 shows a plot of the best value obtained for the shutter effectiveness with reference to the number of generations.

When optimized to create an open surface, the best state found had a shutter effectiveness of 2.1972dB after only 17 generations. No better states were found for the remainder of the generation. The Random search found a slightly higher value for the shutter effectiveness, 2.88dB. A plot of the best shutter effectiveness found for each generation is displayed in Figure 5.54.

The next frequency selected for optimization is 825MHz. As shown in Figure 5.55, the GA set up to optimize for a closed surface failed to find an acceptable state after all 80 generations. The random search was also unable to find an acceptable state.

Figure 5.56 shows a plot of the best shutter effectiveness found for each generation when the GA is set to optimize for an open surface. The GA found an acceptable state right from its first generation. The best state of all 80 generations is found at generation 33, and no improvement was made afterward

At 850MHz, the GA was unable to find a state capable of achieving the desired results. As shown in Figure 5.57, when set up to optimize for a closed surface, the best state found after all 80 generations had a shutter effectiveness of –27.179dB. The best result produced by the random search was only -13.06dB

A plot of the best shutter effectiveness obtained for each generation when the GA is set up to create an open surface is shown in Figure 5.58. A shutter effectiveness higher than the desired value of -6dB was obtained from the first generation and the best of all the generation was found after 4 generations. The best value of 7.016dB remained unchanged from the 4^{th} generation until generation 80.

The next frequency at which the GA was run is 875Hz. As shown in Figure 5.59, the GA set up to optimize for a closed surface was unable to find an acceptable state. The best value returned after all 50 generations were evaluated is -33.55dB. The random search was also unable to find an acceptable state at 875MHz.

When optimized to create an open surface, the best state found had a shutter effectiveness of 4.45dB. A positive effectiveness was recorded from the first start as shown in Figure 5.60. The best shutter effectiveness was found after 15 generation and no better results were obtained for the remaining generations.

At 900MHz, the GA was able to find states capable of achieving the desired results. As shown in Figure 5.61, the best state found when the GA is set to optimize for a closed surface has a shutter effectiveness of -53.713dB. The GA was able to find a switch configuration with a shutter effectiveness less than -40dB on its third generation.

A plot of the best shutter effectiveness obtained for each generation when the GA is set up to create an open surface is shown in Figure 5.62. A shutter effectiveness higher than the desired value of -6dB was obtained from the first generation and the best state found after all 80 generations were run was found to -2.375dB.

After 900MHz, 925MHz was selected for measurement. The best closed surface

optimized switch configuration provided a shutter effectiveness of -54.7485dB, obtained after 26 generations. The GA was able to produce an acceptable state on the 3^{rd} generation as shown in Figure 5.63.

The best open surface optimized switch configuration provided a shutter effectiveness of -3.6004dB as seen in Figure 5.64 An acceptable state was found after only 2 generations.

The next frequency at which the GA was ran is 950MHz. As shown in Figure 5.65, the best closed surface switch configuration found has a shutter effectiveness of -55.78dB. By the 4^{th} generation, the GA had already found a state with a shutter effectiveness of -47.76dB.

When optimized to create an open surface, the best state found had a shutter effectiveness of -0.8682dB. The first initial population contained already some states with a shutter effectiveness above the required value of -6dB. A plot of the best shutter effectiveness found for each generation is displayed in Figure 5.66.

Interesting results are obtained at 975MHz. The initial population generated already contained a state with a shutter effectiveness of -42.013dB. After all 50 generations were run, the best closed surface switch configuration found has a shutter effectiveness of -55.263dB as shown in Figure 5.67

Likewise, the initial population generated when the GA is set to create an open surface already contained states with positive values of shutter effectiveness. The optimization was able to produce a state with an even higher value of shutter effectiveness. the highest value obtained was 1.24dB. A plot of the best shutter effectiveness found for each generation is displayed in Figure 5.68.

The final frequency measured was 1000MHz. As shown in Figure 5.69, the GA set up to optimize for a closed surface was able to find an acceptable state after only 11 generations. The best shutter effectiveness recorded after all 80 generations were evaluated was found to be -56.2342dB.

When optimized to create an open surface, the first population created contained states that already met the requirement of -6dB or higher. The best state found after the GA was ran had a positive value of shutter effectiveness with S_e=1.57dB. The plot of the best shutter effectiveness found for each generation is displayed in Figure 5.70.

For all 13 frequencies considered, the genetic algorithm was able to find states capable of creating an open surface. In most cases, the GA found an acceptable state within the first 5 generations. The GA failed to find states capable of creating a closed surface at 825MHz, 850MHz and 875MHz. This pattern is also observed with the random search. Figure 5.72 and Figure 5.71 show a comparison of the best values obtained for the GA and the random search.

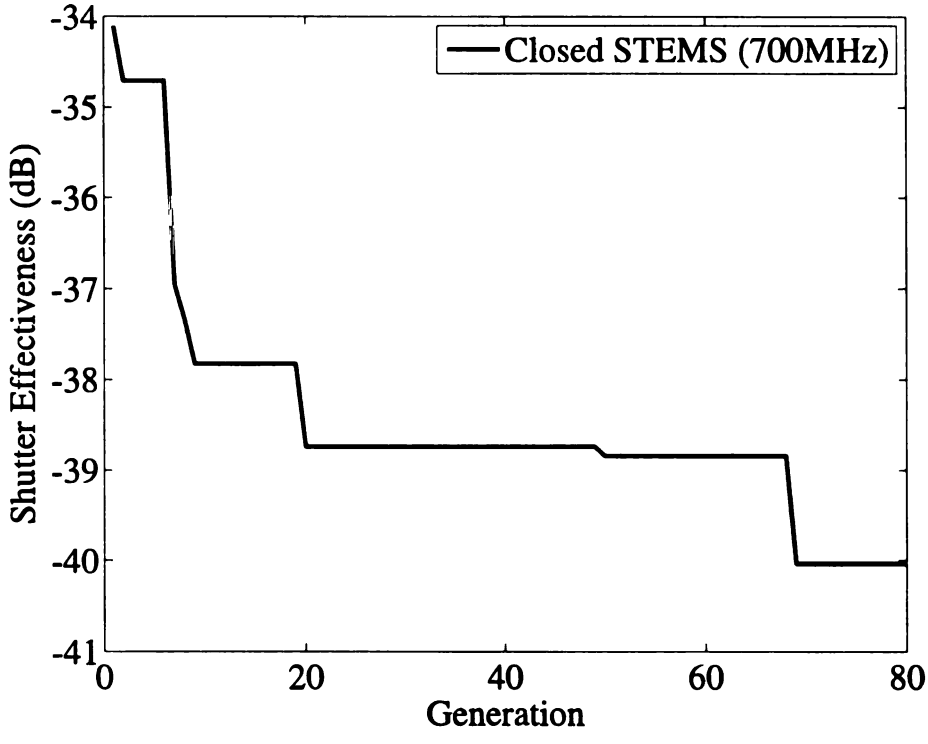

Figure 5.45. Closed STEMS S_e obtained through the GA at 700MHz

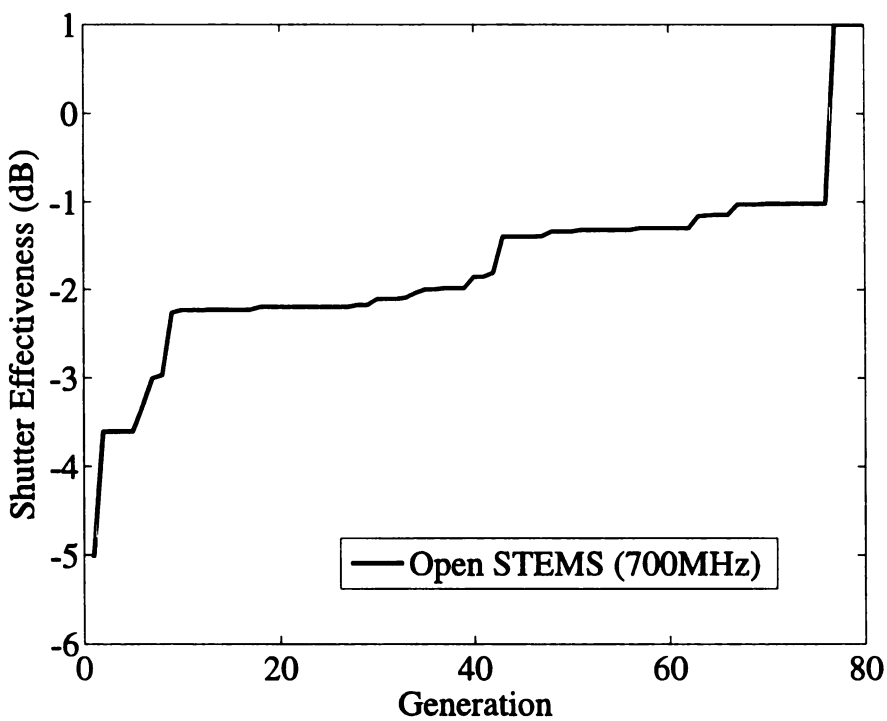

Figure 5.46. Open STEMS S_e obtained through the GA at 700MHz

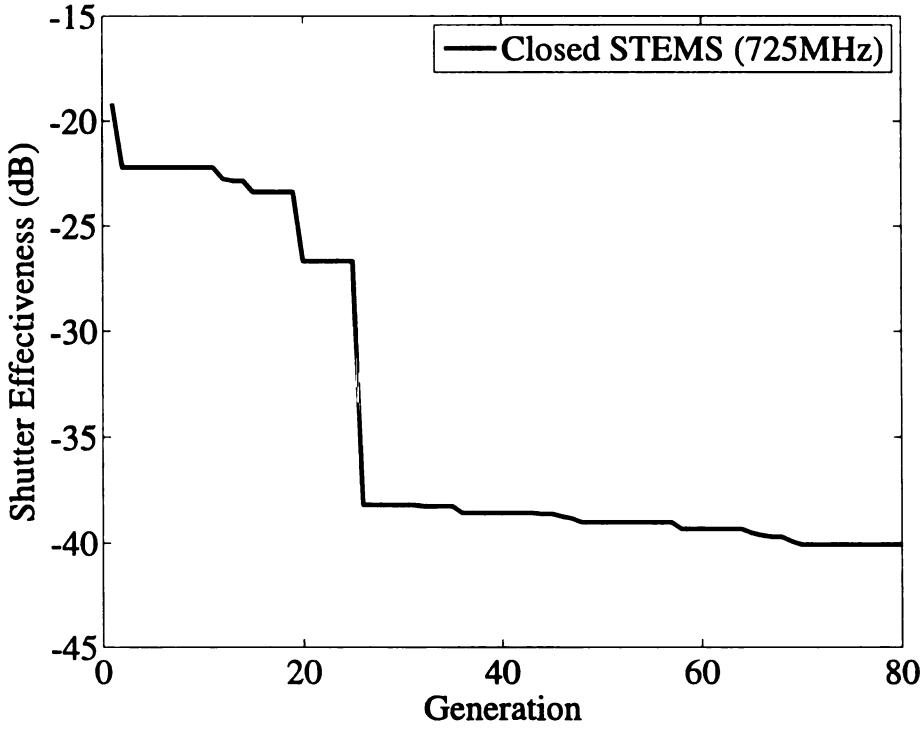

Figure 5.47. Closed STEMS S_e obtained through the GA at 725MHz

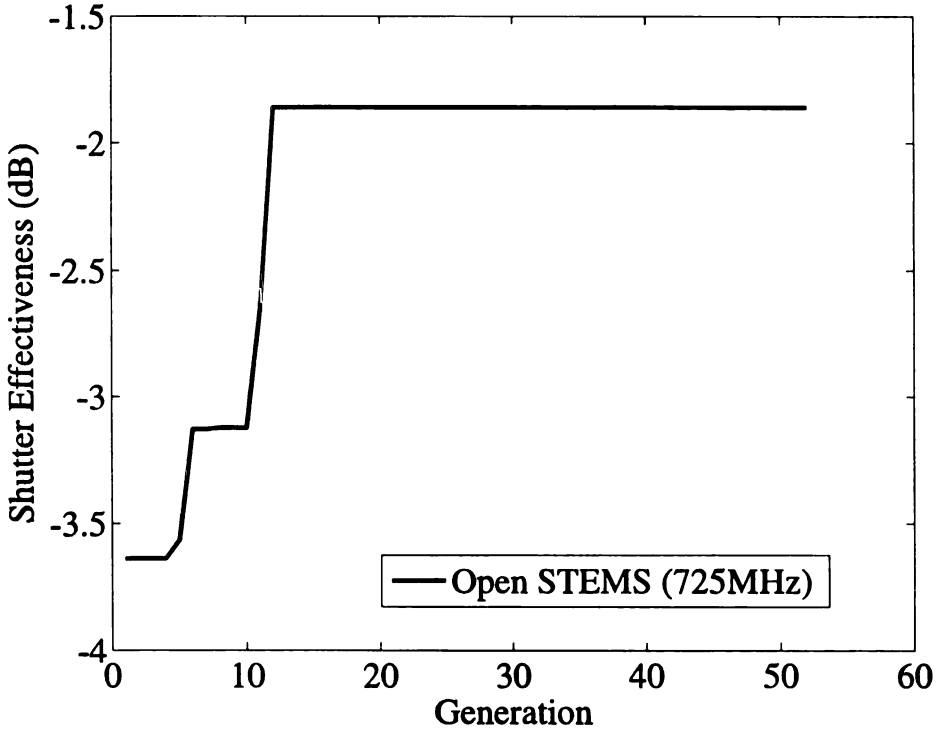

Figure 5.48. Open STEMS S_e obtained through the GA at 725MHz

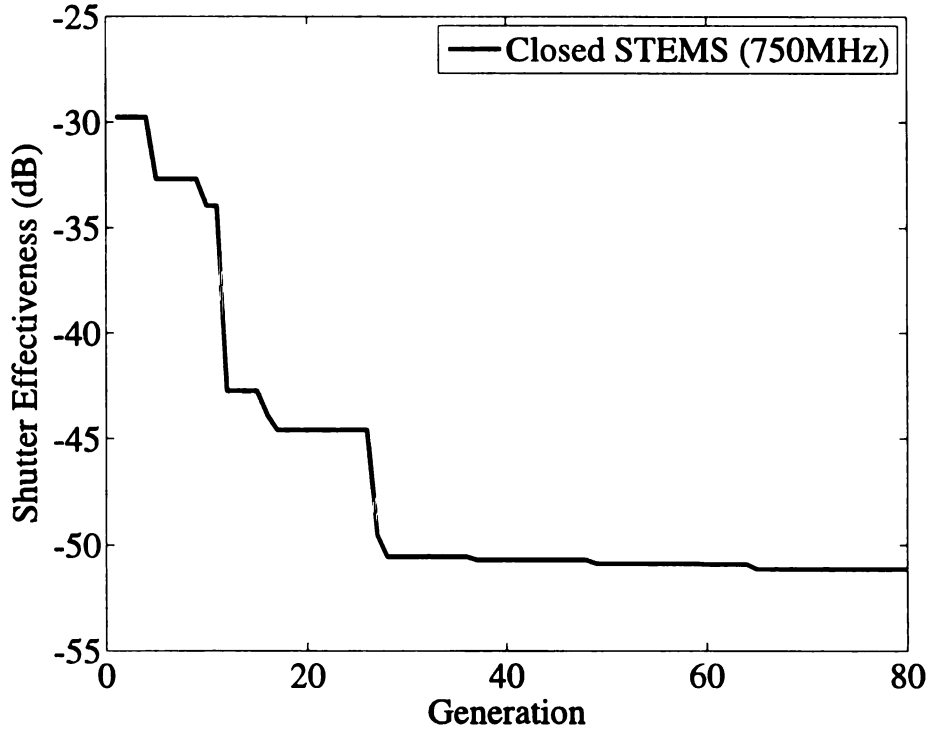

Figure 5.49. Closed STEMS S_e obtained through the GA at 750MHz

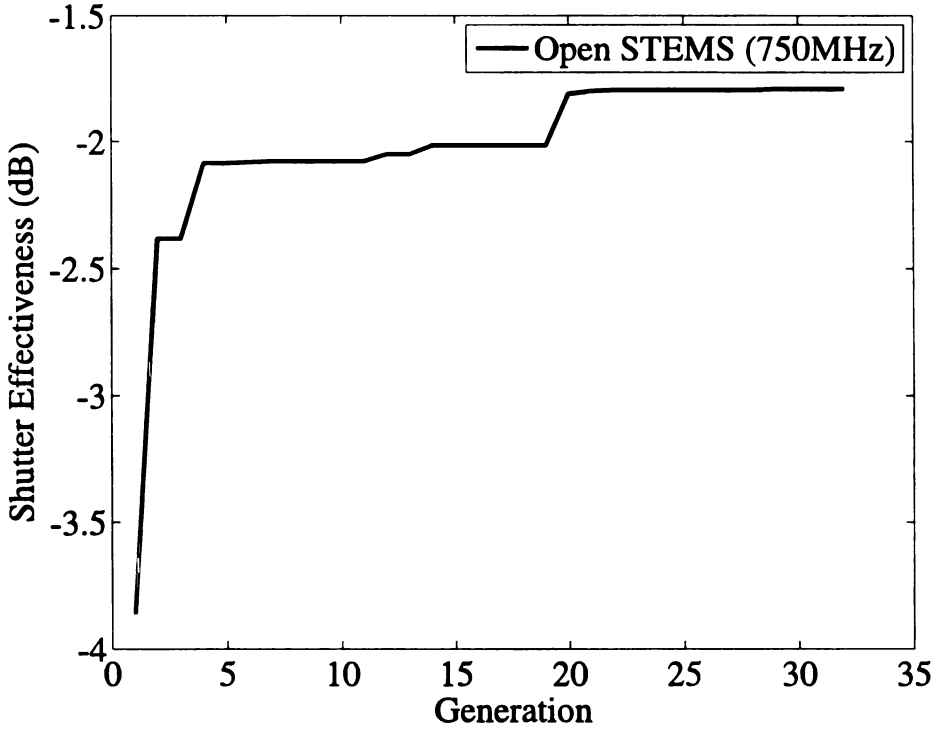

Figure 5.50. Open STEMS S_e obtained through the GA at 750MHz

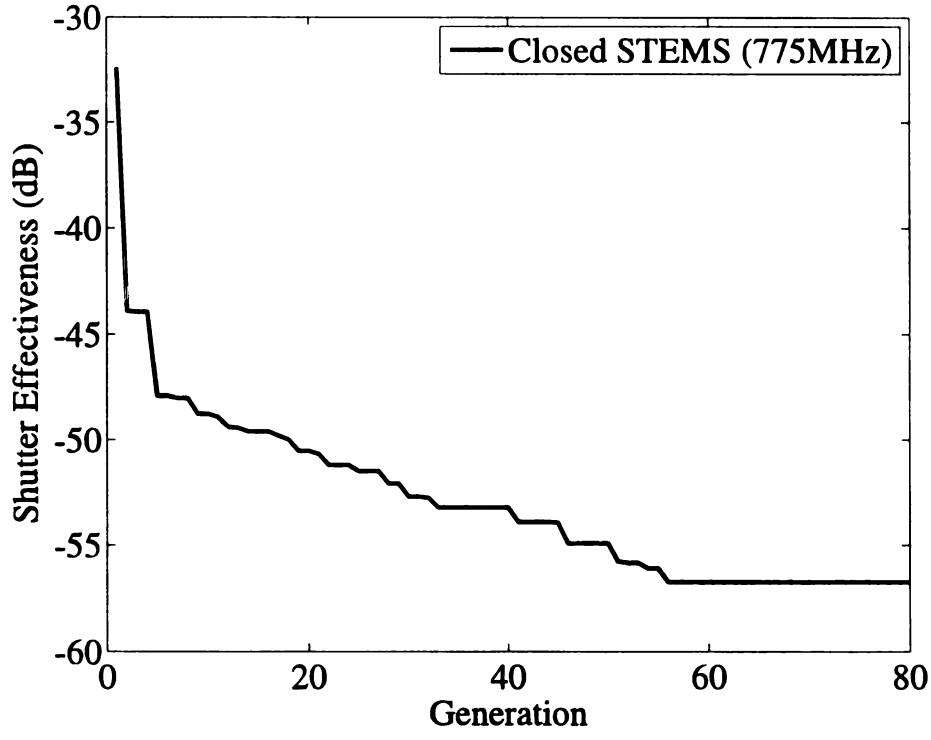

Figure 5.51. Closed STEMS S_e obtained through the GA at 775MHz

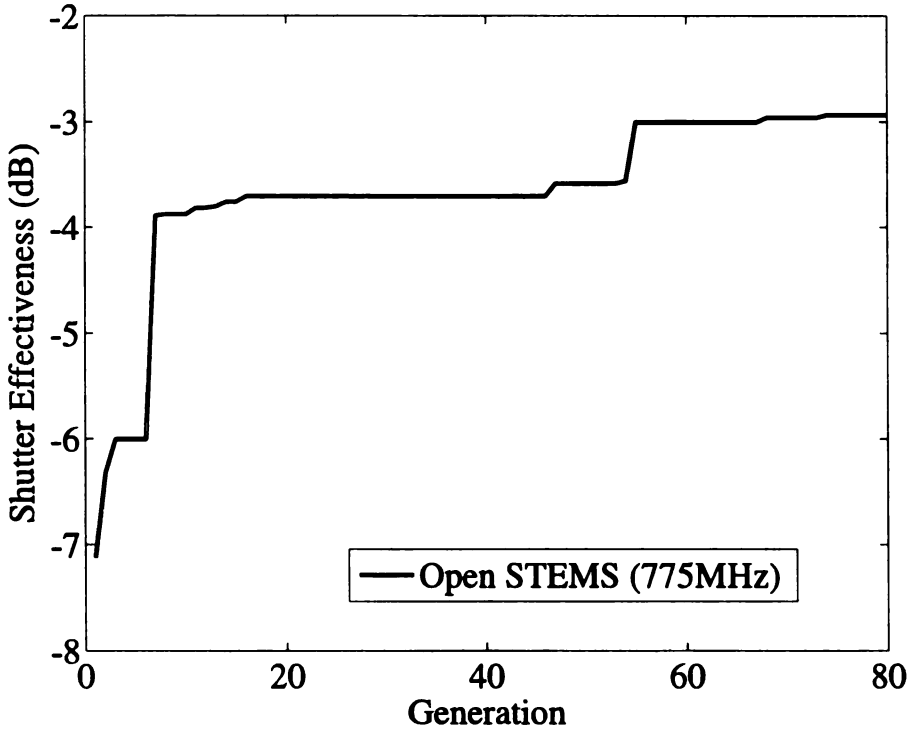

Figure 5.52. Open STEMS S_e obtained through the GA at 775MHz

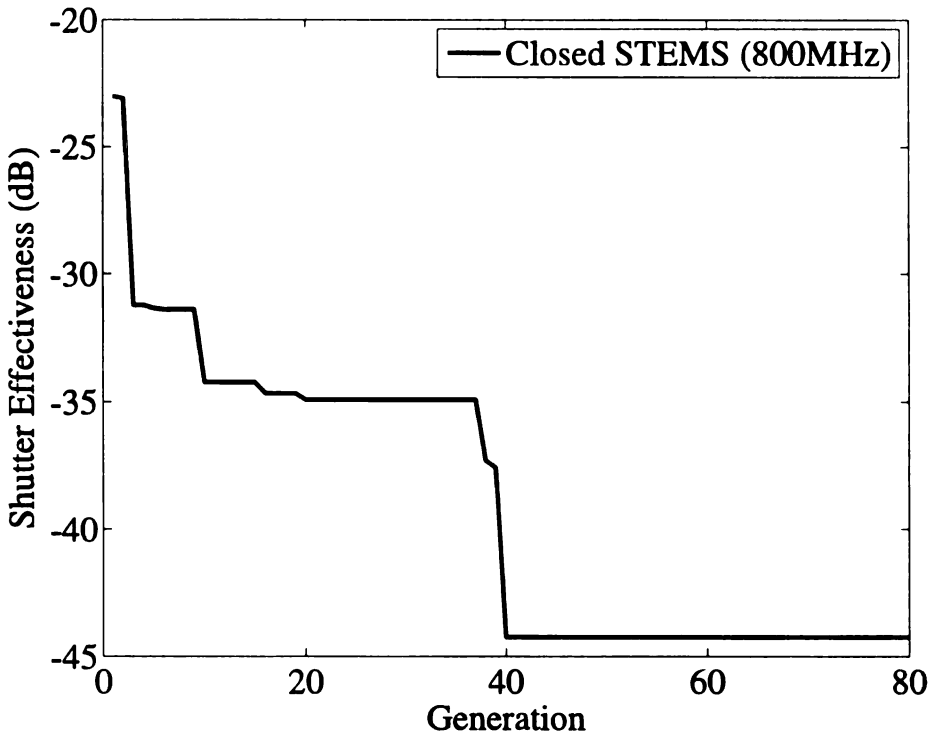

Figure 5.53. Closed STEMS S_e obtained through the GA at 800MHz

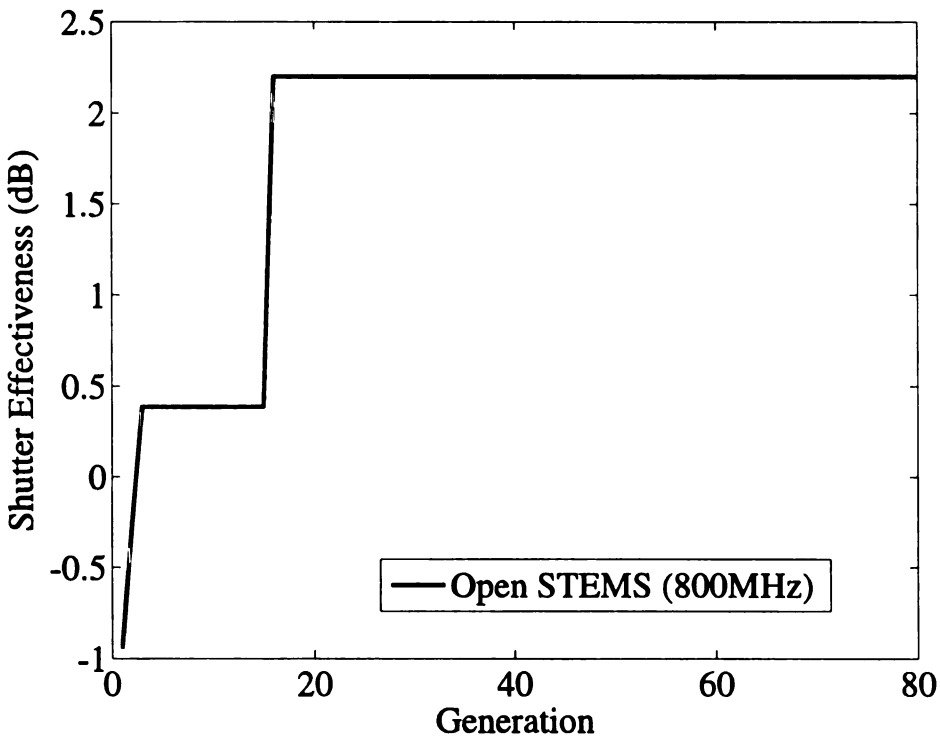

Figure 5.54. Open STEMS S_e obtained through the GA at 800MHz

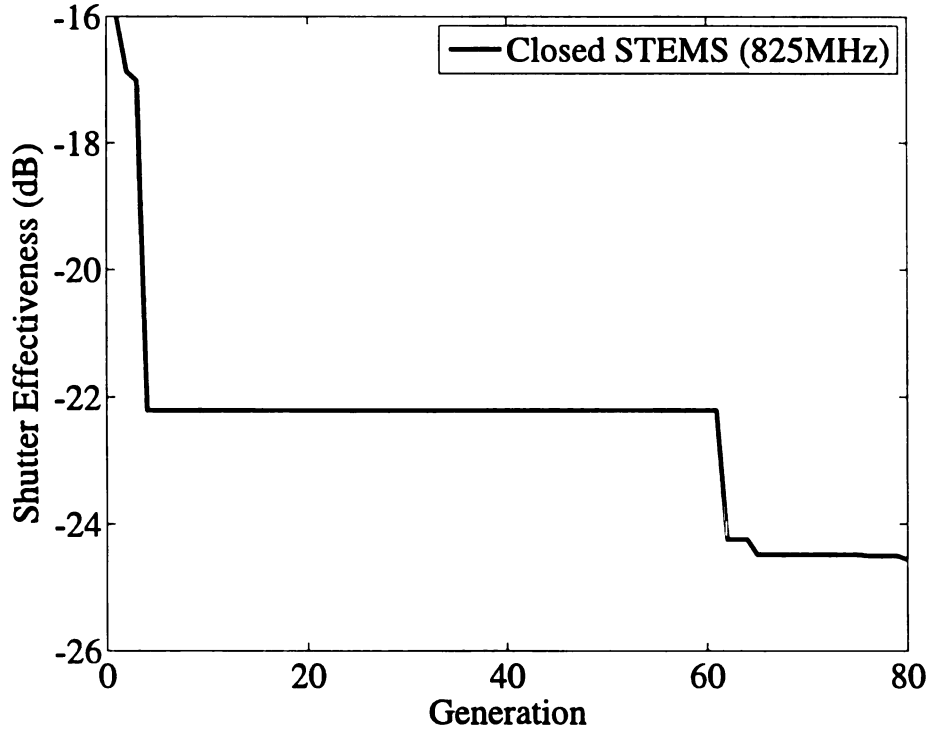

Figure 5.55. Closed STEMS S_e obtained through the GA at 825MHz

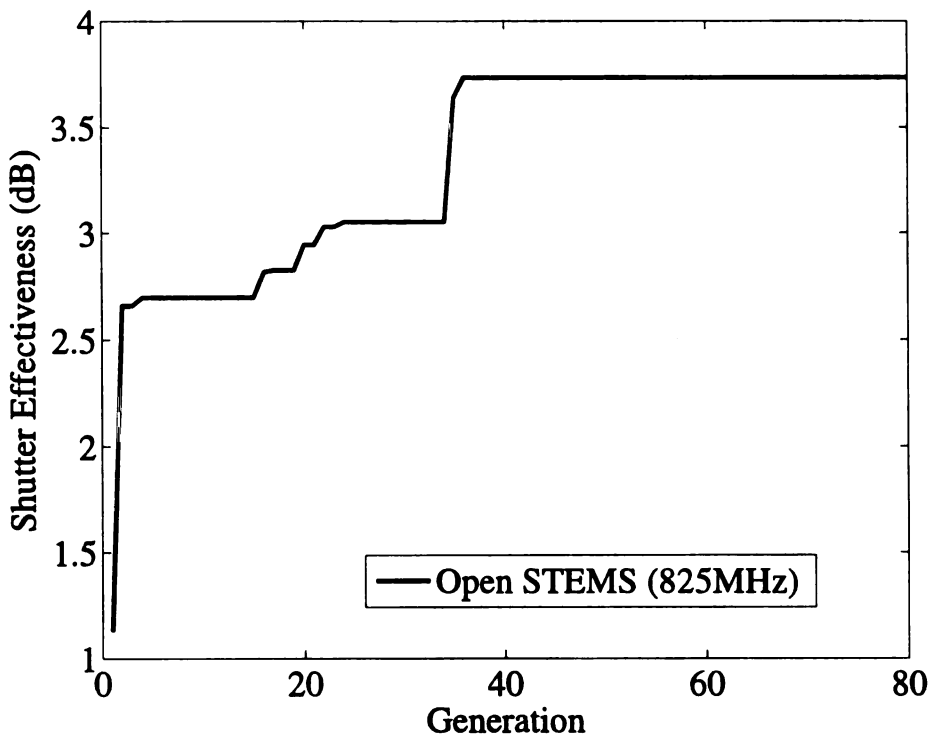

Figure 5.56. Open STEMS S_e obtained through the GA at 825MHz

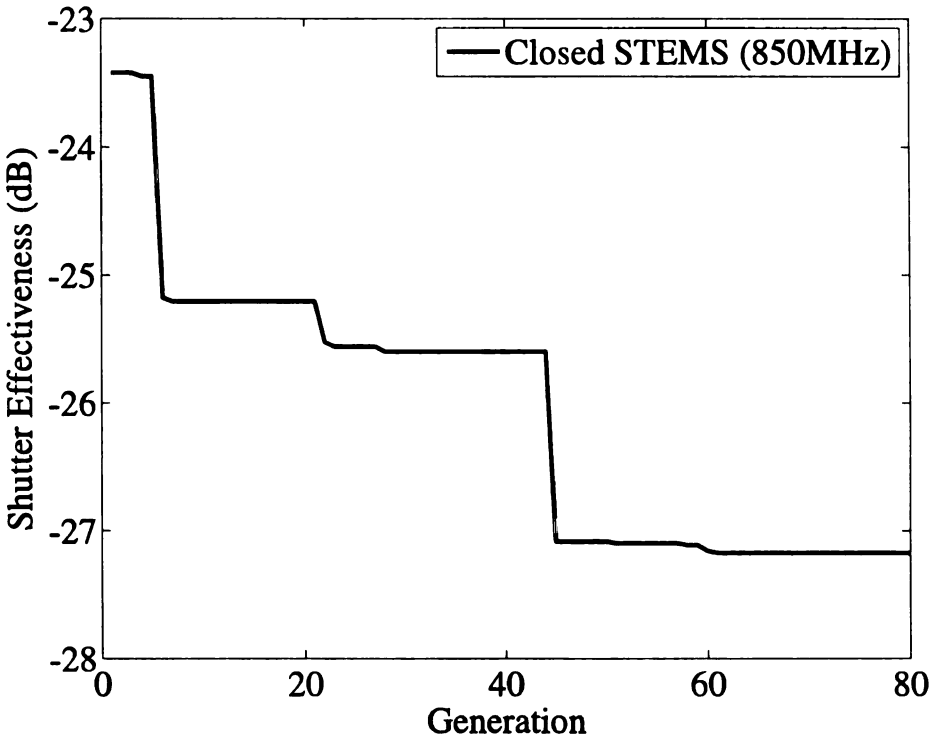

Figure 5.57. Closed STEMS S_e obtained through the GA at 850MHz

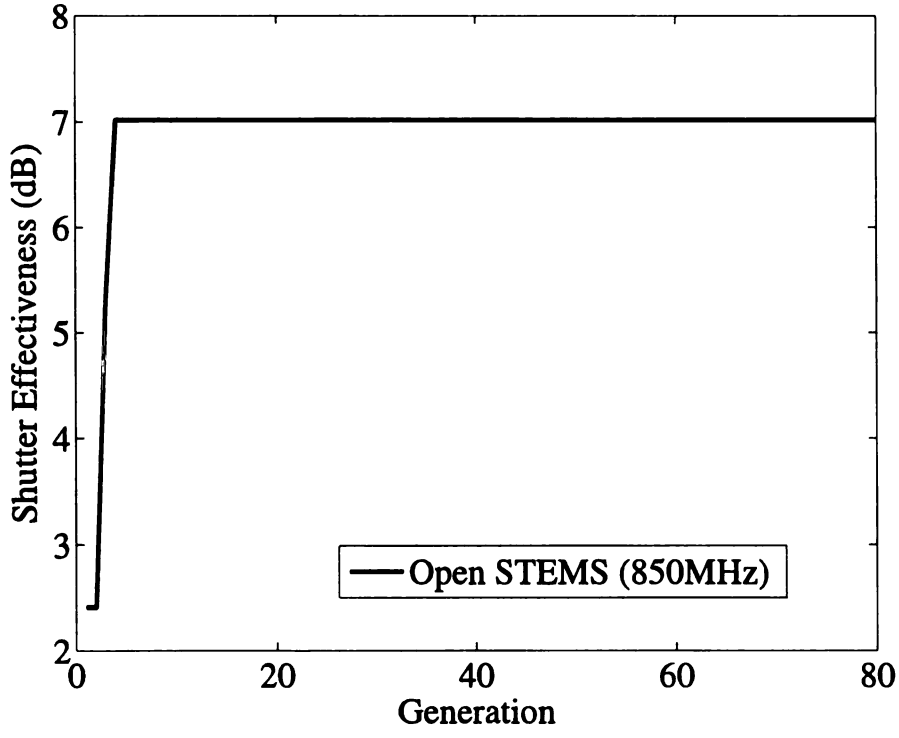

Figure 5.58. Open STEMS S_e obtained through the GA at 850MHz

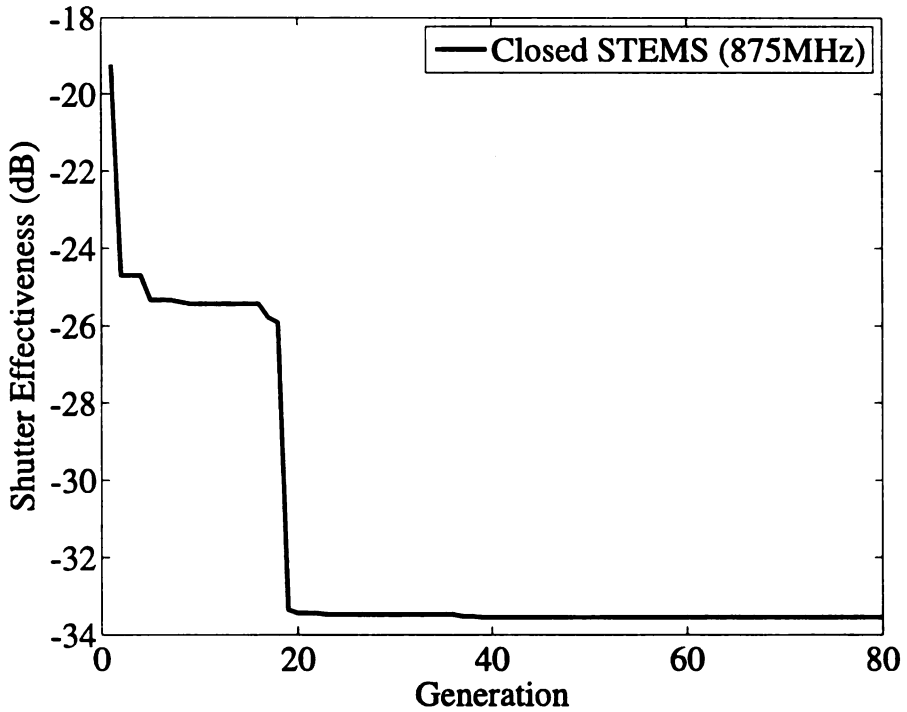

Figure 5.59. Closed STEMS S_e obtained through the GA at 875MHz

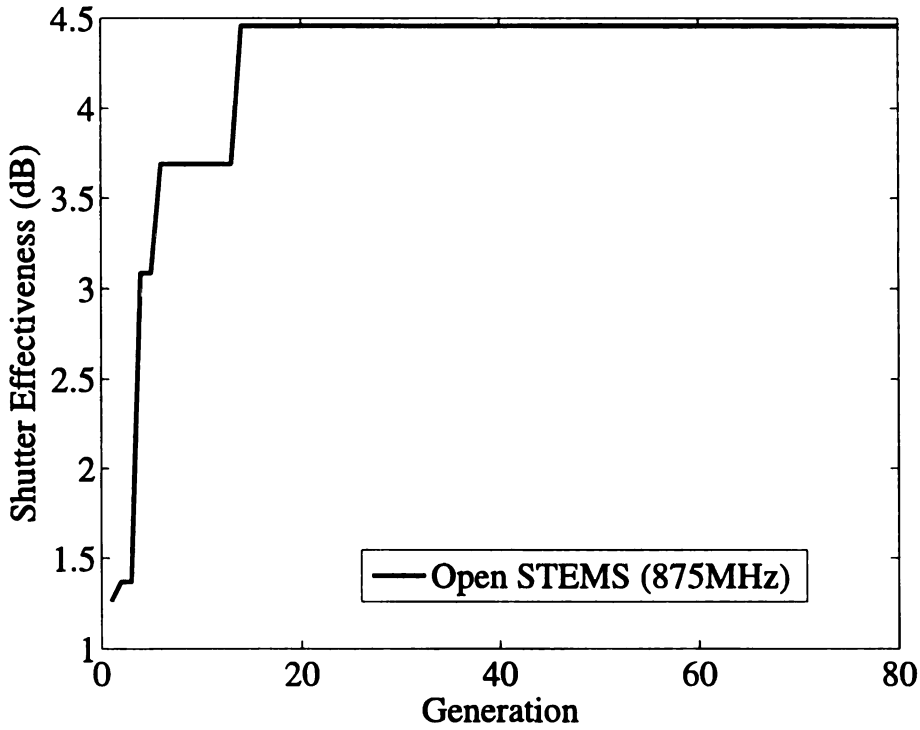

Figure 5.60. Open STEMS S_e obtained through the GA at 875MHz

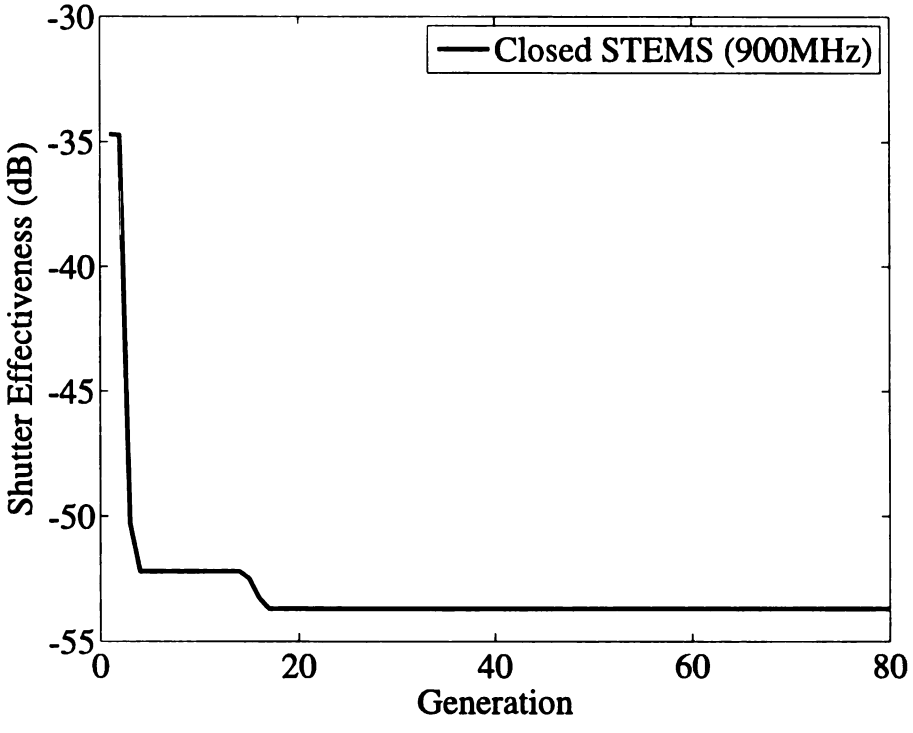

Figure 5.61. Closed STEMS S_e obtained through the GA at 900MHz

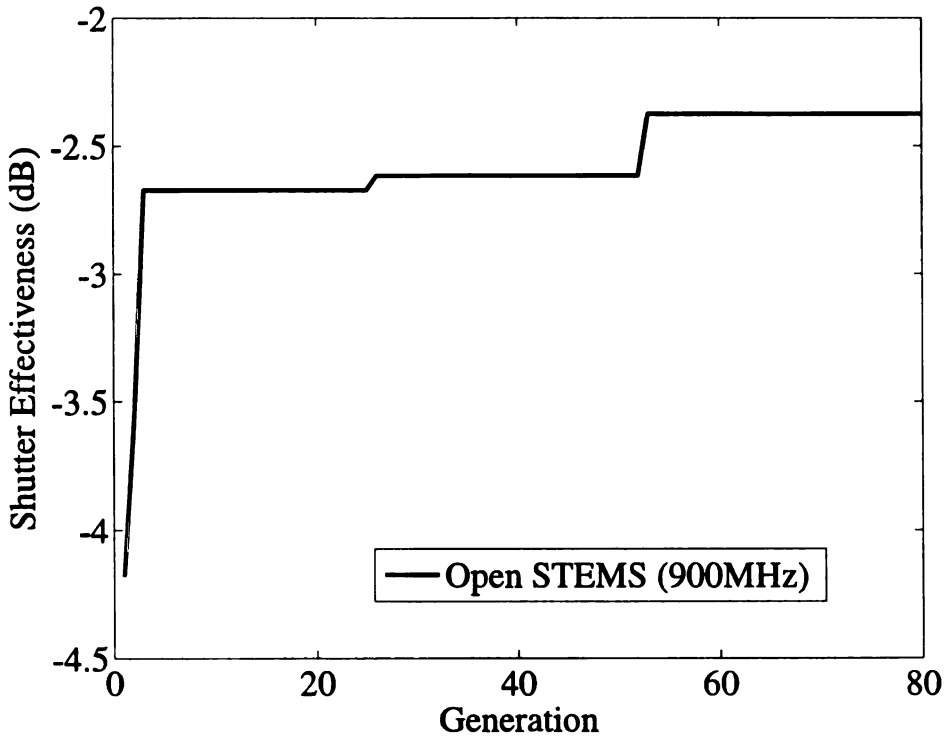

Figure 5.62. Open STEMS S_e obtained through the GA at 900MHz

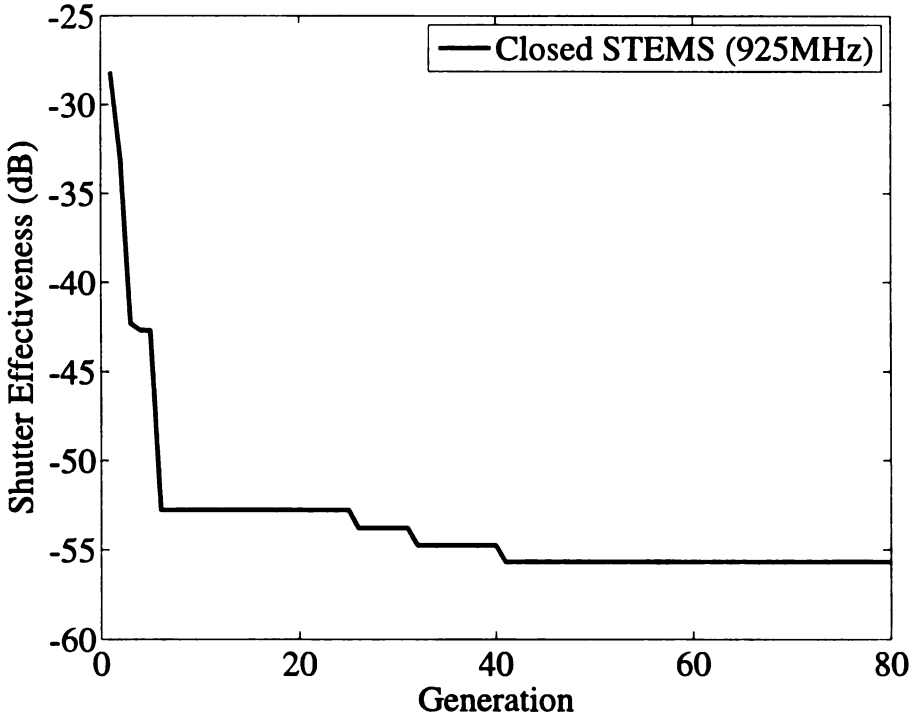

Figure 5.63. Closed STEMS S_e obtained through the GA at 925MHz

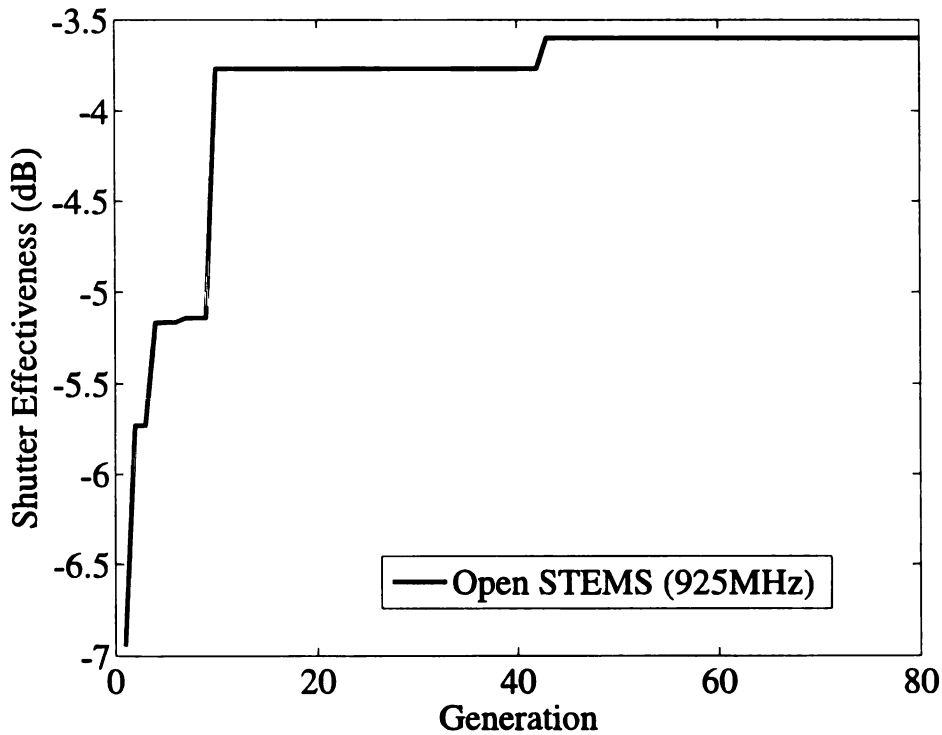

Figure 5.64. Open STEMS S_e obtained through the GA at 925MHz

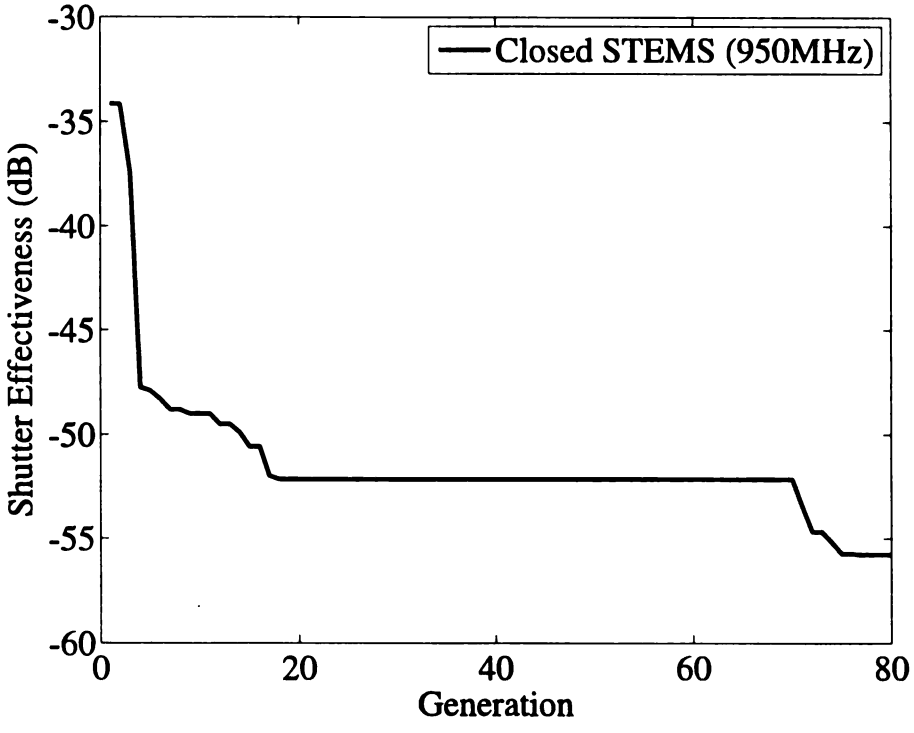

Figure 5.65. Closed STEMS S_e obtained through the GA at 950MHz

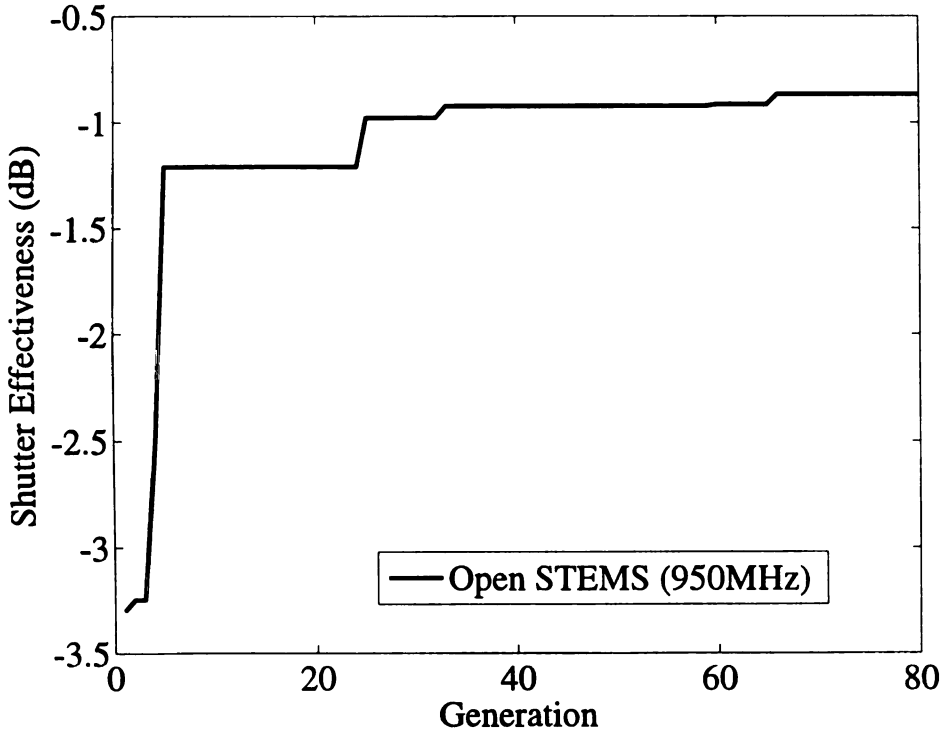

Figure 5.66. Open STEMS S_e obtained through the GA at 950MHz

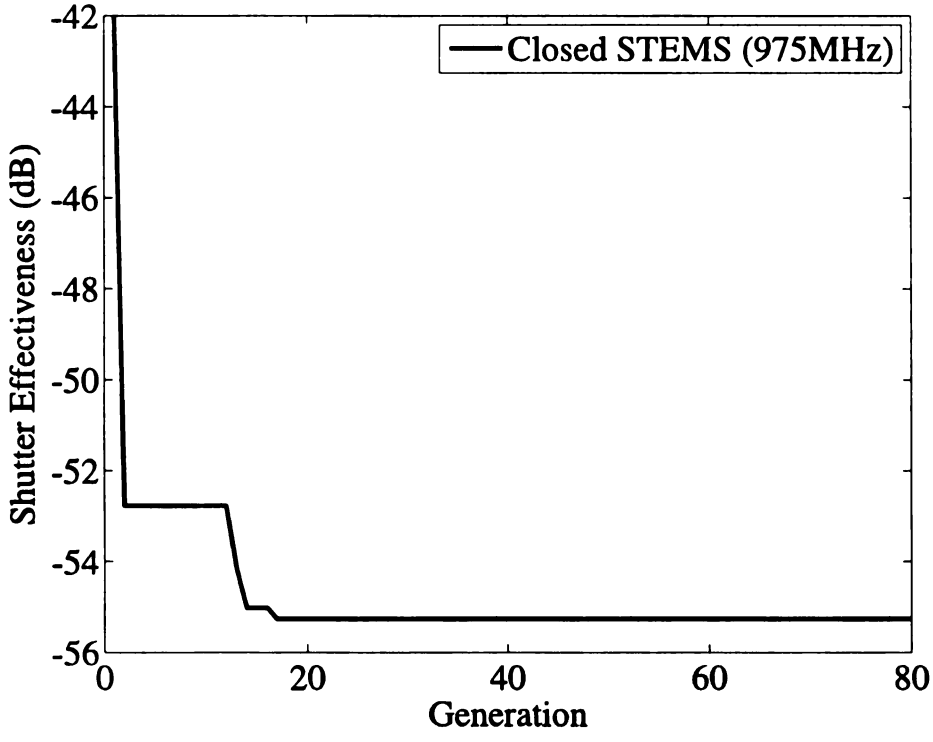

Figure 5.67. Closed STEMS S_e obtained through the GA at 975MHz

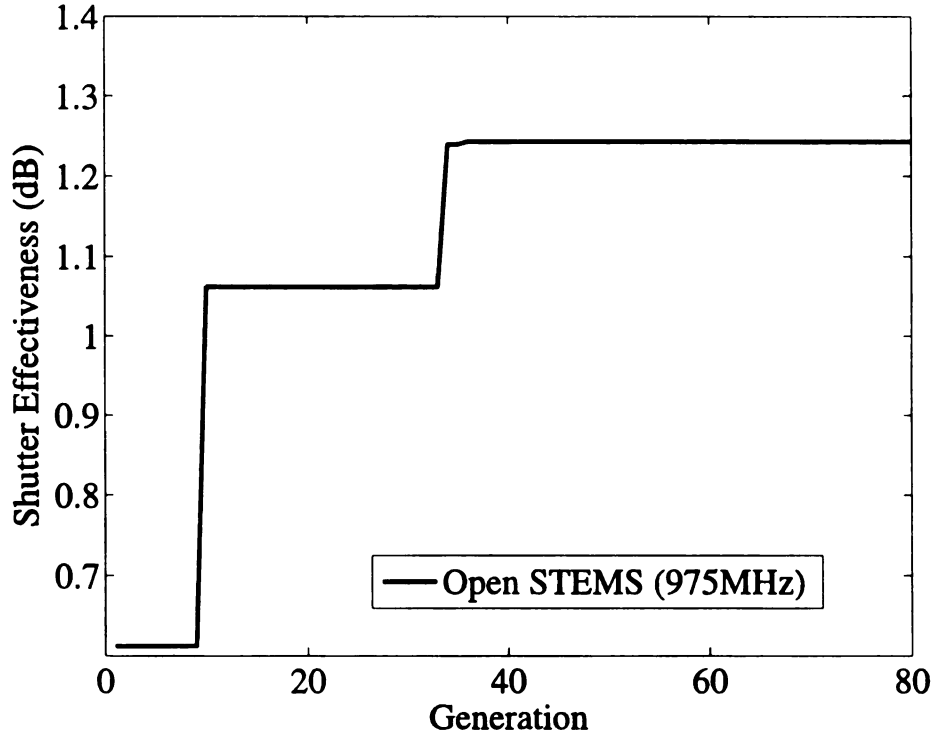

Figure 5.68. Open STEMS S_e obtained through the GA at 975MHz

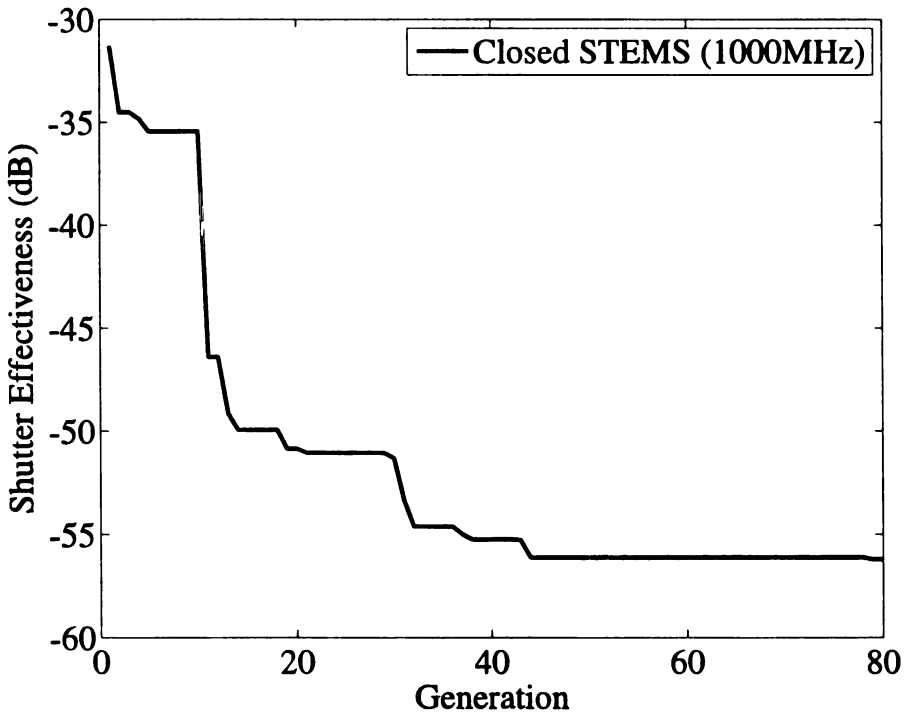

Figure 5.69. Closed STEMS S_e obtained through the GA at 1000MHz

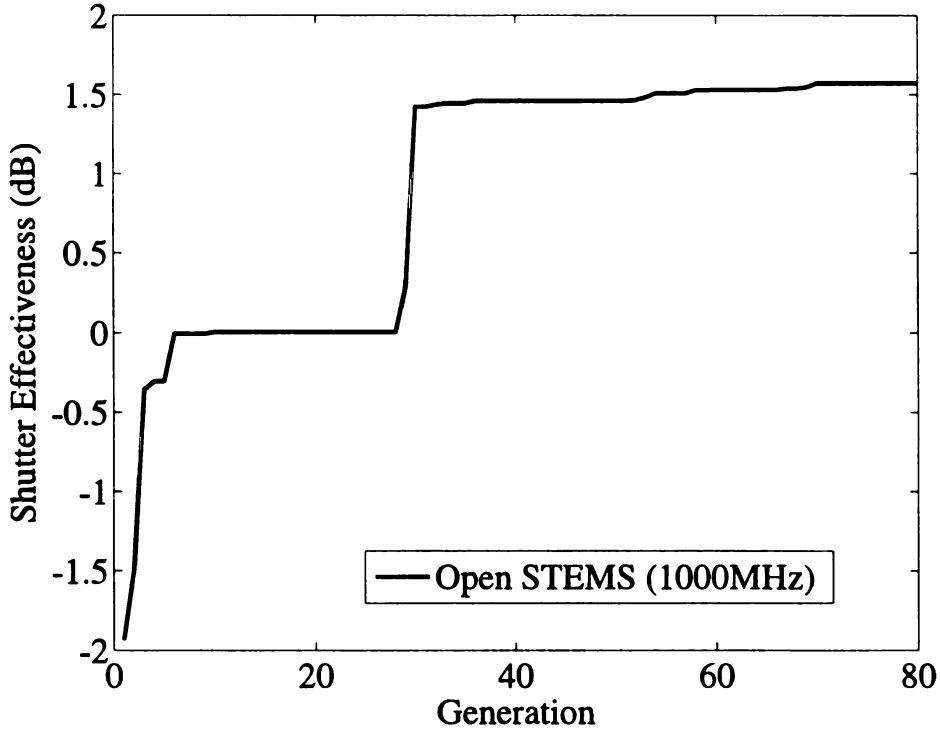

Figure 5.70. Open STEMS S_e obtained through the GA at 1000MHz

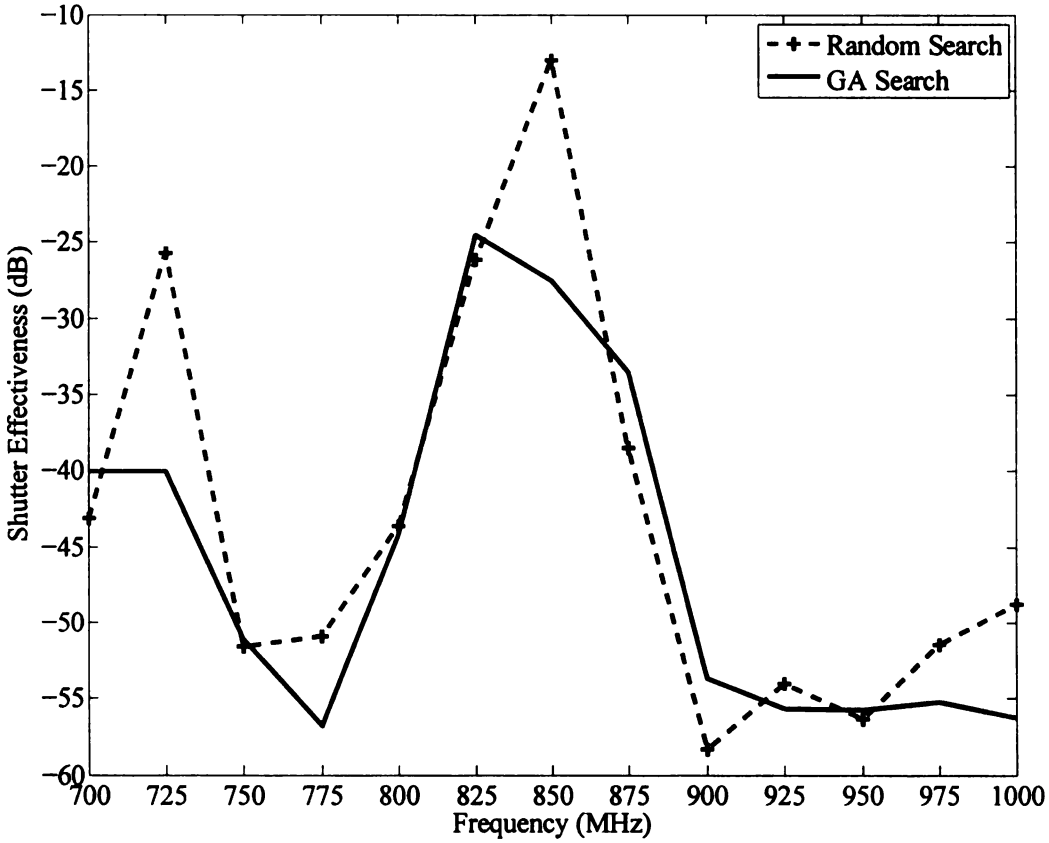

Figure 5.71. Best STEMS S_e for both GA and random search: Closed STEMS

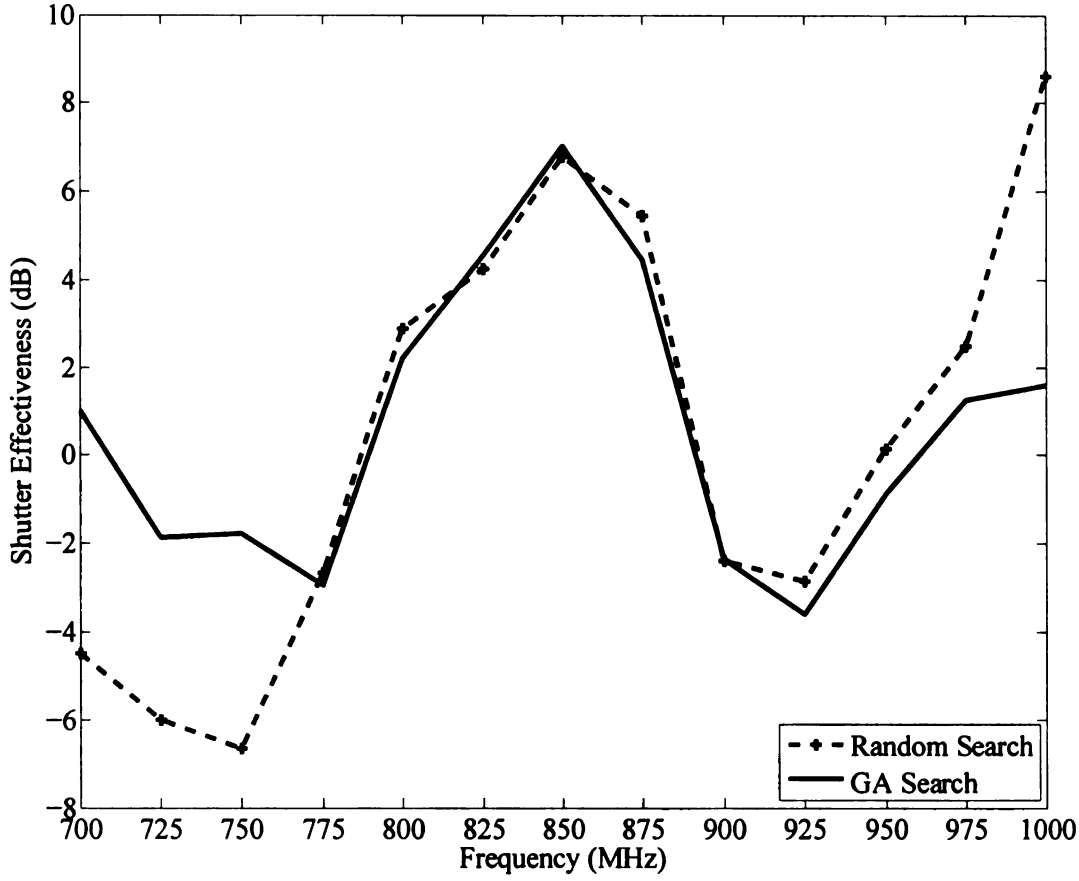

Figure 5.72. Best STEMS S_e for both GA and random search: Open STEMS

5.5.3 STEMS optimized using a GA for an oblique incidence angle

After the GA was completed, the box was moved to a different location still within the anechoic chamber as shown in Figure 5.15. This set up is used to analyzed the performance of STEMS based on location and angle of incidence of incoming waves. Four different frequencies were selected and the genetic algorithm of section 5.5.2 was used to optimize the STEMS to create an open and closed surface. Once an acceptable state was found, a network analyzer was used to obtain a frequency sweep of the state. For every frequency evaluated the system is first calibrated and the open voltage is recorded and saved in the visual basic code for reference. The first frequency selected for analysis was 700MHz. At that frequency, the genetic algorithm was able to optimize the STEMS to create an open and closed surface. Figure 5.73 shows a frequency sweep of the best open and closed STEMS states optimized at 700MHz. This plot shows a positive value of the shutter effectiveness extending over a 50MHz range from 695MHz to 745MHz. the closed STEMS plot show a shutter effectiveness of -48dB at exactly 700MHz. The bandwidth of the closed STEMS is not as wide as that of the open STEMS but more plots provided in the appendix show that the STEMS can be optimized to to be narrow band or broad band.

The next frequency considered for analysis was 775MHz. Using the GA, a closed STEMS state with a shutter effectiveness of -42.7dB and an open STEMS state with a shutter effectiveness of -4.8dB are obtained. Figure 5.74 shows the frequency sweep of the shutter effectiveness obtained using the best switch state obtained for each case.

The third frequency was 872MHz. At that frequency, The shutter effectiveness of the best state found for the closed STEMS is -48dB while the stutter effectiveness of the best state found for the open STEMS is 0dB. Figure 5.75 shows the frequency sweep of the shutter effectiveness obtained using the best switch state obtained for each case.

The last frequency analyzed was 1000MHz. The GA was once more able to find states capable of creating a closed and open surface as shown in Figure 5.76.

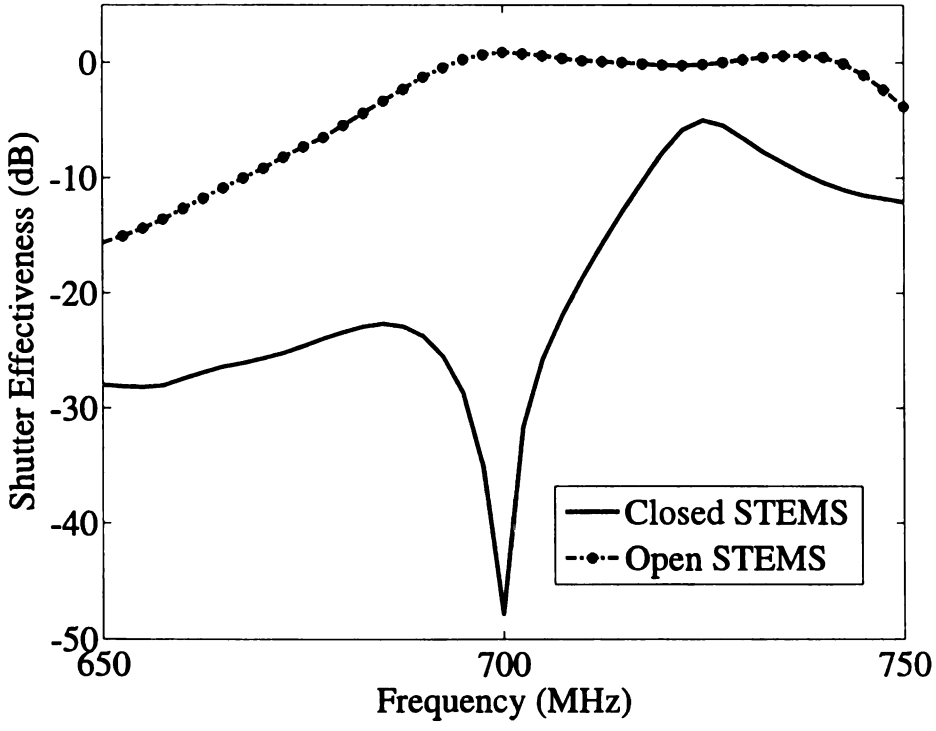

Figure 5.73. Closed and open STEMS best states frequency sweep at 700MHz

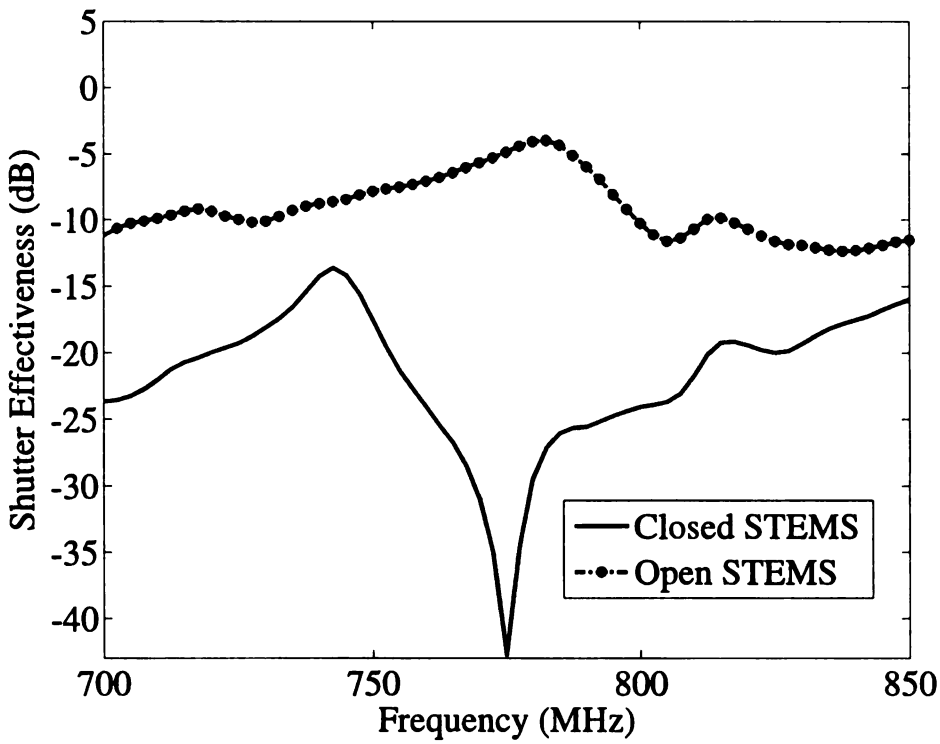

Figure 5.74. Closed and open STEMS best states frequency sweep at 775MHz

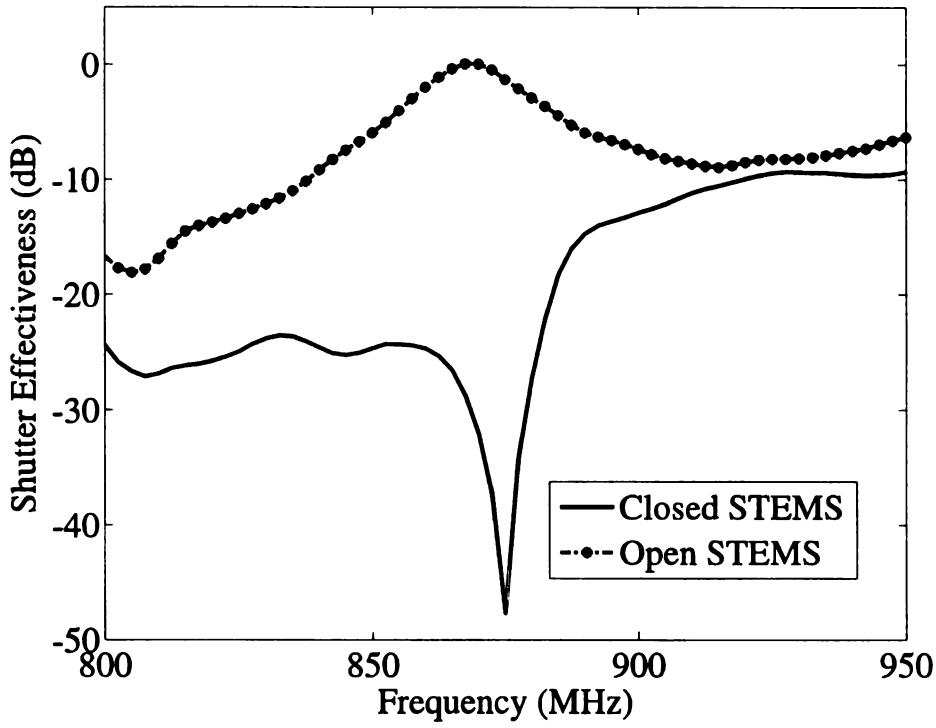

Figure 5.75. Closed and open STEMS best states frequency sweep at 872MHz

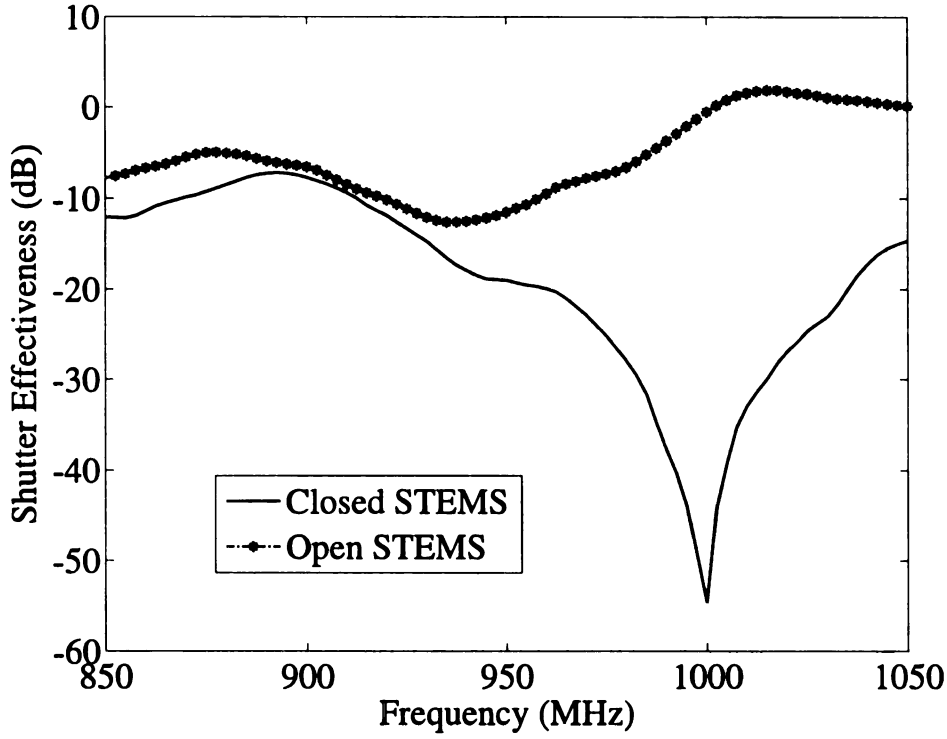

Figure 5.76. Closed and open STEMS best states frequency sweep at 1000MHz

5.6 Conclusion

In this chapter, the fabrication, measurement set-up and measured results of a prototype STEMS are presented. The design and fabrication of the STEMS prototype are presented in section 5.2. Details of the fabricated conducting box and monopole antenna are given in section 5.3. The experimental set-up for measuring the STEMS shutter effectiveness is detailed in section 5.4. The results of the measured shutter effectiveness using a random search code and a genetic algorithm are discussed in section 5.5.

CHAPTER 6

CONCLUSION AND FUTURE WORK

6.1 Conclusion

A new class of electromagnetic devices called self tuning electromagnetic shutters (STEMS) is introduced in this thesis. The STEMS is a slotted metallic surface with computer-controlled switches capable of creating an electronically-controllable iris. An overview of the concept and theory of STEMS is presented in chapter 2. Chapter 3 details the design guidelines of the numerical electromagnetic code NEC4 along with the modeling of closed conducting surfaces using wire grids. The design and simulation of STEMS using GA-NEC is discussed in chapter 4, while chapter 5 presents the details of the fabrication and measurement of a prototype STEMS. Several concluding remarks based on the results of the simulation and the investigations of the prototype STEMS can be drawn as follows:

- STEMS Shutter Effectiveness

  Both simulation and measurement results attest to the effectiveness of STEMS to creating an electronically-controllable iris. The STEMS can behave as a closed or open surface with reference to incident electromagnetic waves by changing the states of the switches on its template.

- Frequency Tunability

  Both simulation and measurement results also prove that the STEMS ability

to exhibit characteristics of an open or closed surface is not limited to a fixed frequency. Through the use of evolutionary search algorithms such as GAs, the frequency of operation of STEMS can be shifted to any desired frequency point within a range of 300MHz. The value 300MHz represents the range in which the prototype was tested and it does not represent the limit of the range of the STEMS frequency tunability.

- STEMS Shutter Effectiveness as a function of Angle of Incidence

  The STEMS ability to create a closed and open surface with respect to different angles of incidences of electromagnetic waves has also been proven through both simulation and measurement. Regardless of the incidence angle of incoming electromagnetic wave, the STEMS can be optimized to produce a shutter effectiveness lower than -40dB or higher than 0dB depending on the task being performed.

6.2 Future Work

Most of the work presented in this thesis has been focused toward the feasibility of STEMS and several of their characteristics are yet to be investigated.

- STEMS Shutter Effectiveness as a function of Location

  The study performed in the measurement section shows that certain switch configurations can produce similar effects at two different locations while others produce very different results. A potential future experiment could be to place

various probes within the box and run an optimization scheme to determine the STEMS shutter effectiveness of all the probes combined.

- STEMS Bandwidth:

  An important property of STEMS that is worth analyzing is their bandwidth. Bandwidth optimization is not possible through the Singer Stoddart NM-37/57 EMI/Field Intensity Meter but this could be realized on the Network Analyzer with LabView. This task could be done through simulation.

- STEMS Multiple Frequencies of Operation:

  Another important property of STEMS that could be investigated is their ability to create a closed or open surface at multiple frequencies. The Field Intensity Meter mentioned above allows for single frequency evaluations and therefore, the Network Analyzer would have to be used for that purpose as well. This could be done through simulation as well to get an insight into the multiple frequency of operation of STEMS

APPENDICES

APPENDIX A

CODES

A.1 Visual Basic Source Code

A.1.1 Random Search

```
%%%%%%%%%%%%%%%%%%%%%%%%%%%%%%%%%%%%%%%%%%%%%%%%%%%%%%%%%%%%%%%%
%   Raoul ouedraogo, ouedraog (at) msu.edu                       %
%   This Visual Basic code reads from a file of random states %
%   to set the switches on the STEMS template                   %
%%%%%%%%%%%%%%%%%%%%%%%%%%%%%%%%%%%%%%%%%%%%%%%%%%%%%%%%%%%%%%%%

Dim StopProcess As Boolean
Dim FilePath, VmFilePath   As String
Dim OUFilePath As String
Dim DBRFilePath As String
Dim Best_StateFilePath, worst_StateFilePath As String
Dim Data As String
Dim n As String
Dim Iter As String
Dim Volt_Out() As Double
Dim Vm As String
Dim Ratio, DBR As String
Dim Vsc As String
Dim LowRatio As String
Dim BeginTime As Date
Dim EndTime As Date
Dim ElapsedTime As Double
Dim In0, Inp0 As String
Dim In1, Inp1 As String
Dim In2, Inp2 As String
Dim In3, Inp3 As String
Dim BinaryCodes As Variant
Dim Voltages As Variant

Private Sub cmdDIOSet_Click()
 Set8PinIO txtDIOSet.Text
End Sub
```

```
Private Sub GetData(VoltAvg)
  CWAI1.AcquireData Voltages, BinaryCodes, 5
  VoltAvg = CWStat1.Mean(Voltages)
  DoEvents
  CWGraph1.PlotY Voltages
End Sub

Private Sub Set24PinIO(Byte0, Byte1, Byte2)
  CWDIO2.Ports.Item(0).SingleWrite Byte0
  CWDIO2.Ports.Item(1).SingleWrite Byte1
  CWDIO2.Ports.Item(2).SingleWrite Byte2
  StopProcess = True
  End Sub

Private Sub Set8PinIO(Byte0)
    CWDIO1.Ports.Item(0).SingleWrite Byte0
End Sub

Private Sub ConfigureCWAI1()
  CWAI1.Configure
End Sub


Private Sub cmdSetState_Click()
  StopProcess = True
'OPEN INPUT FILE
 FilePath = InputBox("Enter file path here")
Open FilePath For Input As #1
'OPEN OUTPUT FILE AND FILE FOR BEST STATE
OUFilePath = InputBox("Enter file path here")
Open OUFilePath For Output As #2
DBRFilePath = InputBox("Enter file path here")
Open DBRFilePath For Output As #3
Best_StateFilePath = InputBox("Enter file path here")
Open Best_StateFilePath For Output As #4
worst_StateFilePath = InputBox("Enter file path here")


Open worst_StateFilePath For Output As #5
'COUNTER & Timer Start
Iter = 1
LowdBR = -2
HighdBR = -200
BeginTime = Now
txtBeginTime.Text = (BeginTime)
```

```
MaxIter = InputBox("Enter number of random iteration", MaxIter)
'START LOOP
Do Until Iter = MaxIter
Line Input #1, Data '(vbTab)
txtByte0.Text = VbCrTab & Data
In0 = Data
Line Input #1, Data
txtByte1.Text = VbCrTab & Data
In1 = Data
Line Input #1, Data
txtByte2.Text = VbCrTab & Data
In2 = Data
Line Input #1, Data
txtByte3.Text = VbCrTab & Data
In3 = Data
Set8PinIO txtByte0.Text
Set24PinIO txtByte1.Text, txtByte2.Text, txtByte3.Text

 'WAIT FOR SWITCHES TO SETTLE
  For ii = 1 To txtWait.Text
  Next ii

'DISPLAY NUMBER OF ITERATIONS
 txtCounter.Text = Iter

'READ VOLTAGE AND RETAIN LOWEST SWR
Dim VoltAvg As Variant
Dim i As Integer
ConfigureCWAI1
GetData VoltAvg
Vm = 10 ^ ((VoltAvg - 0.1040006) / (0.16415))
Vsc = txtVsc.Text
Ratio = Vm / Vsc
DBR = 20 * (Log(Ratio)) / Log(10)
If Abs(DBR) > Abs(LowdBR) Then
LowdBR = DBR
S1 = In0
S2 = In1
S3 = In2
S4 = In3
 Print #4, S1, S2, S3, S4
End If
If Abs(DBR) < Abs(HighdBR) Then
HighdBR = DBR
HS1 = In0
```

```
HS2 = In1
HS3 = In2
HS4 = In3
 Print #5, HS1, HS2, HS3, HS4
End If

'DISPLAY THE PARAMETERS
txtShowVolt.Text = Str$(Vm)
txtShowRatio.Text = Str$(VoltAvg)
txtShowDBR.Text = Str$(DBR)
txtShowLowdBR.Text = Str$(LowdBR)
txtShowHighdBR.Text = Str$(HighdBR)
txtShowIn0.Text = Str$(S1)
txtShowIn1.Text = Str$(S2)
txtShowIn2.Text = Str$(S3)
txtShowIn3.Text = Str$(S4)

'WRITE VOLTAGE TO FILE  "C:\07-08 team\Voultage_Output.txt"
 Print #2, Vm
 Print #3, DBR
 Iter = Iter + 1
 Loop

 'COMPUTE AND DISPLAY ELAPSED TIME
 EndTime = Now
 ElapsedTime = DateDiff("s", BeginTime, EndTime)
    txtEndTime.Text = (EndTime)
    txtElapsedTime.Text = (ElapsedTime)

'CLOSE FILES
Close #1
Close #2
Close #3
Close #4
Close #5
End Sub
Private Sub cmdEndProgram_Click()
    Set8PinIO 0
    Set24PinIO 0, 0, 0
End
End Sub
```

A.1.2 Genetic Algorithm: Closed STEMS

```
%%%%%%%%%%%%%%%%%%%%%%%%%%%%%%%%%%%%%%%%%%%%%%%%%%%
%   Raoul ouedraogo, ouedraog (at) msu.edu        %
%   This Visual Basic code is a genetic algorithm %
%   that optimizes for a closed STEMS             %
%%%%%%%%%%%%%%%%%%%%%%%%%%%%%%%%%%%%%%%%%%%%%%%%%%%

Dim NewPop(1000, 64) As Boolean
Dim OldPop(1000, 64) As Boolean
Dim StateToSet(64) As Boolean
Dim BestinPop(64) As Boolean
Dim WorstinPop(64) As Boolean
Dim Plotit(400) As
Dim Fitness(1000), DBR(1000) As Single
Dim BigFit(500) As Single
Dim GenBest(500)  As Siuiyngle
Dim AvgFitness, MaxFitness, MinFitness, PopSize, As Single
Dim BestFitness, WorstFitness, TotalFitness, As Single
Dim igenno As Integer
Dim BitLength, NGen, IMaxFitness As Integer
Dim ifirst As Integer
Dim ProbCross, ProbMut, Xmin, Xmax, X, Bi, kk, As Singe
Dim ShowDBR, ShowDBRworst, Rate As Single
Dim NO, N1, N2, N3 As String
Dim BO, B1, B2, B3, BinDigit, BestChrome As String
Dim BinaryCodes As Variant
Dim Voltages As Variant
Dim VoltAvg As Variant
Dim i As Integer

Private Sub cmdDIOSet_Click()
 Set8PinIO txtDIOSet.Text
End Sub

Private Sub cmdRunAcquisition_Click()
  ConfigureCWAI1
  GetData VoltAvg
End Sub

Private Sub GetData(VoltAvg)
  CWAI1.AcquireData Voltages, BinaryCodes, 5
  VoltAvg = CWStat1.Mean(Voltages)
```

```
  DoEvents
End Sub

Private Sub Set8PinIO(Byte0)
    CWDIO1.Ports.Item(0).SingleWrite Byte0
End Sub

Private Sub ConfigureCWAI1()
  CWAI1.Configure
End Sub

Private Sub cmdSetIO24_Click()
  Set24PinIO txt0DIO24.Text, txt1DIO24.Text, txt2DIO24.Text
End Sub

Private Sub Set24PinIO(Byte0, Byte1, Byte2)
  CWDIO2.Ports.Item(0).SingleWrite Byte0
  CWDIO2.Ports.Item(1).SingleWrite Byte1
  CWDIO2.Ports.Item(2).SingleWrite Byte2
  StopProcess = True
End Sub

Private Sub cmdRunGa_Click()
  Call RunGA
End Sub

Private Sub RunGA()

Best_StateFilePath = InputBox(" Enter file path here")
Open Best_StateFilePath For Output As #1
 BestReduction_FilePath = InputBox(" Enter file path here")
Open BestReduction_FilePath For Output As #2
 Worst_StateFilePath = InputBox(" Enter file path here")
Open Worst_StateFilePath For Output As #3
WorstReduction_FilePath = InputBox(" Enter file path here")
Open WorstReduction_FilePath For Output As #4

Dim p As String
  BitLength = 32
p = InputBox("Enter population size (<=1000)")
 PopSize = CInt(Val(p))
  p = InputBox("Enter number of generations")
  NGen = CInt(Val(p))
  Randomize
  Call InitPop
```

```
  ifirst = 1
  For igenno = 1 To NGen
    txtGenNo.Text = igenno
    txtGenNo.SetFocus
    Call EvaluateFitness
    Call FitStats
    Call ScaleFitness
    Call SelectPop
    Call CrossPop
    Call MutatePop
    Print #1, BestChrome
  Next igenno

  For j = 1 To 32
    StateToSet(j) = BestinPop(j)
  Next j
  Call SetState
  Close #1
  Close #2
  Close #3
  Close #4
End Sub

Sub InitPop()
'Initializes the population to random values
  For i = 1 To PopSize
    For j = 1 To BitLength
      If Rnd() > 0.5 Then
        OldPop(i, j) = True
      Else
        OldPop(i, j) = False
      End If
    Next j
  Next i
End Sub
Sub EvaluateFitness()
Dim VoltAvg As Variant
For i = 1 To PopSize
  For j = 1 To 32
    StateToSet(j) = OldPop(i, j)
  Next j
Call SetState

'wait while state settles
  For ii = 1 To txtWait.Text
```

```
  Next ii
  Vsc = txtVsc.Text

'read voltage
  ConfigureCWAI1
  GetData VoltAvg
  Fitness(i) = Sqr(0.5841) - (VoltAvg)
  Vm = 10 ^ ((VoltAvg - 0.1040006) / (0.16415))
Ratio = Vm / Vsc
DBR(i) = 20 * (Log(Ratio)) / Log(10)
Next i
End Sub
Sub ScaleFitness()
Dim cmult, a, b As Single
Dim i As Integer

'Scales the fitness of the population
  cmult = 1.2
  If MaxFitness > cmult * AvgFitness Then
    a = (cmult - 1) * (AvgFitness / (MaxFitness - AvgFitness))
    b = (1 - a) * AvgFitness
   If a * MinFitness + b < 0 Then
      a = AvgFitness / (AvgFitness - MinFitness)
      b = -a * MinFitness
    End If
   For i = 1 To PopSize
      Fitness(i) = a * Fitness(i) + b
    Next i
   End If
End Sub
Sub FitStats()
Dim sum As Single
Dim i As Integer

'Calculates the statistics of the population fitness
  If ifirst = 1 Then
    For k = 1 To BitLength
      BestinPop(k) = OldPop(1, k)
    Next k
    BestFitness = Fitness(1)
    WorstFitness = Fitness(1)
    Fmax = Fitness(1)
    Fmin = Fitness(1)
    ifirst = 0
  End If
```

```
 sum = 0
 IMaxFitness = 0
 Fmax = BestFitness
 Fmin = WorstFitness
For i = 1 To PopSize
   sum = sum + Fitness(i)
    If Fitness(i) > BestFitness Then
     BestChrome = ""
     IMaxFitness = i
     Fmax = Fitness(i)
     ShowDBR = DBR(i)
     BestFitness = Fitness(i)
     For j = 1 To BitLength
       BestinPop(j) = OldPop(i, j)
       If BestinPop(j) Then
       BestChrome = 1 & BestChrome
       Else: BestChrome = 0 & BestChrome
       End If
       Next j
   End If
   If Fitness(i) < WorstFitness Then
     Fmin = Fitness(i)
     ShowDBRworst = DBR(i)
     WorstFitness = Fitness(i)
     For k = 1 To BitLength
       WorstinPop(k) = OldPop(i, k)
       If WorstinPop(k) Then
       WorstChrome = 1 & WorstChrome
       Else: WorstChrome = 0 & WorstChrome
       End If
     Next k
   End If
 Next i
 AvgFitness = sum / PopSize
 MaxFitness = Fmax
 MinFitness = Fmin
 TotalFitness = sum
 GenBest(igenno) = MaxFitness
 txtBest.Text = MaxFitness
 txtBest.SetFocus
 txtWorst.Text = MinFitness
 txtWorst.SetFocus
 txtGenAvg.Text = AvgFitness
 txtGenAvg.SetFocus
 txtBestIndividual.Text = BestChrome
```

```
  txtWorstIndividual.Text = WorstChrome
  txtXValue.Text = ShowDBR
  txtYValue.Text = ShowDBRworst
  CWGraph1.PlotY GenBest
    Print #2, ShowDBR
    Print #3, WorstChrome
    Print #4, ShowDBRworst
End Sub
Sub SelectPop()
Dim NNew, NSelect, Nallocate, i, j, k As Integer

'Selects the population for the next generation
'First select by expectd allocation
NNew = 0
For i = 1 To PopSize
Rate = txtRatio.Text
  Nallocate = Int(Fitness(i) / AvgFitness)
  If Nallocate > Rate Then
    For j = 1 To Nallocate
      NNew = NNew + 1
      For k = 1 To BitLength
        NewPop(NNew, k) = OldPop(i, k)
      Next k
    Next j
  End If
Next i
End Sub
Sub CrossPop()
  ProbCross = txtXOver.Text
Dim breed1(64), breed2(64) As Boolean

'performs cross over of breeding population'
ncross = NNew
For i = 1 To NNew Step 2

'select pairs
  i1 = Int(1 + Rnd() * ncross)
  For k = 1 To BitLength
    breed1(k) = NewPop(i1, k)
  Next k
  If i1 < ncross Then
    For j = i1 To ncross
      For k = 1 To BitLength
        NewPop(j, k) = NewPop(j + 1, k)
      Next k
```

```
    Next j
  End If
  ncross = ncross - 1
  i1 = Int(1 + Rnd() * ncross)
  For k = 1 To BitLength
    breed2(k) = NewPop(i1, k)
  Next k
  If i1 < ncross Then
    For j = i1 To ncross
      For k = 1 To BitLength
        NewPop(j, k) = NewPop(j + 1, k)
      Next k
    Next j
  End If
  ncross = ncross - 1
  test = Rnd()
  If ProbCross > test Then
    i1 = Int(1 + (BitLength) * Rnd())
    For k = 1 To i1
      OldPop(i, k) = breed1(k)
      OldPop(i + 1, k) = breed2(k)
    Next k
    For k = i1 + 1 To BitLength
      OldPop(i, k) = breed2(k)
      OldPop(i + 1, k) = breed1(k)
    Next k
    Else
    For k = 1 To BitLength
      OldPop(i, k) = breed1(k)
      OldPop(i + 1, k) = breed2(k)
    Next k
  End If
Next i
End Sub
Sub MutatePop()
Mutate = txtMute.Text
ProbMut = Mutate / (igenno)
i1 = Int(1 + (BitLength) * Rnd())
For i = 1 To NNew
    test = Rnd()
    If ProbMut > test Then
      OldPop(i, i1) = Not (OldPop(i, i1))
    End If
Next i
```

```
'Now fill the rest randomly
Do While NNew < PopSize
NNew = NNew + 1
    For j = 1 To BitLength
      If Rnd() > 0.5 Then
        OldPop(NNew, j) = True
      Else
        OldPop(NNew, j) = False
      End If
    Next j
Loop

'replace last with best result so far
For k = 1 To BitLength
  OldPop(PopSize, k) = BestinPop(k)
Next k
End Sub
Sub SetState()

' create bytes to set switch states
B0 = 0
  For j = 1 To 8
    If StateToSet(j) Then
      B0 = B0 + 2 ^ (j - 1)
    End If
  Next j
  B1 = 0
  N1 = 1
  For j = 9 To 16
    If StateToSet(j) Then
      B1 = B1 + 2 ^ (N1 - 1)
    End If
    N1 = N1 + 1
  Next j
  B2 = 0
  N2 = 1
  For j = 17 To 24
    If StateToSet(j) Then
      B2 = B2 + 2 ^ (N2 - 1)
    End If
    N2 = N2 + 1
  Next j
  B3 = 0
  N3 = 1
  For j = 25 To 32
```

```
    If StateToSet(j) Then
      B3 = B3 + 2 ^ (N3 - 1)
    End If
    N3 = N3 + 1
  Next j

'set switch states
txtByte0.Text = B0
txtByte1.Text = B1
txtByte2.Text = B2
txtByte3.Text = B3
  Set8PinIO B0
  Set24PinIO B1, B2, B3
End Sub
Private Sub cmdEndProgram_Click()
    Set8PinIO 0
    Set24PinIO 0, 0, 0
End
End Sub
```

A.1.3 Genetic Algorithm: Open STEMS

```
%%%%%%%%%%%%%%%%%%%%%%%%%%%%%%%%%%%%%%%%%%%%%%%%%%%
%   Raoul ouedraogo, ouedraog (at) msu.edu        %
%   This Visual Basic code is a genetic algorithm %
%   that optimizes for an Open STEMS              %
%%%%%%%%%%%%%%%%%%%%%%%%%%%%%%%%%%%%%%%%%%%%%%%%%%%

Dim NewPop(1000, 64) As Boolean
Dim OldPop(1000, 64) As Boolean
Dim StateToSet(64) As Boolean
Dim BestinPop(64) As Boolean
Dim WorstinPop(64) As Boolean
Dim Plotit(400) As Boolean
Dim Fitness(1000), DBR(1000) As Single
Dim BigFit(500) As Single
Dim GenBest(500)  As Single
Dim AvgFitness, MaxFitness, MinFitness, TotalFitness As Single
Dim BestFitness, WorstFitness As Single
Dim igenno As Integer
Dim BitLength, NGen, IMaxFitness As Integer
Dim ifirst As Integer
Dim ProbCross, ProbMut, PopSize, Xmin, Xmax, X, Bi, kk As Single
```

```
Dim ShowDBR, ShowDBRworst, Rate As Single
Dim N0, N1, N2, N3 As String
Dim B0, B1, B2, B3, BinDigit, BestChrome As String
Dim VoltAvg As Variant
Dim i As Integer
Dim BinaryCodes As Variant
Dim Voltages As Variant

Private Sub cmdDIOSet_Click()
 Set8PinIO txtDIOSet.Text
End Sub

Private Sub cmdRunAcquisition_Click()
  ConfigureCWAI1
  GetData VoltAvg
End Sub

Private Sub GetData(VoltAvg)
  CWAI1.AcquireData Voltages, BinaryCodes, 5
  VoltAvg = CWStat1.Mean(Voltages)
  DoEvents
End Sub

Private Sub Set8PinIO(Byte0)
    CWDIO1.Ports.Item(0).SingleWrite Byte0
End Sub

Private Sub ConfigureCWAI1()
  CWAI1.Configure
End Sub

Private Sub cmdSetIO24_Click()
  Set24PinIO txt0DIO24.Text, txt1DIO24.Text, txt2DIO24.Text
End Sub

Private Sub Set24PinIO(Byte0, Byte1, Byte2)
  CWDIO2.Ports.Item(0).SingleWrite Byte0
  CWDIO2.Ports.Item(1).SingleWrite Byte1
  CWDIO2.Ports.Item(2).SingleWrite Byte2
  StopProcess = True
End Sub

Private Sub cmdRunGa_Click()
  Call RunGA
End Sub
```

```
Private Sub RunGA()

Best_StateFilePath = InputBox(" Enter file path here")
Open Best_StateFilePath For Output As #1
Worst_StateFilePath = InputBox("Enter file path here")
Open Worst_StateFilePath For Output As #3
BestReduction_FilePath = InputBox(" Enter file path here")
Open BestReduction_FilePath For Output As #2
WorstReduction_FilePath = InputBox(" Enter file path here")
Open WorstReduction_FilePath For Output As #4


Dim p As String
  BitLength = 32
p = InputBox("Enter population size (<=1000)")
 PopSize = CInt(Val(p))
  'ProbMut = 1 / PopSize
  'p = InputBox("Enter probability of crossover (<=1)")
  'ProbCross = CSng(Val(p))
  'ProbCross = 0.5
  p = InputBox("Enter number of generations")
  NGen = CInt(Val(p))
  Randomize

'Vsc = txtVsc.Text
  Call InitPop
  ifirst = 1
  For igenno = 1 To NGen
    txtGenNo.Text = igenno
    txtGenNo.SetFocus
    Call EvaluateFitness
    Call FitStats
      Call SelectPop
    Call CrossPop
    Call MutatePop
    Print #1, BestChrome
  Next igenno
  For j = 1 To 32
    StateToSet(j) = BestinPop(j)
  Next j
  Call SetState
  Close #1
  Close #2
  Close #3
```

```
  Close #4
End Sub
Sub InitPop()

'Initializes the population to random values
  For i = 1 To PopSize
    For j = 1 To BitLength
      If Rnd() > 0.5 Then
        OldPop(i, j) = True
      Else
        OldPop(i, j) = False
      End If
    Next j
  Next i
End Sub
Sub EvaluateFitness()
Dim VoltAvg As Variant
For i = 1 To PopSize
  For j = 1 To 32
    StateToSet(j) = OldPop(i, j)
  Next j
Call SetState

'wait while state settles
  For ii = 1 To txtWait.Text
  Next ii
  Vsc = txtVsc.Text

'read voltage
  ConfigureCWAI1
  GetData VoltAvg
  Fitness(i) = Sqr(0.5841) - (VoltAvg)
  Vm = 10 ^ ((VoltAvg - 0.1040006) / (0.16415))
Ratio = Vm / Vsc
DBR(i) = 20 * (Log(Ratio)) / Log(10)
Next i
End Sub

Sub FitStats()
Dim sum As Single
Dim i As Integer
'Calculates the statistics of the population fitness
  If ifirst = 1 Then
    For k = 1 To BitLength
      BestinPop(k) = OldPop(1, k)
```

```
    Next k
    BestFitness = Fitness(1)
    WorstFitness = Fitness(1)
    Fmax = Fitness(1)
    Fmin = Fitness(1)
    ifirst = 0
  End If
  sum = 0
  IMaxFitness = 0
  Fmax = BestFitness
  Fmin = WorstFitness
For i = 1 To PopSize
    sum = sum + Fitness(i)
     If Fitness(i) < BestFitness Then
      BestChrome = ""
      IMaxFitness = i
      Fmax = Fitness(i)
      ShowDBR = DBR(i)
      BestFitness = Fitness(i)
      For j = 1 To BitLength
        BestinPop(j) = OldPop(i, j)
        If BestinPop(j) Then
        BestChrome = 1 & BestChrome
        Else: BestChrome = 0 & BestChrome
        End If
        Next j
    End If
    If Fitness(i) > WorstFitness Then
      Fmin = Fitness(i)
      ShowDBRworst = DBR(i)
      WorstFitness = Fitness(i)
      For k = 1 To BitLength
        WorstinPop(k) = OldPop(i, k)
        If WorstinPop(k) Then
        WorstChrome = 1 & WorstChrome
        Else: WorstChrome = 0 & WorstChrome
        End If
      Next k
    End If
  Next i
  AvgFitness = sum / PopSize
  MaxFitness = Fmax
  MinFitness = Fmin
  TotalFitness = sum
  GenBest(igenno) = MaxFitness
```

```
  txtBest.Text = MaxFitness
  txtBest.SetFocus
  txtWorst.Text = MinFitness
  txtWorst.SetFocus
  txtGenAvg.Text = AvgFitness
  txtGenAvg.SetFocus
  txtBestIndividual.Text = BestChrome
  txtWorstIndividual.Text = WorstChrome
  txtXValue.Text = ShowDBR
  txtYValue.Text = ShowDBRworst
  CWGraph1.PlotY GenBest
    Print #2, ShowDBR
    Print #4, ShowDBRworst
    Print #3, WorstChrome
End Sub

Sub SelectPop()
Dim NNew, NSelect, Nallocate, i, j, k As Integer
'Selects the population for the next generation
'First select by expectd allocation
NNew = 0
For i = 1 To PopSize
Rate = txtRatio.Text
  Nallocate = Int(Fitness(i) / AvgFitness)
  If Nallocate < Rate Then
    For j = 1 To Nallocate
      NNew = NNew + 1
      For k = 1 To BitLength
        NewPop(NNew, k) = OldPop(i, k)
      Next k
    Next j
  End If
Next i
End Sub
Sub CrossPop()
  ProbCross = txtXOver.Text
Dim breed1(64), breed2(64) As Boolean

'performs cross over of breeding population'
ncross = NNew
For i = 1 To NNew Step 2

'select pairs
  i1 = Int(1 + Rnd() * ncross)
  For k = 1 To BitLength
```

```
    breed1(k) = NewPop(i1, k)
  Next k
  If i1 < ncross Then
    For j = i1 To ncross
      For k = 1 To BitLength
        NewPop(j, k) = NewPop(j + 1, k)
      Next k
    Next j
  End If
  ncross = ncross - 1
  i1 = Int(1 + Rnd() * ncross)
  For k = 1 To BitLength
    breed2(k) = NewPop(i1, k)
  Next k
  If i1 < ncross Then
    For j = i1 To ncross
      For k = 1 To BitLength
        NewPop(j, k) = NewPop(j + 1, k)
      Next k
    Next j
  End If
  ncross = ncross - 1
  test = Rnd()
  If ProbCross > test Then
    i1 = Int(1 + (BitLength) * Rnd())
    For k = 1 To i1
      OldPop(i, k) = breed1(k)
      OldPop(i + 1, k) = breed2(k)
    Next k
    For k = i1 + 1 To BitLength
      OldPop(i, k) = breed2(k)
      OldPop(i + 1, k) = breed1(k)
    Next k
    Else
    For k = 1 To BitLength
      OldPop(i, k) = breed1(k)
      OldPop(i + 1, k) = breed2(k)
    Next k
  End If
Next i
End Sub
Sub MutatePop()
Mutate = txtMute.Text
ProbMut = Mutate / (igenno)
i1 = Int(1 + (BitLength) * Rnd())
```

```
For i = 1 To NNew
    test = Rnd()
    If ProbMut > test Then
      OldPop(i, i1) = Not (OldPop(i, i1))
    End If
Next i

'Now fill the rest randomly
Do While NNew < PopSize
NNew = NNew + 1
    For j = 1 To BitLength
      If Rnd() > 0.5 Then
        OldPop(NNew, j) = True
      Else
        OldPop(NNew, j) = False
      End If
    Next j
Loop

'replace last with best result so far
For k = 1 To BitLength
  OldPop(PopSize, k) = BestinPop(k)
Next k
End Sub

Sub SetState()
' create bytes to set switch states
B0 = 0
  For j = 1 To 8
    If StateToSet(j) Then
      B0 = B0 + 2 ^ (j - 1)
    End If
  Next j
  B1 = 0
  N1 = 1
  For j = 9 To 16
    If StateToSet(j) Then
      B1 = B1 + 2 ^ (N1 - 1)
    End If
    N1 = N1 + 1
  Next j
  B2 = 0
  N2 = 1
  For j = 17 To 24
    If StateToSet(j) Then
```

```
      B2 = B2 + 2 ^ (N2 - 1)
    End If
    N2 = N2 + 1
  Next j
  B3 = 0
  N3 = 1
  For j = 25 To 32
    If StateToSet(j) Then
      B3 = B3 + 2 ^ (N3 - 1)
    End If
    N3 = N3 + 1
  Next j

'set switch states
txtByte0.Text = B0
txtByte1.Text = B1
txtByte2.Text = B2
txtByte3.Text = B3
  Set8PinIO B0
  Set24PinIO B1, B2, B3
End Sub
Private Sub cmdEndProgram_Click()
    Set8PinIO 0
    Set24PinIO 0, 0, 0
End
End Sub
```

A.2 Matlab Code

A.2.1 Random Search Histogram, histogram.m

```
%%%%%%%%%%%%%%%%%%%%%%%%%%%%%%%%%%%%%%%%%%%%%%%%%%%%%%%%
% histogram.m                                          %
% Random search result histograms                      %
% Andrew Temme, temmeand (at) msu.edu                  %
% This m file uses random search results for various   %
% frequencies to produce histograms of the shutter     %
% effectiveness found for each frequency.              %
%%%%%%%%%%%%%%%%%%%%%%%%%%%%%%%%%%%%%%%%%%%%%%%%%%%%%%%%

%frequencies
```

```
freq = [600 620 650 675 700 725 750 775 801 825...
 850 875 900 925 950 975 1000];


%number of divisions for the histogram
num_bins = 200;
%process each file
for j=1:max(size(freq))
 path = [int2str(freq(j)) '-Random-DB_R.txt'];
 dB_data = load(path);
 %hist(dB_data,200);
 max_dB = max(dB_data); %find the max and min
 min_dB = min(dB_data);
 dB_range = ceil(max_dB - min_dB);
 dB_step = dB_range / num_bins;
 dB_data = dB_data + -1*min_dB;

    histo = zeros(num_bins,1);
    data_size = max(size(dB_data));

    for i=1:data_size   %process each result
        bin = ceil( dB_data(i)/dB_range * num_bins);
        if ( bin == 0 )
            bin = 1;
        end
        histo(bin) = histo(bin) + 1;
    end

    %plot
    figure(j)
    subplot(2,1,1)  %full histogram
    stairs(histo)
    title(['dB Reduction for ' int2str(freq(j)) ' MHz']);
    xlabel('Current Reduction (dB)')
    tick = floor(min_dB):dB_range/10:ceil(max_dB);
    set(gca,'XTickLabel',tick);
    ylabel('Number of States');
    subplot(2,1,2)
    stairs(histo)   %zoomed in histogram (smaller y range)
    title(['dB Reduction for ' int2str(freq(j)) ' MHz']);
    xlabel('Current Reduction (dB)')
    tick = floor(min_dB):dB_range/10:ceil(max_dB);
    set(gca,'XTickLabel',tick);
    ylabel('Number of States');
    ylim([0 50])
```

```
    save_file_as = [int2str(freq(j)) 'MHz-rand-histo.pdf'];
    saveas(j,save_file_as)
end
```

A.2.2 GA Nec Switch State Histogram, gaNecHisto.m

```
%%%%%%%%%%%%%%%%%%%%%%%%%%%%%%%%%%%%%%%%%%%%%%%%%%%%%%%%%%%%%%%%%%%%%%%%
% gaNecHisto.m                                                          %
% GA Nec Switch State Histogram                                         %
% 21 Jul 2008                                                           %
% Andrew Temme, temmeand (at) msu.edu                                   %
% This m file generates a histogram showing how many                    %
% times a switch is turned on in a set GA NEC results                   %
% files, both vertical orientation and oblique                          %
% orientation, maximum and minimum searches.                            %
%%%%%%%%%%%%%%%%%%%%%%%%%%%%%%%%%%%%%%%%%%%%%%%%%%%%%%%%%%%%%%%%%%%%%%%%

% frequencies of result files
freq = [625 650 675 700 725 750];
num_freq = size(freq);    %number of frequencies
hist = zeros(32,7);       %histogram variable
%maximum
for i = 1:num_freq(2)
    vert_name = ['max' int2str(freq(i)) '-0-0.ni4'];
    obli_name = ['max' int2str(freq(i)) '-30-60.ni4'];
    vert = load(vert_name);     %load files
    obli = load(obli_name);
    for j = 1:32
        if vert(j,5) == 0.100000001490116
            hist(j,1) = hist(j,1)  + 1;
        end
        if obli(j,5) == 0.100000001490116
            hist(j,2) = hist(j,2)  + 1;
        end
    end
end
hist(:,3) = hist(:,1) + hist(:,2);  %sum vert. and oblique
% minimum
for i = 1:num_freq(2)
    vert_name = ['min' int2str(freq(i)) '-0-0.ni4'];
    obli_name = ['min' int2str(freq(i)) '-30-60.ni4'];
    vert = load(vert_name);     %load files
    obli = load(obli_name);
```

```
    for j = 1:32
        if vert(j,5) == 0.100000001490116
            hist(j,4) = hist(j,1)  + 1;
        end
        if obli(j,5) == 0.100000001490116
            hist(j,5) = hist(j,2)  + 1;
        end
    end
end
hist(:,6) = hist(:,4) + hist(:,5);
hist(:,7) = hist(:,3) + hist(:,6);
%plot all on one figure
figure(1)
subplot(4, 2, 1)
stairs(hist(:,1))
title('Vertical Orientation Maximum Best Switch States')
xlabel('Swtich')
ylabel('Num. of Occurrences')
xlim([1,32])
ylim([0,10])
subplot(4, 2, 3)
stairs(hist(:,2))
title('Obligue Orientation Maximum Best Switch States ')
xlabel('Swtich')
ylabel('Num. of Occurrences')
xlim([1,32])
ylim([0,10])
subplot(4, 2, 5)
stairs(hist(:,3))
title('All Maximum Best Switch States Histogram')
xlabel('Swtich')
ylabel('Num. of Occurrences')
xlim([1,32])
ylim([0,15])
subplot(4, 2, 2)
stairs(hist(:,4))
title('Vertical Orientation Minimum Best Switch States')
xlabel('Swtich')
ylabel('Num. of Occurrences')
xlim([1,32])
ylim([0,10])
subplot(4, 2, 4)
stairs(hist(:,5))
title('Obligue Orientation Minimum Best Switch States')
xlabel('Swtich')
```

```
ylabel('Num. of Occurrences')
xlim([1,32])
ylim([0,10])
subplot(4, 2, 6)
stairs(hist(:,6))
title('All Minimum Best Switch States Histogram')
xlabel('Swtich')
ylabel('Num. of Occurrences')
xlim([1,32])
ylim([0,15]
subplot(4, 2, 7)
stairs(hist(:,7))
title('All Best Switch States Histogram')
xlabel('Swtich')
ylabel('Num. of Occurrences')
xlim([1,32])
ylim([0,30])
saveas(1,'NEC_switch_histogram.pdf')
%plot each on an individual figure
figure(2)
stairs(hist(:,1))
xlabel('Swtich')
ylabel('Num. of Occurrences')
xlim([1,32])
ylim([0,10])
saveas(2,'max-vert-hist.pdf')
figure(3)
stairs(hist(:,2))
xlabel('Swtich')
ylabel('Num. of Occurrences')
xlim([1,32])
ylim([0,10])
saveas(3,'max-obli-hist.pdf')
figure(4)
stairs(hist(:,3))
xlabel('Swtich')
ylabel('Num. of Occurrences')
xlim([1,32])
ylim([0,15])
saveas(4,'max-all-hist.pdf')
figure(5)
stairs(hist(:,4))
xlabel('Swtich')
ylabel('Num. of Occurrences')
xlim([1,32])
```

```
ylim([0,10])
saveas(5,'min-vert-hist.pdf')
figure(6)
stairs(hist(:,5))
xlabel('Swtich')
ylabel('Num. of Occurrences')
xlim([1,32])
ylim([0,10])
saveas(6,'min-obli-hist.pdf')
figure(7)
stairs(hist(:,6))
xlabel('Swtich')
ylabel('Num. of Occurrences')
xlim([1,32])
ylim([0,15])
saveas(7,'min-all-hist.pdf')
figure(8)
stairs(hist(:,7))
xlabel('Swtich')
ylabel('Num. of Occurrences')
xlim([1,32])
ylim([0,30])
saveas(8,'all-hist.pdf')
```

BIBLIOGRAPHY

BIBLIOGRAPHY

[1] B. A. Munk, *Frequency Selective Surfaces: Theory and Design* John Wiley, New York, 2000.

[2] T.K. Wu, "Double-square-loop FSS for multiplexing four (S/X/Ku/Ka) bands," IEEE Antenna and Propagation Magazine, vol. 3, pp. 1885-1888, June 1991.

[3] T.K. Wu, S.W. Lee "Multiband Frequency Selective Surface with Multiring Patch Elements," IEEE Antenna and Propagation Magazine, vol. 42, no. 11, pp. 1484-1490, December 1994.

[4] T.K. Wu, "Four-Band Frequency Selective Surface with Double-Square-Loop Patch Elements," IEEE Antenna and Propagation Magazine, vol. 42, no. 12, pp. 1659-1653, December 1994.

[5] J. Romeu, Y. Rahmat-Samii,"Dual band FSS with fractal elements," IEEE Electronics Letters, vol. 35, no. 9, pp. 702-703, April 1999.

[6] J. Romeu, Y. Rahmat-Samii,"Fractal FSS: A Novel Dual-Band Frequency Selective Surface," IEEE Electronics Letters, vol. 48, no. 7, pp. 702-703, July 2000.

[7] J.P. Gianvittorio, J. Romeu, S. Blanch, Y. Rahmat-Samii,"Self-Similar Prefractal Frequency Selective Surfaces for Multiband and Dual-Polarized Applications," IEEE Electronics Letters, vol. 51, no. 11, pp. 3088-3096, July 2003.

[8] D.H. Kim, J.I. Choi,"Frequency Selective Surface for the blocking of multiple frequency bands," IEEE Antenna and Propagation Magazine, vol. 1, pp. 4195-4198, 2006.

[9] M. Lambea, J.A Encinar, "Analysis of multilayer frequency selective surfaces with rectangular geometries," IEEE Antenna and Propagation Magazine, vol. 1, no.407 pp. 528-531, April 1995.

[10] C. Wan, J.A Encinar, "Analysis of Multilayered FSS by Efficient Computation of Generalized Scattering Matrix," IEEE Antenna and Propagation Magazine, vol. 3, pp. 2270-2273, June 1994.

[11] J.M. Johnson, Y. Rahmat-Samii, "Genetic algorithms in engineering electromagnetics," IEEE Antenna and Propagation Magazine, vol. 39, pp. 7-21, August 1997.

[12] G. Manara, A. Monorchio, R. Mittra,"Frequency selective surface design based on genetic algorithm," IEEE Electronics Letters, vol. 35, no. 17, pp. 1400-1401, August 1999.

[13] E. A. Parker, A. D. Chuprin, J. C. Batchelor, S. B. Savia,"GA optimization of crossed dipole FSS array geometry," IEEE Electronics Letters, vol. 37, no. 16, pp. 996-997, August 2001.

[14] Y. Yuan, C. H. Chan, K. F. Man, R. Mittra, "A genetic algorithm approach to FSS fi lter design," IEEE Antenna and Propagation Magazine, vol. 4, pp. 688-691, July 2001.

[15] S. Chakravarty and R. Mittra, "Application of the micro-genetic algorithm to the design of spatial fi lters with frequency-selective surfaces embedded in dielectric media," IEEE Antenna and Propagation Magazine, vol. 44, no. 2, pp. 338-346, May 2002.

[16] A.C. de C. Lima, E.A. Parker and R.J. Langley,"Tunable frequency selective surface using liquid substrates," IEEE Electronics letters, vol. 30, no. 4, pp. 281-282, February. 1994.

[17] T. K. Chang, R. J. Langley, E. A. Parker,"Active frequency-selective surfaces," IEEE Microwaves, Antennas Propagation., vol. 143, pp. 62-64, February. 1996.

[18] Y. C. Chan, G. Y. Li, T. S. Mok, J. C. Vardaxoglou,"Analysis of a tunable frequency-selective surface on an in-plane biased ferrite substrate," Microwave and Optical Technology Letters., vol. 13, no. 2, pp. 5963, October 1996.

[19] J.P. Gianvittorio, J. Zendejas, Y. Rahmat-Samii, J. Judy, "Reconfigurable MEMS-enabled frequency selective surfaces," IEEE Electronic Letters., vol. 38, no. 25, pp.16271628, Dec. 2002

[20] C. Mias,"Frequency selective surfaces loaded with surface-mount reactive components," IEE Electronics Letter, vol. 39, no. 9, May 2003.

[21] J. A. Bossard, D. H. Werner, T. S. Mayer, and R. P. Drupp,"A Novel Design Methodology for Reconfigurable Frequency Selective Surfaces Using Genetic Algorithms," IEEE Transactions on Antennas and Propagation, Vol. 53, No. 4, pp. 1390 - 1400, April 2005.

[22] J. A. Bossard, D. H. Werner, T. S. Mayer, and R. P. Drupp,"Reconfigurable Infrared Frequency Selective Surfaces," IEEE Transactions on Antennas and Propagation, Vol. 2, No. 4, pp. 1911 - 1914, June 2004.

[23] J. A. Bossard, D. H. Werner, T. S. Mayer, and R. P. Drupp,"A Novel Design Methodology for Reconfigurable Frequency Selective Surfaces Using Genetic Algorithms," IEEE Transactions on Antennas and Propagation, Vol. 53, no. 4, pp. 1390 - 1400, April 2005.

[24] X. Liang, L. Li, J. A. Bossard, D. H. Werner,"Reconfigurable frequency selective surfaces with silicon switches," IEEE Transactions on Antennas and Propagation, Vol. 1, pp. 189-192, July 2006.

[25] F. Bayatpur, K. Sarabandi, "A tunable, band-pass, miniaturized-element frequency selective surface: Design and measurement," IEEE Antenna and Propagation Magazine, vol. 1, pp. 3964-3967, June 2007.

[26] C.M. Coleman, E.J. Rothwell, J.E. Ross, "Self-Structuring Antenna," IEEE Antenna and Propagation Magazine, vol. 3, pp. 1256-1259, July 2000.

[27] C.M. Coleman, E.J. Rothwell, J.E. Ross, B.T. Perry and B.F. Basch, "Self-Structuring Antenna for Television Reception," IEEE Antenna and Propagation Magazine, vol. 1, pp.162-165, July 2001.

[28] C.M. Coleman, E.J. Rothwell, J.E. Ross, and L.L. Nagy, "Self-Structuring Antenna," IEEE Antenna and Propagation Magazine, vol. 44, no. 3, pp. 11-22, June 2002.

[29] C.M. Coleman, E.J. Rothwell, and J.E. Ross, "Investigation of simulated annealing, ant-colony optimization, and genetic algrithm for self-structuring antenna," IEEE Antenna and Propagation Magazine, vol. 52, no. 4, pp. 1007-1014, April 2004.

[30] E.J. Rothwell, J.E. Ross, and S. Preschutti, "A complimentary self-structuring antenna for use in a vehicle environment," IEEE Antenna and Propagation Magazine, vol. 3, pp. 2321-2324, June 2004.

[31] B.T. Perry, E.J. Rothwell, J.E. Ross, and L.L. Nagy, "Self-structuring antenna concept for FM-band automotive backlight antenna design," IEEE Antenna and Propagation Magazine, vol. 1B, pp. 92-95, 2005.

[32] B.T. Perry, E.J. Rothwell, and L.L. Nagy, "Analysis of switch failures in a self-structuring antenna system," IEEE Antenna and Propagation Magazine, vol. 4, pp. 68-70, 2005.

[33] G. Burke and A. Poggio, *Numerical Electromagnetic Code-Method Of Moment*, Livermore CA: Lawrence Livermore National Laboratory, Report no. UCID-18834, 1981.

[34] John Ross & Associate, *GA-Suite with NEC analysis Version 7.0.*

[35] Tom Wallace, *Speeding up NEC using LAPACK*, Applied Computational Electromagnetics society Newsletter, Vol 15, no. 1, ISSN 1056-9170.

[36] A. Sarolic, B. Modlic, and D. Poljak, *Measurement validation of ship wiregrid models of different complexity in EMC*, IEEE International Symposium on Electromagnetic Compatibility, vol. 1, pp. 651656, August 2001.

[37] M. McKaughan, *Coast guard applications of nec*, IEEE Antennas and Propagation Society Symposium, vol. 3, pp. 28792882, June 2004.

[38] C. W. Trueman and S. J. Kubina, *Fields of complex surfaces using wire grid modeling*, IEEE Transactions on Magnetics, vol. 27, no. 5, pp. 42624267, September 1991.

[39] Lt P. Ellhiadis (Hellenic Navy) and J. K. Breakall, *An investigation of the near fields for shipboard antennas using the numerical electromagnetics code (NEC)*, IEEE Antennas and Propagation Society International Symposium, vol.1, pp. 236-239, Year 1989.

[40] Robert Stratman Elliott, *Antenna Theory and Design*, Prentice-Hall, Englewood Cliffs, NJ, 1981.

[41] A. Rubinstein, M. Rubinstein, and F. Rachidi, *'A physical interpretation of the equal area rule*, In IEEE Transactions on Electromagnetic Compatibility, 2005, submitted.

[42] A. C. Ludwig *Wire grid modeling of surfaces*, IEEE Transactions on Antennas and Propagation, vol. AP-35, no. 9, pp. 10451048, September 1987.

[43] Abraham Rubinstein, Cyrous Rostamzadeh, Marcos Rubinstein, Farhad Rachidil, *On the Use of the Equal Area Rule for the Wire-Grid*, 17th International Zurich Symposium on Electromagnetic Compatibility, 2006

[44] R.F. Harrington, *Time-Harmonic Electromagnetic fields*, IEEE Press, Classic Reissues, 2001.

[45] D.M. Pozar, *Microwave Engineering* John Wiley, New York , Third edition, 2005.

[46] *home.ict.nl/ arivoors/*

[47] G. Lynn, *A self-structuring patch antenna*, Michigna State University, 2008.